

BOTSWANA INTERNATIONAL UNIVERSITY
OF SCIENCE & TECHNOLOGY

FALL OF GROUND CHARACTERIZATION AND ITS IMPLICATIONS FOR GROUND CONTROL AT BCL MINE

by

PAKO TUMELO PHUMAPHI

A Thesis Submitted to the Faculty of Engineering and Technology in Partial Fulfillment of the Requirements for the Award of the Degree of Master of Engineering in Geological Engineering of Botswana International University of Science and Technology.

JULY, 2018

BOTSWANA INTERNATIONAL UNIVERSITY OF SCIENCE & TECHNOLOGY

FALL OF GROUND CHARACTERIZATION AND ITS IMPLICATIONS FOR GROUND CONTROL AT BCL MINE

by

PAKO TUMELO PHUMAPHI

Student Number: 14100124

BSc (Geology), University of Botswana

Department of Mining and Geological Engineering,

Faculty of Engineering and Technology,

Botswana International University of Science and Technology.

E-mail Address: tumelo.phumaphi@studentmail.biust.ac.bw, Phone Number: +26772771051

A Thesis Submitted to the Faculty of Engineering and Technology in Partial Fulfillment of the Requirements for the Award of the Degree of Master of Engineering in Geological Engineering of Botswana International University of Science and Technology.

Supervisors: Dr, Amoussou Coffi Adoko

School of Mining and Geosciences, Nazarbayev University, Kazakhstan

E-mail Address: amoussou.adoko@nu.edu.kz, Phone Number: (+77057834744)

Signature: _____ Date: 09/07/2018

Dr, Jerome Anabannye Yendaw

Department of Mining and Geological Engineering,

Faculty of Engineering and Technology (FET), BIUST

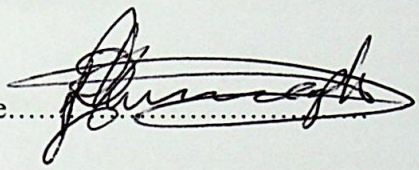
E-mail Address: yendawj@biust.ac.bw , Phone Number :(+26775323627)

Signature: _____ Date: 09/07/2018

July, 2018

DECLARATION AND COPYRIGHT

I, **Tumelo Pako Phumaphi**, declare that this thesis is my own original work and that it has not been presented and will not be presented to any other university for a similar or any other degree award.

Signature..... 

This thesis is copyright material protected under the Berne Convention, the Copyright Act of 1999 and other international and national enactments, in that behalf, on intellectual property. It must not be reproduced by any means, in full or in part, except for short extracts in fair dealing; for researcher private study, critical scholarly review or discourse with an acknowledgement, without the written permission of the office of the Provost, on behalf of both the author and the Botswana International University of Science and Technology.

CERTIFICATION

The undersigned certifies that he has read and hereby recommends for acceptance by the Faculty of Engineering and Technology a thesis titled: **Fall of Ground characterization and its implications for ground control at BCL Mine**, in fulfillment of the requirements for the degree of Master of Engineering in Geological Engineering of the Botswana International University of Science and Technology.

.....

Dr. A.C Adoko

(Supervisor)

Date: 09/07/2018

.....

Dr. J.A Yendaw

(Co-Supervisor)

Date: 09/07/2018

Acknowledgement

I would like to thank the all mighty high, the Lord for guiding me throughout this Rock Mechanics Engineering research work that was conducted for two years at the Department of Mining and Geological Engineering at Botswana International University of Science and Technology.

Secondly, I would like to express my very great appreciation to Dr. Amoussou Coffi Adoko, my knowledgeable supervisor who had faith in me from the starting day until the day I submitted this thesis. He gave me the opportunity to improve my skills and constantly provided me with invaluable guidance, encouragement, and suggestions. I cannot possibly count every lesson that I learned from him throughout this period. I also would like to thank him for having the patience to review and correct multiple versions of this document.

I would like to thank Dr Jerome Yendaw for having the patience to review some chapters of this document and being the internal supervisor. Special thanks to my dearest friend, Molaodi Ntuane, for his continued guidance and constant support, Tiro Lebane, Dithebe Moesi, Oratile Kgaodi, Physics team, Mining and Geological engineering technicians and many others were more than just colleagues, but good friends, and the best support team I have ever worked with. Without their help and support, this thesis could not have been possible. This study was carried out in collaboration with the BCL mine. My gratitude to Mr. Maswebe Dimapo and rock mechanics team for their assistance and guidance during my data collection period at BCL mine. I learned so much more than I could ever imagine about working at a mining environment in a very short period of time.

Love, thanks and gratitude to my beloved family for always being there for me during my time as a student, friends for their understanding throughout the duration of my studies in BIUST (Palapye). A special thanks to my mother for always believing in me, providing me with the confidence and support during my studies to reach goals I did not think I could reach. Aunt, thank you for listening to me and encouraging me along the way.

Finally, my thanks to Botswana International University of Science and Technology (BIUST) for their financial support which made this research work possible.

List of symbols and abbreviations

NIOSH: National Institute for Occupational Safety and Health

FoG: Fall of Ground

UCS: Uniaxial Compressive Strength (MPa)

E: Young's modulus (GPa)

MPa: Mega Pascal

GPa: Giga Pascal

Ga: Giga Annum (Billion Years)

SLOS: Sublevel Open Stoping

CSIRO: Commonwealth Scientific and Industrial Research Organization of Australia

SEE: South East Extension

c: Cohesion (MPa)

H: Overburden or tunnel depth (m)

GSI: Geological Strength Index

K: Horizontal to vertical stress ratio

MN/m^3 : Meganewton per cubic metre

S: Strength factor

Φ: Internal friction angle (°)

ρ: Density of the rock (kg/m^3)

σ_c: Uniaxial compressive strength (MPa)

σ_h: Horizontal stress (MPa)

σ_v: Vertical stress (MPa)

BPNN: Back propagation neural network

ANN: Artificial neural Network

RES: Rock engineering system

GBI: Ground behavior index

RMSE: Root mean square error

C=E: Cause-effect

Table of Contents

Acknowledgement iii
List of symbols and abbreviations iv
Table of Contents v
List of Figures viii
List of Tables x
List of Equations xi
Abstract xii
Chapter 1: Introduction 1
1.1 The research background 1
1.2 Problem description 2
1.3 Motivation 4
1.4 Aim of the research project 4
1.5 Objectives of this study 4
1.6 Methods 5
1.7 Thesis Outline 6
Chapter 2: Fall of Ground Review 8
2.1 Introduction 8
2.1.2 Occurrence of FoG 10
2.1.3 Types of FoG 11
2.1.4 Factors influencing excavation instability and FoG. 11
2.1.5 Characteristics of an effective fall of ground assessment method 16
2.1.6 Hazards in underground mines 16
2.1.7 Coal bumps 17
2.1.8 Rock bursts 18
2.2 Ground Control 18
2.2.1 Ground Control in underground mining 19
2.3 Failure mode 19
2.3.1 General ground behavior and failure 21
2.3.2 Structurally controlled failures 25
2.3.3 Spalling failure 25

2.4 Summary 26
Chapter 3: Fall of Ground (FoG) Characterization at BCL Mine 28
3.1 Introduction 28
3.1.1 Location of study area 28
3.2 Geo-engineering setting of the study area 30
3.2.1 Geology 30
3.2.2 Structural geology 31
3.2.3 Ore body 32
3.3 The stress field around BCL mine and other mining districts 33
3.3.1 Primary stress state 34
3.3.2 Mining method 36
3.4 Characterization of FoG data 37
3.4.1 Compiling a FoG database 37
3.4.2 Analysis of FoG 39
3.4.3 Unplanned fall of Ground Evaluation 41
3.4.4 FoG accident statistics 45
Chapter 4: Constructing the Ground Behavior Index (GBI), (Data Analysis) 49
4.1 Quantifying Rock Mass Behavior around BCL excavations 49
4.1.1 The rock engineering systems (RES) 49
4.1.2 Artificial Neural Network Background (ANN) 51
4.1.3 Defining the ground behavior index (GBI) 56
4.2 Developing the GBI 56
4.2.1 Dataset preparation 56
4.2.2 Results 60
4.2.3 Validation of the results 70
4.3 Conclusions 71
Chapter 5: Numerical Modeling 73
5.1 Introduction 73
5.2 Structure controlled failure mode analysis 73
5.3 Stress controlled failure mode analysis 79
5.3.1 Examine^{2D} stress analysis 79

5.3.2 Rock and Soil 2-dimensional (RS2) analysis 80
5.3.3 Model setup 81
5.3.4 Stress distribution 81
5.3.5 Strength factor 83
5.3.6 Yielded elements 84
Chapter 6: Discussions 85
6.1 Failure 89
6.2 Rock mass quality 90
6.3 Summary 91
Chapter 7: Conclusion 92
7.1 Recommendations and future numerical modeling 94
7.2 Future Research 95
Reference 96

List of Figures

Figure 1: Fall of ground at 835 m/ 3450 in Phikwe stope. 4
Figure 2: Different modes of failure in underground openings (Kaiser and Kim, 2008). 24
Figure 3: Ground behavior in underground mine opening (Rahimi and Sharifzadeh, 2017). 26
Figure 4: Location of study area. 29
Figure 5: Location map of BCL mine shafts. 29
Figure 6: Generalized stratigraphy of BCL mine (Gallon, 1986). 31
Figure 7: Position of BCL mine ore bodies and geology of the area modified after (Gallon, 1986). 32
Figure 8: Schematic long section through BCL mines ore bodies (Maswebe, 2011). 33
Figure 9: Various excavation width (X_9) at Selebi mine (left) and Phikwe Central mine (right). 40
Figure 10: Different excavation heights (X_{10}) in the mine. 41
Figure 11: Mine wide excavation heights (X_{10}) distribution. 41
Figure 12: Unplanned fall of ground length (left) and fall of ground height (right). 42
Figure 13: Shows fall of ground width. 43
Figure 14: Illustrates unplanned fall of ground weight (X_{14}) distribution in the mine. 43
Figure 15: Rock material dislodged description classification. 44
Figure 16: Fall of ground occurrence relation grouping. 44
Figure 17: Rock mass failure mode distribution. 45
Figure 18: Number of fatalities at BCL mine by 5 year period. 47
Figure 19: Occupational fatalities and injuries by mine location. 48
Figure 20: Principle of the interaction matrix (Hudson, 1992). 50
Figure 21: Artificial neural network structure (Fausett, 1994). 53
Figure 22: Schematic diagram of a BPNN in training phase (Shin et al., 2009). 54
Figure 23: Training performance using the FoG datasets. 62
Figure 24: Cause-effect diagram for the GBI system. 64
Figure 25: Interaction intensity for the parameters of the GBI. 65
Figure 26: Comparison between predicted and actual FoG. 69
Figure 27: The GBI with the associated hazard level (H.L.). 69
Figure 28: Stereonet projection with density contour and major geological structures forming sliding wedges in sill drive. 75
Figure 29: Pole plot of geological structures forming vital sliding and falling wedges in Phikwe stopes. 76
Figure 30: Contour plot of joint density concentrations in Phikwe stopes. 77
Figure 31: Pole plot of geological structures forming vital sliding and falling wedges in Phikwe 835 m/ 3420 stopes. 77
Figure 32: Kinematic analyses accounting for wedge sliding in Selebi 950 m/ 3875 stope. 78
Figure 33: The distribution of major principal stress around Phikwe 3420 stope (left) and Selebi 3875 stope (right). 79

Figure 34: Stress distribution of minor principal stress after stope excavation in Phikwe 3420 (left) and Selebi 3875 (right). 80
Figure 35: Strength factor around Phikwe stope (left) and Selebi stopes (right) after excavation..... 80
Figure 36: A general model setup for the Selebi sill drive. 81
Figure 37: Stress distribution of major principal stress in Selebi 850 m sill drive (elastic model)..... 82
Figure 38: Stress distribution (major principal stress) around 835 m/ 3100 stope. 82
Figure 39: Stress distribution (minor principal stress) for the sill drive (elastic model). 83
Figure 40: Potential brittle failure areas with strength factor less than 1 in an unsupported cut and fill 835 m/ 3100 stope (elastic model). 83
Figure 41: Yielded elements in a plastic model of Phikwe 835 m/ 3100 stope. 84
Figure 42: Shear and tension failure along discontinuities at Phikwe 835 m/ 3100 stope..... 84

List of Tables

Table 1: BCL mine fatalities and injuries data BCL mine (BCL, 2016). 3
Table 2: Methods employed to acquire the objectives of this study. 6
Table 3: Group of parameters influencing ground behaviors (Cai et al., 2004). 13
Table 4: Rock damage scale used to classify the case history data (Mikula, 2013, Duan, 2016). 21
Table 5: Ground behavior type and instability in underground opening for geomechanical planning (Goricki et al., 2004). 23
Table 6: Summary of stress components at BCL mine (Van der Heever et al., 2014). 36
Table 7: Raw data sample. 39
Table 8: Fall of ground accident statistics by mine location (BCL, 2016). 46
Table 9: ESQ method for interaction intensity coding (Hudson, 1992). 51
Table 10: GBI parameter classification rating. 58
Table 11: Statistical description of the data. 60
Table 12: The interaction matrix derived from the trained BPNN using the FoG datasets 63
Table 13: Calculated parameter weights for ground behavior. 65
Table 14: Calculated GBI with a sample of encoded datasets. 67
Table 15: Calculated GBI for a sample of validation datasets. 70
Table 16: Major dip and dip direction measurements selected in Dips software (Rocscience, 2016a). 78

List of Equations

Equation 1: Damage index expression used for calculating stress induced failure. 20
Equation 2: The vertical stress estimation expression. 35
Equation 3: The horizontal stress approximation relationship..... 35

Abstract

Mining at great depth is associated with many principal stability and ground control problems. One of the challenges currently facing underground mines is changes in ground conditions leading to the fall of ground (FoG) hazards. Fall of ground refers to rock material dislodged from roof and sidewalls of an underground excavation usually unintentionally induced. This study focuses on FoG characterization. A FoG database has been compiled. In order to quantify the rock mass behavior around underground excavations and fully characterize the FoG events, statistical analysis, numerical methods, rock engineering system (RES) and artificial neural networks (ANN) have been used. The Bamangwato Concessions Limited (BCL), an underground mine located in Selibe-Phikwe, Botswana was used as case study where FoG events that occurred in various stopes and other mine openings were recorded. Overall, two aspects of the FoG characterization were investigated. In the first part of this thesis, the concept of ground behaviour index was introduced to predict the ground class associated with FoG hazard. To this end, ANN was used to determine the weights of input parameters involved and the RES was employed as a tool to quantify the non linear interactions of parameters via the interaction matrices and the hazard class evaluated. Meanwhile, in the second part of the thesis, numerical modelling was implemented to analyse the modes of rock failure around the underground openings which had led to FoG. Several models were established in Rocscience software package to simulate the structure-induced and stress-induced failure modes or a combination of both that had been observed in the field. In general, the obtained results were in agreement with the field results. It is concluded that this study has enhanced the understanding of ground conditions, fall of ground characteristics and provided ground control improvements in BCL mine.

Keywords: Fall of ground characterization; failure mode; ground control; ground behavior index; rock engineering system; Artificial Neural Networks; and Numerical Methods

Chapter 1: Introduction

1.1 The research background

Over the years, Bamangwato Concessions Limited (BCL) mine has been a key driving factor to Botswana's economy, enormously contributing to the gross domestic product (GDP) (Newman, 2013). The depletion of surface mineral resources compels mining in deeper ground to extract valuable mineral resources that account for country's economy. The development of mines into greater depths, unexploited ground conditions is accompanied by risk, unique challenges for engineers and researchers that are associated with underground excavation instability and ground control issues.

A wide range of rock fall events can be used in the literature to describe fall of ground (FoG). FoG can be defined as rock detached from roof and sidewalls of an underground excavation usually unintentionally induced (Adoko et al., 2017). Ground falls refer to rock dislodged by falling from roof, sliding from sidewalls, that falls by gravity on the excavated site (Varnes, 1978). In this thesis the author defined fall of ground as when the rock material is discharged from the roof and sidewalls as blocks posing serious threat to the underground activities such as causing injuries, fatalities and damaging equipment.

Falls of ground (FoG) are an intrinsic danger and one of the leading hazards in underground mines eroding workers safety and mine operations. Falls of ground dangers exist in every underground mine across the world due to uncertainties in ground conditions and are a result of excavation instability. Thus, ground fall is a serious unwelcome global challenge affecting underground miners and mining investment. Fall of ground characterization is of critical importance to the design and mining of underground rock engineering projects.

In recent years, ground falls have been reported as a problem in BCL mine and underground mines from many countries, including South Africa (Koldas, 2003, Stacey and Gumede, 2007), USA (Bertoncini and Hinders, 2010), Peru (Iramina et al., 2014) and Zambia (Katongo, 2005). In BCL, underground mining operations have been affected by FoG leading to mine economic loss and accidents to miners. The mine accidents reveal the hazardous nature of FoG. Historically rock falls have always been accountable for the loss of lives and it is the leading hazard causing most fatalities in mining and tunnel works. For example, nine miners died in a violent coal bump at Crandall Canyon mine in United States in 2007 (Mark et al.,

2011). Since 1999 through to 2010, fall of ground integrated with rockbursts have in the past been responsible and remains the leading cause of most fatalities and injuries in underground mines. The development of ground control procedures and ground support standards to tackle these hazards has resulted in reduction of fatalities and enhanced mining operations (Pappas and Mark, 2012).

Ground conditions, geological discontinuities, excavation geometry, support design measures and mining methods are fundamental contributors of underground excavation rock falls. Ground control has been and continues to be a major problem facing underground mines around the world. The reduction of geo-engineering hazards including fall of ground to an acceptable degree, while maintaining safe excavations in surrounding rock mass is the principal objective of ground control in mining, civil and tunneling operations. Therefore, the knowledge of rock mass structure, ground behavior and failure mode is essential in managing the ground and designing of ground control procedures for future mining. The consequence of FoG have led to personal harm, equipment damage accompanied with enormous economic losses in worker's compensation and production delay (Lang, 2010).

1.2 Problem description

Over the past two decades, annual fatalities in Bamangwato Concessions Limited (BCL) underground mine have been decreasing steadily while production was rising. The downward trend in fatalities and injuries classified in 5 year periods can be observed through the two decades in Table 1. 2005 to 2009 were the safest years for BCL mining recording the lowest number of fatalities and injuries, with 2 fatalities and 2 lost time injuries according to the statistics. Fall of ground events are accountable for most of the fatalities and injuries of the BCL underground mine according to mine accident statistics. This shows that unplanned falls of ground are an important problem. On the BCL fall of ground reports, 89 fatalities and injuries occurred from March 1995 through January 2016 with an enormous number of these accidents taking place in stopes areas posing danger to miner's safety (BCL, 2016).

Table 1: BCL mine fatalities and injuries data BCL mine (BCL, 2016).

BCL Mine Year	Fatalities	Reportable Injuries (RI)	Lost Time Injuries (LTI)	Minor Injuries (MI)
1995-1999	12	16	1	-
2000-2004	8	13	9	6
2005-2009	2	-	2	-
2009-2016	2	7	7	4
Total	24	36	19	10

New challenges of excavation stability arise due to increased depths of mining, changing ground conditions and changes of rock mass response to mining has resulted in fall of ground occurring in BCL mine. Table 1 illustrates FoG fatalities and injuries that have occurred in BCL mine caused by fall of ground from excavation roof and side walls. Increasing concern of hazard occurrences in BCL mines has led to demand for improvement and efficient ground control measures. Accordingly, instability of rock mass surrounding underground mine excavations has become a serious safety issue and challenging problem for BCL and mining industry worldwide. Currently numerous number of FoG are registered in the mine with varying fall out size. Figure 1 shows fall of ground damage that occurred at 835 m depth/ 3450 stope. In order to deal with these challenges, design methodologies must take into consideration all risk modifiers that influence manifestations of instability in surrounding rock mass. This research focuses on considerable fundamental fall of ground characterization for effective ground control in BCL mine as a case study. Ground control forms a significant part of mine planning to ensure, improve safety and production. Peng (2015) stated that implementation of ground control methods is required for improving miners safety and accomplishing desired mine design as many rock engineering applications would have not functioned without it.

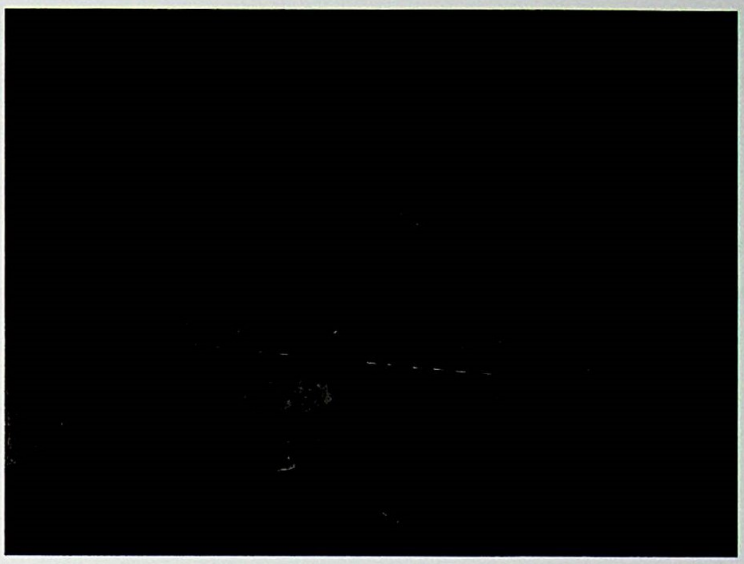


Figure 1: Fall of ground at 835 m/ 3450 in Phikwe stope.

1.3 Motivation

Underground excavations are located in vast variety of ground conditions with different modes of behavior and failure. This has led to an imperative challenge of understanding of surrounding rock mass response to underground mining activities since it can aid in eliminating hazards, improving safety and ground control approaches. The motivation for this research work was driven by problems associated with excavation instability such as falls of ground necessitating to make underground mines a safer place to work. The problems and consequences of changing ground conditions led to the requirement to characterize and understand the cause of ground falls in different stope environments in the mine.

1.4 Aim of the research project

The aim of this research is to characterize fall of ground events that occurred at BCL mine in order to propose practical recommendations in terms of ground control.

1.5 Objectives of this study

The main objectives of the research project are to:

i. Compile fall of ground data including the rock mass characteristics, excavation geometry, excavation support and mining methods.
ii. Describe the FoG events at BCL mine.
iii. Quantify the rock mass behavior around the stopes subject to fall of ground using the concept of Ground Behavior Index (GBI).

iv. Analyze the fall of ground features including the factors influencing the excavations instability, failure types and modes in selected stopes using numerical methods.
v. Formulate recommendations for ground control at BCL Mine.

1.6 Methods

In order to achieve the objectives of this study, a set of methods were implemented including field observations, statistical methods, Rock Engineering System (RES), Artificial Neural Network (ANN) and numerical modeling methods as summarized in Table 2.

Table 2: Methods employed to acquire the objectives of this study.

Objectives	Methods
(i). Compile fall of ground data including the rock mass characteristics, excavation geometry, support and mining methods.	Field observations. Literature review. Followed by collection of underground data from the field, underground mapping, studying and assembling geotechnical reports. Laboratory rock mechanical properties testing results data was availed. Fall of ground data gathered from ground fall directory.
(ii). Describe the FoG events at BCL mine. Quantify the rock mass behaviour around the stopes subject to fall of ground using the concept of Ground Behaviour Index.	Assembled FoG database was screened to determine the fall of ground properties and factors influencing instability. Statistical methods, RES, ANN, GBI conception and empirical methods.
(iii). Analyze the fall of ground features including the factors influencing the excavations instability, failure types and modes in selected stopes using numerical methods.	Simulate different rock material models to reproduce the rock failure mode occurring around the stopes and sill drive using Rocscience software package (Dips, Examine^{2D} and RS2.)
(iv). Formulate recommendations for ground control at BCL Mine.	Based on the results of the GBI and numerical analysis as well as the field observations, ground control suggestions can be devised.

1.7 Thesis Outline

In this thesis, an assessment into characteristics of the rock mass and ground falls, failure mode and factors impacting ground instability leading to fall of ground was carried out. The

current chapter introduces the nature of the work, starting with background, defines the problem that is being studied and methodology and objectives of the thesis.

Chapter 2 provides a detailed literature review on fall of ground characterization and ground control in underground mining and methods used to pinpoint factors influencing fall of ground and methods that can be used to compile, analyze and group FoG data. In this chapter an evaluation of the necessary information on characterization of ground falls and ground control methods, the importance of controlling ground movement in mines and mine design technique was carried out. This involved the theory of hazards presented as FoG and the types of FoG. Key concepts of rock falls and rock fall events are explained. The factors that can influence FoG are also reviewed. Finally, the different techniques that are used to control ground movement are explained.

Chapter 3 presents the methodology that aims at compiling BCL mine fall of ground data and analyzing the data using statistical methods. The geological setting, mining methods and the stress field of the mine are explained. The methodology of compiling FoG data and quantifying the fall of ground characteristics is discussed.

Chapter 4 illustrates the application of ANN and RES to quantify ground behavior of BCL mine. Empirical, analytical and statistical analysis together with numerical approaches will be used to determine the rock mass behavior and the hazard level of FoG as well as identifying principal parameters influencing fall of ground.

Chapter 5 discusses the Rocscience software package used in this work to examine structure induced gravity driven failure and stress failure modes occurring in the mine. Kinematic analysis is used to assess potential failure around the excavations. Numerical modeling is utilized to analyze stress and combined stress and structural failures.

Chapter 6 provides a discussion of this research work's summary results.

Chapter 7 provides conclusions of this research project incorporating recommendations for future work.

Chapter 2: Fall of Ground Review

2.1 Introduction

The stability of underground openings is critical to sustainable safe mining in underground metalliferous hard rock mines. The evaluation of ground behavior around underground mine excavations and characterization of ground falls is required because they have a considerable influence on engineering decision making when choosing suitable mine design techniques, application of ground control measures and maintaining underground openings stability. The excavation failure mode may be altered by mining induced stresses. The applicable engineering methods may need to be changed due to changes in excavation behavior during mining (Kaiser, 2016). In rock engineering projects involving underground excavations in rock with discontinuities, many instability problems are caused by failure and deformation (Hao and Azzam, 2005). The rock mass failure can result in falls of ground. The major challenge encountered in underground metalliferous mining today is managing geo-hazards such as fall of ground which is connected to ground control problems.

Ground falls pose a great significant challenge in underground mines and tunnels, as it is the source of injuries, fatalities, damage to machinery and production delay. This serious hazard has been responsible for numerous casualties, excavation and equipment damage in underground mines. In underground mines, FoG and ground control problems demands attention for ensuring miners safety and stability of excavations. Underground metalliferous hard rock mines continues to experience many types of ground failures and have developed comprehensive ground support standards and ground control procedures to address the hazards. From underground observations, studies and experience acquired from rock mass failure events around excavations indicates that fall of ground is relentless and the requirement of understanding ground behavior compels advances in rock mechanics to reduce excavation failures (Kaiser, 2016). It is important to assess fall of ground characteristics, failure mode, ground conditions connected with hazards to mitigate this unwanted problem by coming with reliable improved ground control technology. The system used as a line of resistance to lessen any form of ground movement is ground control (Kaiser and Cai, 2012). The method has been successful in many underground opening across the world.

Statistics recorded around the world show that mechanized mining practices and ground conditions play a key role in driving instabilities. Previous statistical data of non fatal and

fatal injuries confirm the seriousness of this unwanted safety issue in underground mines in USA, Poland, South Africa and Australia (Mark et al., 2011, Martyka and Hetmanczyk, 2013). Advancement in ground control methods such as pillar design and ground movement control technology have remarkably reduced injuries and fatalities caused by fall of ground but they remain the major cause of injuries in underground mines stated by Mark and Gauna (2017). Koldas (2003), Peng (2015), Katongo (2005), Kashyap et al. (2008), Mark and Gauna (2017), Mark (2016), Zhu et al. (2017), Direk (2015) and Queensland (2004) have been assessing this safety issue for years and research work still ongoing worldwide. One of the principal problems faced by past and current industry, academic research engineers and research students is to advance methods of managing FoG and mitigate the hazards associated with ground instabilities. According to Stacey and Gumede (2007), Koldas (2003), Cai (2016), Mark (2016), Prusek et al. (2017), Mark et al. (2011), Shahriar et al. (2009), Mark and Barczak (2010), Sinkala and Krishna (2014) and Peng (2015) the optimum approaches have been developed to diminish these hazards with continuous observations, experience and research to upgrade mine safety, but further growth can be achieved in underground mining ground control. Such dramatic reduction can be observed in the industry safety statistics, which illustrates a crucial downward direction in ground fall injuries and fatalities (Potvin et al., 2001). Furthermore, reduction in ground fall injuries can be attributed to other factors such as reduction of underground workers, advances in new ground control technologies especially innovation of roof bolts implemented for ground support, application of these technologies and alteration of safety cultures (Mark, 2015). According to Mark and Barczak (2010) utilization of roof control plan and the growth in shield support for long wall mining principally contributed in enhancing ground control technology. Research has shown that continuous development of ground control technologies and methods would result in advances of ground fall prevention plans, improved safety and excavation stability.

2.1.1.1 Coal Mine ground falls

Esterhuizen and Bajpayee (2012), Molinda and Mark (2010), Mark et al. (2011), Ndlovu and Stacey (2007), van der Merwe et al. (2001), Kashyap et al. (2008), Esterhuizen et al. (2007) and Xie et al. (2018) previously carried out different studies and examination on roof fall causes and factors influencing it. The strength of rock mass, excavation's geometry and the magnitude and the orientation of in situ stresses determine the extent of rock failure around an

excavation (Hoek et al., 2002). Failures around mine structures stabilize after strata movements and in other places continue throughout before final collapse takes place. Research indicates that many roof falls occur in underground mines with weak roofs than in strong roofs (Lehmann and Konietzky, 2015, Pappas and Mark, 2010). The stability of excavations can be reduced by geological discontinuities. Roof falls in underground coal mines are generated by a number of various factors. Esterhuizen et al. (2007), Esterhuizen and Bajpayee (2012) and Molinda and Mark (2010) conducted a study on the factors that influence excavation stability and found that geological conditions, roof quality, moisture, in-situ stress level, mining methods, multiple seam mining and inadequate strata support are the leading factors that cause strata movements and FoG. Bajpayee et al. (2014) investigated the factors influencing roof instabilities in underground coal mines. Roof falls investigations have yielded a list of common types of roof falls that are the chief hazards to miners (Molinda, 2003).

2.1.2 Occurrence of FoG

Falls of ground occur when rocks become displaced from the roof or sidewalls of an underground excavation. The amount of dislodged geological material can vary in size from hundreds of kilograms to thousands of tons of material. The ejected material can be a serious hazard to workers, equipment and production as it causes injuries, fatalities, damage to equipment and production delays as well as economic loss to mine operations. There are situations demanded in order for fall of ground incident to happen, such as ground element domain, human factor element domain and inadequate ground support system (Biswas and Zipf, 2003). Ground control measures are implemented to stabilize underground excavations and prevent falls of ground. Ground control is the art of maintaining and preventing ground movements in underground mine openings to an acceptable level utilizing various techniques. It is essential that fall of ground events are thoroughly investigated in order to comprehensively understand the factors that contributed to the occurrence and for improving ground control measures as well as preventing recurrence of similar events for future control. Every mine is required to conduct falls of ground investigations.

2.1.3 Types of FoG

Instability in underground openings presents itself as fall of ground. Falls of ground in underground mines can be mainly categorized into: Induced/ intentional ground fall and unplanned/ unintentional fall of ground (Biswas and Zipf, 2003). Induced fall of ground expresses the ground falls that are expected to occur promoted by mining methods such as caving rock in block caving mining method in hard rock mine and room and pillar mine where the roof collapses. Unintentional FoG signify that fall of ground from around the excavation arise without prior warning to miners in mine workings due to underground opening instability. This work focuses on unplanned falls of ground characterization and prediction. Fall of ground includes, rock falls, cave-in and stress-induced instabilities which is rock spalling and rock burst (Martin et al., 2003, Adoko et al., 2017). The types of ground instabilities are gravity induced structurally controlled, block movement and stress induced (Martin et al., 1999). Cave in is where the overlying ground immediately falls into the excavation. The dimensions of the falls are blocks of dissimilar sizes and fracturing dominates in these collapses. Understanding and recognition of ground failure mechanisms resulting in the hazardous failure process and evaluation of roof and side wall fall danger are essential in eliminating injuries and ground falls.

2.1.4 Factors influencing excavation instability and FoG.

Today, ground falls is the most significant hazard that underground workers have to tackle. In order to design satisfactory ground control measures and minimize falls of ground it is essential to understand ground movement mechanisms as a result of mining operation and elements influencing instability in underground openings triggering fall of ground. The causes of rock falls can be broadly categorized into geologic, ground control components and ground control system design. In underground hard rocks, there are many factors that are related to the occurrence of falls of ground such as rock blasting, excavation geometry including size and shape, rock mass strength and type, geological structures of the rock mass, ground water, geo-stress condition and the mining method. Other factors that influence the behavior of the rock mass, occurrence of ground falls around underground excavations include mechanical properties of rocks, nature of geological discontinuities, the method of excavation and the rock reinforcement and ground support systems (Brown and Hoek, 1978). Over the years, several researchers have reported the factors associated with rockbursts events in hard rock

using prediction methods (Wang and Park, 2001, Mansurov, 2001, Zhou et al., 2010, Jian et al., 2012).

Although rock is naturally stable, there are different factors when combined which influence the rock behavior and stability of rock mass (Cai et al., 2004). It is therefore important to understand rock mass characteristics, rock mass extrinsic parameters and rock engineering design parameters affecting rock mass behavior since they have a great significance on the long term stability of underground excavations, ground control measures and in choosing suitable mine design techniques (Adoko et al., 2017).

Cai et al. (2004) proposed parameters that guide the ground behavior and organized them into three groups: Rock mass intrinsic parameters, rock mass extrinsic parameters and excavation design parameters as depicted in Table 3 below. Table 3 shows the specific parameters which influence rock behavior of the rock in underground excavations. Among the intrinsic parameters, the uniaxial compressive strength, joint orientation has been used in this study to evaluate the ground behavior around BCL mine openings. Between the rock mass extrinsic parameters, the in situ stress conditions and blasting has been used and from excavation design factors excavation size and blasting has been used to quantify the ground behavior index in this research work. From Cai et al. (2004)'s work on parameters influencing ground behavior, improvements in rock engineering design parameters can be made. The author proposes that the mining methods and ground support system be added in the excavation design parameters as it greatly influences the ground behavior. Ground support and mining methods are significant to the long term stability of underground excavations.

Table 3: Group of parameters influencing ground behaviors (Cai et al., 2004).

Group of parameter		Individual parameters
Rock mass intrinsic parameters	Intact rock parameters	Strength of intact rock
		Rock modulus
	Joint parameters	Number of joint sets
		Joint frequency
		RQD
		Joint condition (roughness, infilling, weathering)
		Joint size/length, persistency
		Joint orientation
Rock mass extrinsic parameters	Not applicable	In situ stress
		Ground water
		Dynamic condition (earthquake, blasting)
		Excavation size
Design (excavation) parameters	Not applicable	Excavation shape
		Construction method
		Blasting damage

2.1.4.1 Geological discontinuities

Mines are constructed in rocks which are greatly affected by geological discontinuities. In rock engineering excavation projects, geological discontinuities are one of the most vital elements of an excavation and greatly influence excavation instability problems leading to ground falls. The frequent encountered geological discontinuities in rock mass are faults, joints, bedding and foliations. The discontinuities occurrence in underground openings weakens the rock mass strength, control failure and deformation (Liu et al., 2010, Chikande and Zvarivadza, 2016). Most FoGs occurrences are associated to rock mass with considerable

discontinuities creating ground control challenges (Koldas, 2003). The rock mass geological structures heavily control the magnitude and frequency of fall of ground occurrence where underground excavations take place. The geological discontinuity properties such as orientation, persistence, infilling and roughness play a vital role in controlling the probability of FoG occurrence. Thus, the evaluation of geological structures is significant based on structural collected field data of excavated stopes and other underground mine excavations. Kainthola (2015), Li et al. (2015) stated that over the years underground rock engineering constructions have been facing considerable challenge on deformation and failure of surrounding rock mass along geological structures. Schubert (1998) investigated the impact of geological discontinuities on the failure and deformation behavior of rock mass surrounding underground excavations.

2.1.4.2 Blasting

The backbone of underground mine openings excavation technique is blasting. Numerous safety and mining operations problems are a result of blasting practices that are not optimized to the specific site ground conditions (Iverson et al., 2007). Blasting practices generates seismic disturbances, damages the surrounding rock mass, roof, ribs, walls and ground support system initiating hazardous conditions in underground excavation (Singh et al., 2015). Rock damage caused by blasting can result in instability, unplanned falls of ground which is a safety threat to workers and equipment. Moreover, blast damage contributes to rock mass quality reduction leading to demand in ground support increase (Iverson et al., 2007). Statistics show that most of injuries sustained during scaling and installation of ground support are the result of unplanned falls of ground originated from blast damage. Blast induced damage and unplanned falls of ground can be reduced by utilizing better perimeter control blasting (Badal, 1994, Iverson et al., 2007). Ground control consideration and stability of underground excavations are commonly connected to the strength of rock mass. Therefore the enhancement of better careful perimeter blasting will improve rock quality, minimize scaling and ground control requirements. Whyatt et al. (2003) employed controlled blasting approaches to improve ground control safety in underground mines. Kidybinski (1986) recorded small and large roof falls and floor heave in underground coal mine openings being caused by blast damage when the peak particle velocity (PPV) increases. Currently National Institute of Occupational Safety and Health (Iverson et al., 2013, Verma et al., 2014) is

conducting research on reducing rock damage around underground excavations. Methods have been developed to quantify blast induced damage and future investigations are directed towards documenting the location and orientation of cracks surround the opening and measuring seismic velocity changes.

2.1.4.3 Ground water

Ground water is water located in the subsurface filling up soil pore spaces and rock mass cracks. It is stored and moves by hydraulic gradient through geological lithologies. It is this ground water that affects the excavation conditions and long term stability (Palmström and Stille, 2010). When designing underground excavations during analysis of potential water problems it is critical to consider regional geology and ground water pattern (Flaten, 2015). Significant ground water encountered in rock mass is associated with many forms of instability. The stability of the mine openings is affected by reduction in friction, strength of the rock material and the shear strength of discontinuities caused by groundwater pore pressure. Increase in water content increases the rock weight resulting in increased shear stress. Nilsen and Palmström (2000) stated that the evaluation of ground water pressure is key as it may contribute to instability by corroding the ground support and reducing rock mass strength.

2.1.4.4 Weathering

The interaction of water with the rock system favors rock dissolution, mineral deposition and clay mineral formation (Watters et al, 2005). Irfan (1999), Zimbelman et al. (2004) and Watters et al. (2000) have focused on weathering factors causing chemical and mineral alteration process and few attempts on the weathering effects on strength reduction of altered rock material have been investigated (Zimbelman et al., 2003). Finn et al. (2007) proposed that material degradation is an essential factor in inducing excavation instability and fall of ground. Also, progressive alterations of rock materials by physical and chemical systems that could promote instability in underground excavations understanding is limited (Pola et al., 2014). Instability in mine openings produces hazardous conditions and fall of ground. The correlation between an increase in porosity and decreasing the uniaxial compressive strength (UCS) of rock has been widely accepted worldwide. Marques et al. (2010) and Pola et al. (2014) illustrated that physical characterization (porosity, water content, P-S wave velocity),

chemical characterization, deterioration of UCS and Young's modulus could be employed to demonstrate the degree of alterations in rocks. Therefore, detailed descriptions of the rock mass behavior and assessment of failure mode is a fundamental requirement for effective ground control measures to hamper fall of ground and stability challenges.

2.1.5 Characteristics of an effective fall of ground assessment method

The fall of ground occurrence evaluation approaches can be thought of as steps that characterize the fall of ground events and implement controls to handle these events to an acceptable level. The first step is to identify ground fall location, measure the excavation geometry and estimate FoG dimensions, FoG size, determine the geology and ground support type within active portions of the mine. By executing this process, the distinguishing parameters are recognized and quantitatively analyzed using rock engineering system, artificial neural networks, statistical methods and qualitative numerical methods. The aim is to establish the most important parameters influencing the ground behavior leading to FoG taking place. The identified influential parameters are rated from the most important to least significant. The next step uses a wide variety of analysis techniques to determine the potential of FoG, forecasting areas that are highly susceptible to ground falls linked with specific ground conditions and ground behavior of the mine. In underground mine the hazards can be graded by their severity and ground management procedure can be applied to determine how to minimize the hazard.

2.1.6 Hazards in underground mines

In underground mining rock explosion from excavations are considered to as rock burst in metalliferous (nickel copper) mines and coal burst in coal mines, which are described as hazards caused by mining and ground behavior around excavation (Cai, 2016). Geological conditions in the mining area such as the rock mass in situ stresses, bumping features contained in the rock mass and ability to maintain large amounts of strain energy influence the mechanism and mode of rock explosion. Fall of ground, coal bumps and rock bursts as regarded as hazards in underground mines are discussed as they take place in similar geological conditions and induced by mining excavations (Kaiser and Cai, 2013, Cai, 2016). Whenever a fall of ground, coal burst and rock burst occurs, there are always contributing

geological conditions, excavation geometry and mining induced stress related to it. The hazards in underground mines are described in the following sections.

2.1.6.1 Scaling

Ground condition observations in underground mines become intricate as the excavations spans and height increase creating visibility challenges when taking down loose after blasting. Failure to remove loose ground causes fall of ground. Scaling in underground mines is important to remove loose ground after blasting from sidewalls and roof. There are two ways of carrying out scaling namely: hand scaling and mechanical scaling. Mechanical scaling separates the miner from unsupported ground reducing the risk of rock falls. According to Grau and Prosser (1997) approximately one third of the fall of ground injuries in underground mines are caused by hand scaling contributing 90% of injuries leading the statistics. Iannacchione et al. (1998) stated that ground control hazards can be reduced by making underground excavations stable.

2.1.7 Coal bumps

Coal bumps refers to abrupt and forceful ejection of coal and rock fragments from the walls or pillars caused by stress release. In the 1960s, studies on coal bumps and rock burst began using micro seismic techniques to pinpoint areas of high stress concentration (Peng, 2015). Already with more than 50 years of sustained study and examination, numerous coal bumps continue to cause problems to excavation damage and miner's safety resulting in injuries and fatalities. The coal bump phenomena continue to be encountered in underground coal mines without prior awareness even though lots of coal bump concepts have improved and ground monitoring procedures to control them have developed. Several researchers studied causes of coal bumps and rock bursts and deduced ground control measures to avoid high stress concentrations (Saharan and Mitri, 2011, Konicek et al., 2011). Calleja and Porter (2016) and other researchers (Mark and Zelanko, 2005, Dou et al., 2009, Mark et al., 2011, Cai, 2016, Zhang et al., 2015, Mark and Gauna, 2017) explained that there are preventative and mitigating methods that have been successfully employed and are currently in operation to control and prevent coal bursts and rock bursts in underground mines, such as destress blasting, pillar design, long term water infusion, optimization of mining methods, mining sequence, implementation of rock bolts as ground support and hydrofracking.

2.1.8 Rock bursts

Over the past years, artificial intelligence has been used to predict rock burst occurrence utilizing important parameters that influence rock burst as inputs. Rock burst prediction can be classified into long term prediction and short term prediction (Peng et al., 2010). Several researchers have studied rock burst prediction using parameters that affect ground behavior related rock burst occurrence. Peng et al. (2014) classified rock burst based on support vector machines. Li and Liu (2015) and Li et al. (2016) employed Bayesian networks technique to predict rock burst hazard. Furthermore, Adoko et al. (2013), Yu et al. (2009), Guo and Jiang (2009) used fuzzy networks technologies to deduce rock burst hazard. Miao et al. (2016) stated that geo-stress is one of the critical factors in forecasting rock burst. A similar methodology was adopted in this research using parameters that influence ground behavior causing hazards to predict fall of ground.

2.2 Ground Control

Ground control is a technique of sustaining stability around underground openings to minimize the hazards related with different ground failures and displacement appearances to ensure and prolong safety of mines. Ground control may be described as the art of maintaining and preventing ground movements and predicting rock behavior in underground mine openings to an acceptable level utilizing various techniques to ensure safety of workers and serviceability of openings (MOSHAB, 1997). Ground represents all forms of rock ranging from very weak, weathered to high strength material and rock mass. Ground control is a principal problem, which affects safety and productivity in underground mining. Ground control deals with the adaptation of a system by which ground movement can be regulated to accepted level of safe workplace and extraction of mineral resources. Rock mass properties such as cohesion, strength and friction angle as well as detailed knowledge of any geological structures, stress field details are needed to examine the ground response to mining activities. The requirement for effective ground control may extend into its components. The three key elements that make up successful ground control maybe considered to be:

- Site Ground characteristics
- Mine planning and design
- Ground support and reinforcement

2.2.1 Ground Control in underground mining

Ground control encompasses different engineering and operational measures to control, monitor and restrain falls of ground from occurring. The procedure to manage ground movements and instabilities require understanding of rock mass behavior, failure mechanisms and failure modes in order to design measures that prevents falls of ground. Mine planning and sequencing strategies can be utilized to minimize the effects of stress on ground support, adequate ground support installation to stabilize underground mine openings and monitoring system to measure ground displacements and rock mass stress levels around the excavations. The stope mining sequence plays a central role in determining the redistribution of mining induced stresses around the openings. Different mining induced stresses are the results of varied mining sequences, which are one of the important factors affecting instability, assisted by the dip, thickness of ore body and excavation geometry (Abedellah et al., 2014).

All forms of ground displacement are addressed by ground control use to try and solve the challenges associated with mining operations such that appropriate methods and technologies could be improved to grow the craft ground control to tackle critical mining issues. Fundamental problems in underground mines are tackled by ground control such as sidewall control, floor control, pillar design, roof control, bump failures and subsidence of overlying ground and stress changes (Peng, 2015). In mining operations, Ground control measures, namely design of support and reinforcement, mining method, ground conditions as well as excavation methods and sequencing can greatly affect the stability of underground openings. In a variety of rock engineering fields the stability of underground excavations is a persistent challenge for engineers.

2.3 Failure mode

Failure mode is the manner in which the rock mass will fail also identifying their causes and effects to the ground behavior. It is the result of failure mechanisms. The way failure happens is reported by failure mode. The description of the rock mass failure mode can be a qualitative analysis to indicate that it is a central and fundamental task in rock mechanics engineering. The general rock mechanics modes of failure that are commonly experienced in underground mine openings are structurally controlled gravity driven failure, stress induced spalling / slabbing type failure and a mixture of structurally controlled gravity driven action along structures and stress induced failure. The failure modes involving geological discontinuities

and intact rock are buckling, shearing and sliding as well as block falls. The failure modes involving only intact rock are rockbursting, squeezing and spalling (Deng, 2000).

Shear failure along geological structures is related with majority of ground behavior types around underground excavations (Kaiser and Kim, 2008). The Damage index (D_i) introduced by (Martin et al., 1999) endeavored to quantify the potential for stress induced brittle failure is given by Equation 1:

$$D_i = \frac{\sigma_{max}}{\sigma_c} \qquad (1)$$

Equation 1: Damage index expression used for calculating stress induced failure.

Where σ_{max} is the maximum tangential stress on the boundary of excavation and σ_c is the uniaxial compressive strength.

Table 4 denotes fall of ground damage scale occurring in underground mine (Duan, 2016). The rock damage scale was established based on case history data (Mikula, 2013).

Table 4: Rock damage scale used to classify the case history data (Mikula, 2013, Duan, 2016).

Rock Damage Scale (RDS)	Tonnes Displaced	Rating	Operational Implications	Support Damage
R1	Nil	Acceptable	Damage is sufficiently limited that it does not need repair	No damage
R2	1	Acceptable	Damage is sufficiently limited that it does not need repair. Minor damage	Support system is loaded, loose in mesh, plates deformed
R3	<10	Tolerable	Damage requires a level of repair or rehabilitation, however, effort and cost can be tolerated	Some broken bolts
R4	<100	Intolerable	Damage is extensive that effort and cost would be high	Major damage to support system
R5	>100	Intolerable		Complete failure of support system

2.3.1 General ground behavior and failure

Stability challenges occur in underground openings when the excavated rock does not function to its normal state of physical balance (Andreev, 1995). The topic connecting rock strength, stress and rock mass damage contributing to rock mass behavior has been investigated, accepted and advanced the mining rock engineering subject. A few critical references are discussed here.

It is understood that a combination of elements affecting the rock behavior can cause stability problems to take place (Palmström and Stille, 2007). This is determined by several parameters such as the rock mass characteristics, mining induced stress, excavation geometry and rock mass extrinsic parameters. In Hoek and Brown (1980)'s study at Zambian metalliferous mines and gold hard rock mines at South Africa, observed the ground behaviors and connected the ground behavior to various failure modes. The failure types were studied under high and low in situ stresses as a function of the ratio between applied stress (σ_1) and laboratory rock strength (σ_c). Hoek and Brown (1980) recognized high rock stress failure,

structurally controlled failure, swelling rock failure and groundwater induced failure as the four primary types of failure causing underground instability based on the ground behavior. Moreover, the examination found that rock mass brittle fracturing, violent failure mechanisms such as spalling and rockbursts was caused by elevated stresses and low stress involved localized brittle failure of rock and movement of blocks along discontinuities. The low mining induced stresses and negative tangential stresses around the excavations influence structurally controlled failure mechanisms to take place (Kaiser and Kim, 2008). Furthermore, Martin et al. (1999) expanded (Hoek and Brown, 1980)'s concept founded on considerable research work on rock damage mechanisms with respect to failure mode.

The comparison between the mining induced stresses and rock strength by (Kaiser et al., 2000, Gorícki et al., 2004, Kaiser and Kim, 2008) further developed the rock damage mechanism theory. It illustrated that the quality of rock mass regarding the geological strength index (GSI) reduced with continuation of increasing rock damage related to rising stress to strength ratio. The damage index (Di) is described as the ratio rock mass demand regarding the maximum tangential stress (σ_1) to capacity concerning the uniaxial compressive strength (σ_c). The ground behavior around underground excavations is measured and predicted by damage index (Kaiser et al., 2000). Table 5 below illustrates the principal rock mass behavior and failure modes of underground excavations in hard rock (Gorícki et al., 2004). Figure 2 shows the main failure modes in underground excavations (Kaiser and Kim, 2008).

Table 5: Ground behavior type and instability in underground opening for geomechanical planning (Goricki et al., 2004).

Basic behaviour type	Description of potential failure mode/mechanics during excavation of the tunnel/underground mine
1. Stable	Stable rock mass with potential of small local gravity induced falling or sliding of blocks
2. Stable with the potential of discontinuity controlled block fall	Deep reaching, discontinuity controlled, gravity induced falling and sliding of blocks, occasional local shear failure
3. Shallow shear failure	Shallow stress induced shear failures in combination with discontinuity and gravity controlled failure of the rock mass
4. Deep seated shear failure	Deep seated stress induced shear failures and large deformation
5. Rockburst	Sudden and violent failure of the rock mass, caused by highly stressed, brittle rocks and the rapid release of accumulated strain energy
6. Buckling failure	Buckling of rocks with a narrowly spaced discontinuity set, frequently associated with shear failure
7. Shear failure under low confining pressure	Potential for excessive over break and progressive shear failure with the development of chimney type failure, caused mainly by a deficiency of side pressure
8. Ravelling ground	Flow of cohesion less dry or moist, intensely fractured rocks or soil
9. Flowing ground	Flow of intensely fractured rocks or soil with high water content
10. Swelling	Time dependent volume increase of the rock mass caused by physio-chemical reaction of rock and water in combination with stress relief, leading to inward movement of the tunnel/ excavation perimeter
11. Frequently changing behaviour	Rapid variation of stresses and deformations, caused by heterogeneous rock mass conditions or block-in-matrix rock situation of a tectonic melange (brittle fault zone)

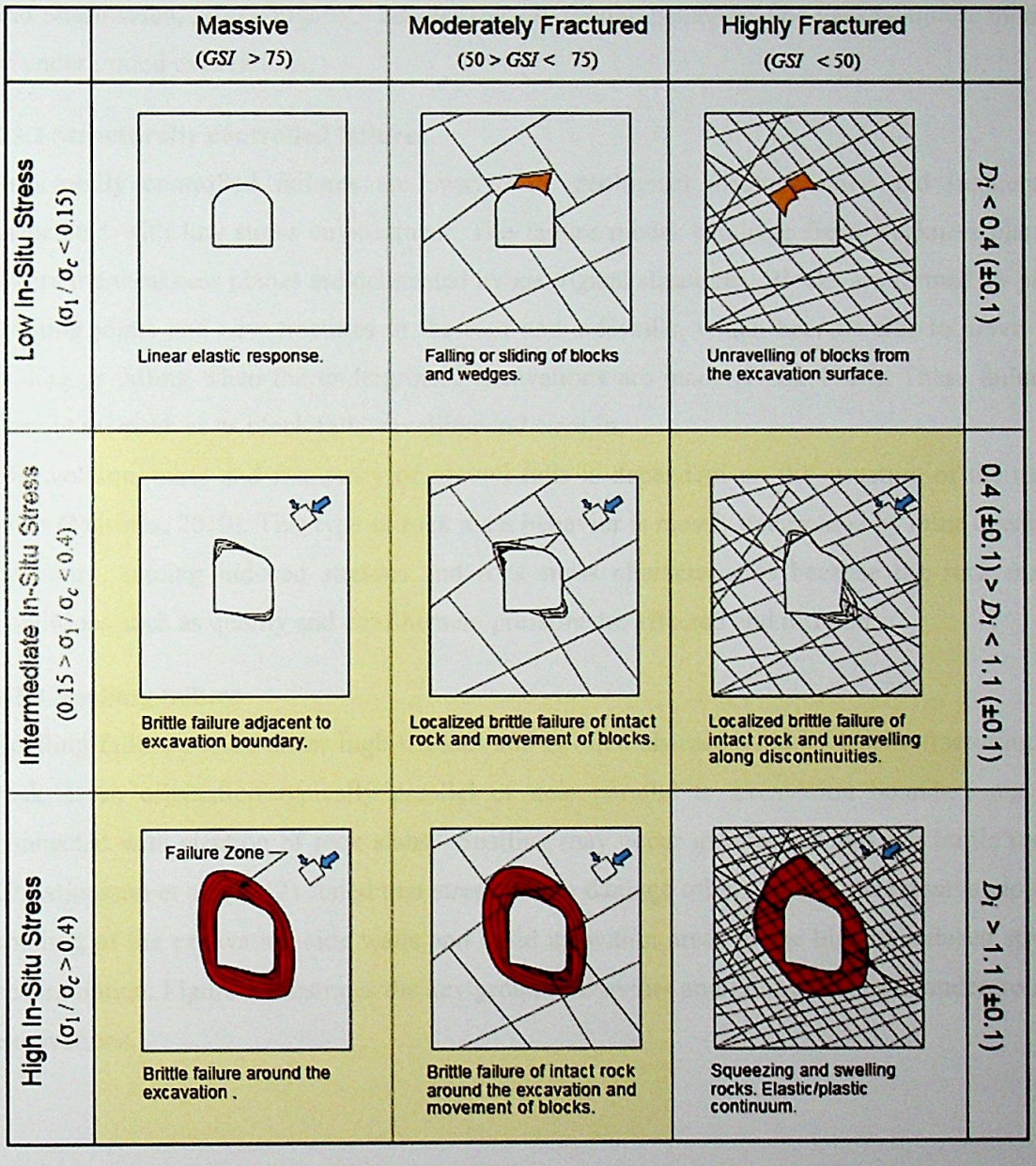


Figure 2: Various modes of failure in underground openings (Kaiser and Kim, 2008).

Martin et al. (2001) further studied the effect of stresses on the rock behavior. Spalling and slabbing failure occurs in massive intact hard rock and high stresses. Ductile failures are anticipated to take place in heavily faulted, foliated and jointed rock mass. Structurally controlled failures occur in rock masses that comprises of many intersecting discontinuities forming blocks that have the potential of falling and sliding into the opening. Figure 3 shows the rock mass failure behavior in underground excavations (Kaiser et al., 2000) and (Rahimi

and Sharifzadeh, 2017). Figure 3 denotes the key ground behaviors and various failure modes in underground excavations.

2.3.2 Structurally controlled failures

Structurally controlled failures are swayed by geological discontinuities and frequently associated with low stress environment. The failure modes originate from weakness planes where the weakness planes are delineated by geological structures. Blocks are formed by pre-existing joints and new fractures in the roof and sidewalls, which become free to move by sliding or falling when the underground excavations are made (Hoek 1980). These failures present themselves as block falls, ravelling and cave-in.

The volume, mass and frequency of ground falls is dependent on the structure of the rock mass (Marinos, 2010). This type of rock mass behavior is mostly determined by mine opening geometry, mining induced stresses and rock mass characteristics because the rock mass conditions such as quality and confinement pressure are affected and different.

2.3.3 Spalling failure

Spalling failure occurs under high stresses and is often characterized by tensile fracturing of rock in an orientation typically parallel or near parallel to excavation boundary and is connected with ejection of rock slabs. Spalling may occur in intact or massive brittle rock. Christiansson et al. (2012) stated that stress driven damage often starts as progressive violent spalling of the excavation side walls and build up within areas of the highest induced stress accumulation. Figure 3 illustrates the key ground behaviors and failure modes in underground excavations.

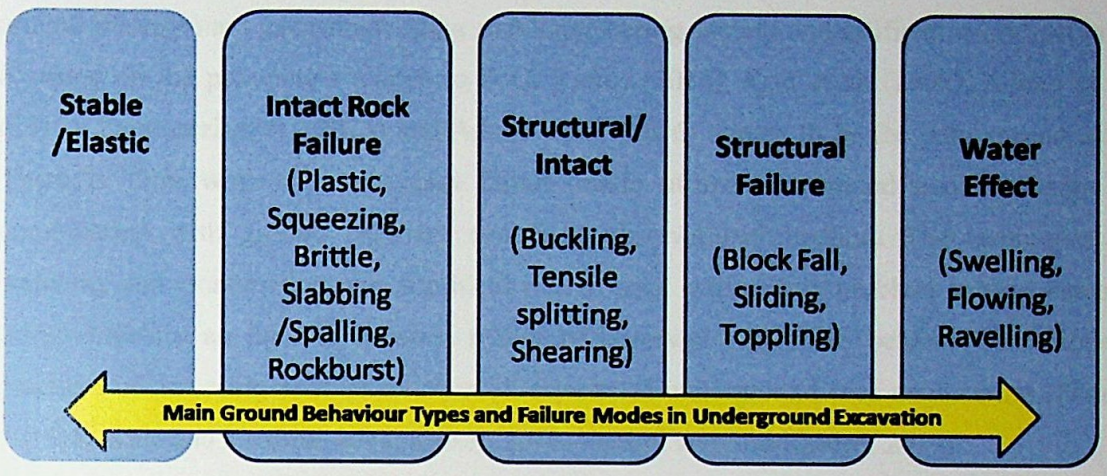


Figure 3: Ground behavior in underground mine opening (Rahimi and Sharifzadeh, 2017).

2.4 Summary

Sinkala and Krishna (2014), Katongo (2005), Koldas (2003), Peng (2015), Rahimi and Sharifzadeh (2017) and Kaiser (2016) have studied and described the mechanisms of fall of ground in underground metalliferous hard rock nickel copper and other metal deposits mines and ground control methods. Katongo (2005) investigated that difference in rock strength and structure, excavation geometry and mining induced stresses leads to alteration of ground conditions which have the potential to cause FoG as well as changes in mining methods. Stacey and Gumede (2007) stated that fall of ground occurs when there is no support, rocks falling between support and inadequate ground support system causing ground falls.

As can be seen from reviewed journals, reports and thesis, rock engineering system, artificial neural network and numerical methods have been used in a wide variety of applications for characterizing the ground behavior and failure mode around underground hard rock excavations. Previous ground behavior investigations methods of the surrounding rock mass in underground openings have been concentrating on the general rock mass behavior, failure mode and ground control. However, the conclusions deduced from the works are widespread. A small number of studies have been reported on the ground behavior, failure mode, ground control and assessment of geohazards resulting from excavation instability in complex geological conditions. There is very little work done on quantification of ground behavior

around underground excavation using rock engineering system and artificial neural network focusing on the parameters related to FoG. Rafiee (2014), Kim et al. (2008), Adoko et al. (2017), Faramarzi et al. (2014) and Adoko et al. (2016) appear to be the only special case. There is little work on rock mass failure mode utilized in ground control design in combination with ground behavior and field observational method. The techniques of watching and examination play a critical role in rock engineering problem solving since it brings together an interval between reality of observed rock mass behavior and modern practices of assuming rock behavior in all aspects of underground rock engineering (Flaten, 2015, Sinkala and Krishna, 2014, Kaiser, 2016, Rahimi and Sharifzadeh, 2017).

Rock engineering practices in underground mining are conducted in complex and unique geomechanical conditions. There is a requirement to evaluate the hazard level associated with that particular rock engineering site. At the present time, there is no literature that have been reported on parameters influencing ground behavior associated with fall of ground and utilizing parameters in underground metalliferous mining ground control designs.
Grounded on a thorough rock engineering context of underground mine opening, numerous factors that influence ground behavior, failure modes and excavation stability have been employed to maintain excavation stability and safety. This study's contribution includes quantifying parameters that influence ground behavior associated with fall of ground and use in ground designs to assess the hazard level. This has practical significance for BCL mine underground openings that experience fall of ground as well as other underground mine engineering setting with corresponding complicated geological conditions and engineering methods.

Chapter 3: Fall of Ground (FoG) Characterization at BCL Mine

3.1 Introduction

As presented in the previous chapters, the main focus of this thesis is the assessment of ground fall characteristics in an underground mine in three different shafts. The BCL mine site will be used as a case study for the thesis and this chapter presents the case study. Firstly, a general description of the mine is given along with location, mining methods, geological and geomechanical data. Field work was conducted to collect FoG data, characterize rock mass and observe FoG events that took place in the mine. In addition the FoG directory is compiled, analyzed and the results are presented in the next sections of this chapter. FoG data was studied using histograms and graphs.

3.1.1 Location of study area

The BCL Mine is located in north-eastern Botswana, approximately 405 kilometers from the capital city Gaborone and 139 kilometers from Palapye, Botswana. Figure 4 shows location of the study area and Figure 5 illustrates location of BCL mine site. The mine manages four shafts, namely Number 2 (Selebi), Number 1 (Phikwe central), Number 3 (South East Extension) and Number 4 (Selebi North) which all mine nickel-copper deposits. Selebi North and Selebi are located 8 km and 15 km south of Number 3 shaft as shown on Figure 5. The copper- nickel ore was magmatically deposited in fractures and openings of the Phikwe complex metamorphic rocks.

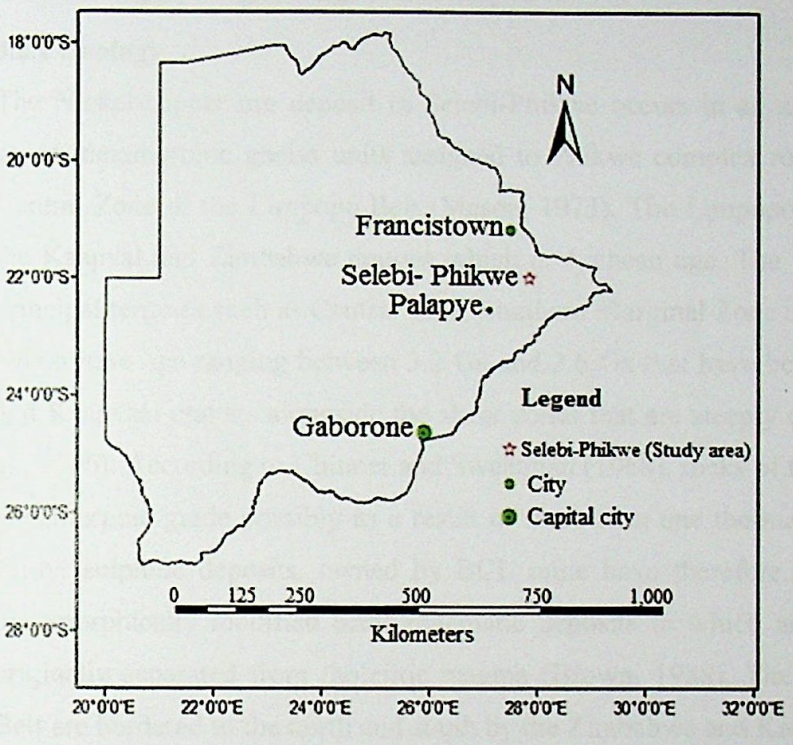


Figure 4: Location of study area.

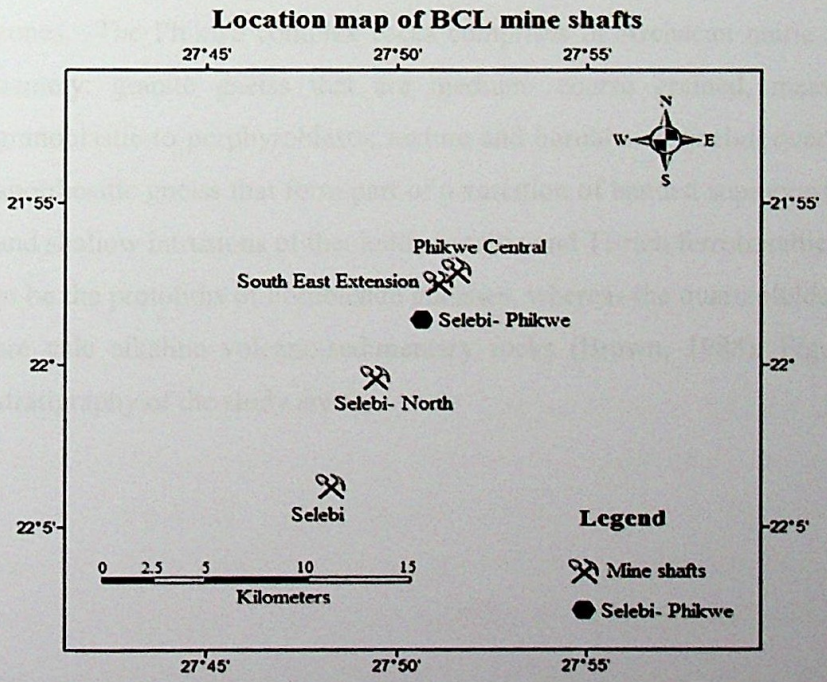


Figure 5: Location map of BCL mine shafts.

3.2 Geo-engineering setting of the study area

3.2.1 Geology

The Nickel-copper ore deposit in Selebi-Phikwe occurs in an area dominated by the high-grade metamorphic gneiss units assigned to Phikwe complex rocks which form part of the Central Zone of the Limpopo Belt (Mason, 1973). The Limpopo Belt is positioned between the Kaapval and Zimbabwe cratons which is Archean age. The Limpopo Belt comprises of principal terranes such as Central zone, Southern Marginal Zone and Northern Marginal Zone which have age ranging between 3.2 Ga and 2.6 Ga that have been accreted onto Zimbabwe and Kaapvaal cratons alongside the shear zones that are steeply dipping and wide (Barton et al., 2006). According to Chinner and Sweatman (1968), rocks of the Central Zone are of high metamorphic grade possibly as a result of more than one thermal event. The Selebi-Phikwe Cu-Ni sulphide deposits, owned by BCL mine have therefore been described as tectono-metamorphically modified ortho-magmatic deposits in which an immiscible sulphide melt originally separated from tholeiitic magma (Brown, 1988). The granulites of the Limpopo Belt are bordered to the north and south by the Zimbabwe and Kaapvaal Cratons respectively. The shear zones and strike slip zones are classified by a high proportion metasediments and highest metamorphic grades. The reworked Granite Greenstone material defines the thrust zones. The Phikwe complex rocks comprises of Archaean mafic and ultramafic intrusions namely: granite gneiss that are medium- coarse grained, massive to weakly foliated, granoblastic to porphyroblastic texture and hornblende gneiss, quartzofeldspathic gneiss and anorthositic gneiss that form part of a variation of banded supracrustal gneisses. The volcanic and shallow intrusions of theoleiitic basaltic and Ti-rich ferrobasaltic constitution are accepted to be the protoliths of hornblende gneisses, whereas the quartzofeldspathic gneisses protoliths are calc alkaline volcano-sedimentary rocks (Brown, 1988). Figure 6 shows the general stratigraphy of the study area.

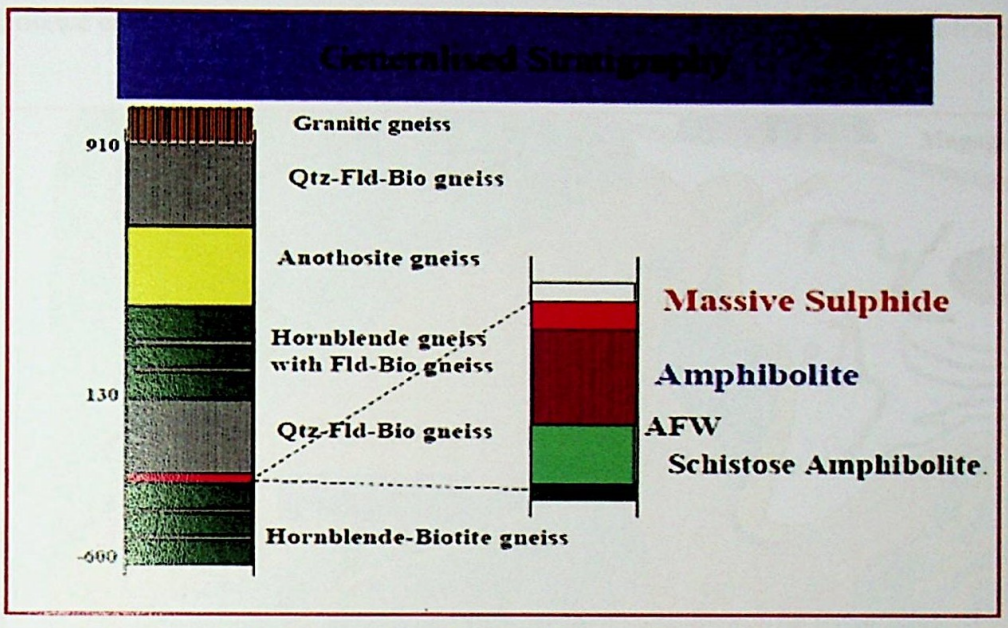


Figure 6: Generalized stratigraphy of BCL mine (Gallon, 1986).

3.2.2 Structural geology

Structural geology in BCL is mainly characterized by rocks that have been deformed by shearing and folding events. Intense folding and shearing occurrence produced ore bearing intrusions that are relatively thin (Lear, 1979). High horizontal stresses are due to different geological environments and the influence of geological structures and regional tectonic forces. McCourt et al. (2004) suggested that dykes, faults and regional shear zones are evidence of geological structures showing the region has been exposed to tectonic deformation. Geological structures are caused by constructional, high grade metamorphism where the fold axis and foliation is parallel to lineation. Van der Heever et al. (2014) stated that the rocks that have been overworked by faults and dykes are characterized by prominent foliation. High grade deformation events are categorized by coarse-grained granoblastic mineral textures and a coarse gneissic layering in which the fold axis are parallel to mineral lineation. Fold structures which occurred at a later stage covering the dominant mineral lineation are folded. These typical deformation events are witnessed in Selibe-Phikwe sulphide ore bodies that have been dismembered, isoclinically folded and sheared the original host of the sulphide body (McCourt et al., 2004). Mining activities provides evidence of the host and the sulphide ore bodies being complicatedly folded. The structural geology of the

Phikwe complex and location of ore bodies of the various mine shafts are illustrated in Figure 7.

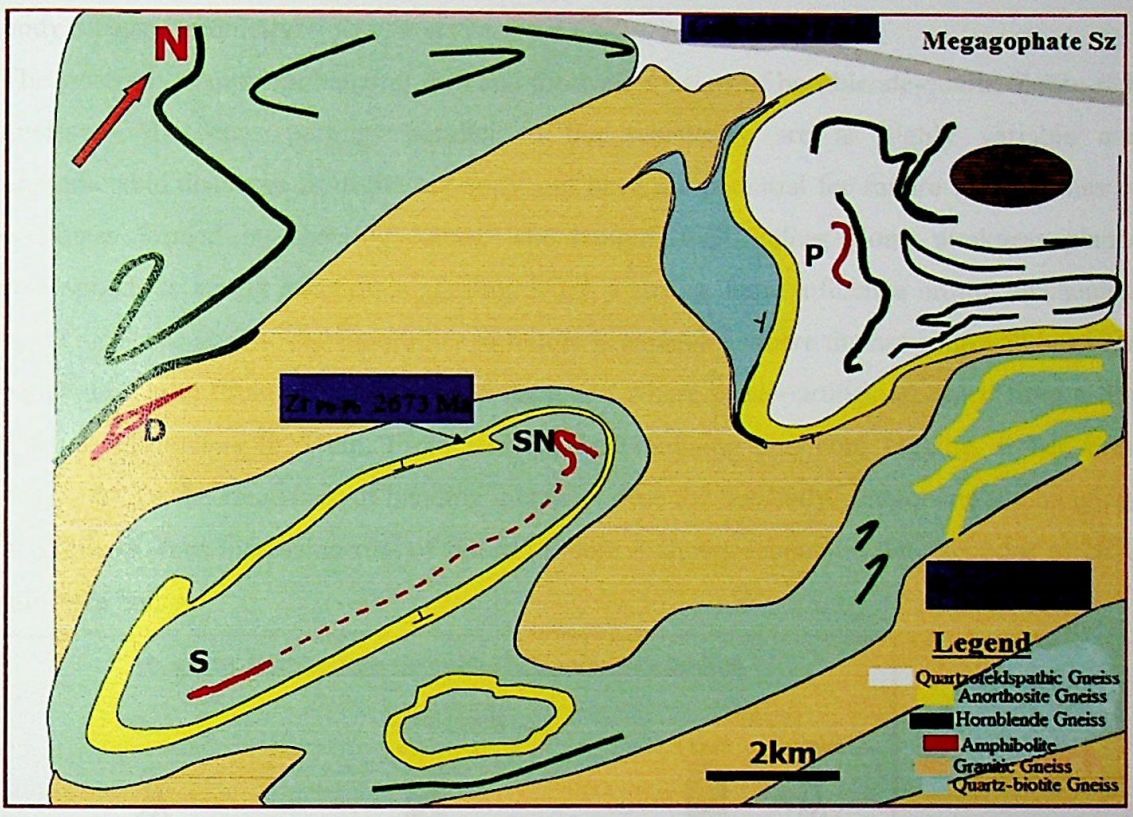


Figure 7: Position of BCL mine ore bodies and geology of the area modified after (Gallon, 1986).

Where P – *Phikwe, SN - Selebi North, S – Selebi, D - Dikoloti*

3.2.3 Ore body

The ore body is essentially a strata bound sulphide body occurring as amphibolites sill confined within the structurally complex biotite, quartz-biotite, and hornblende rich gneisses (Key, 1976, Gallon, 1986). The ore body is generally homogeneous and has a tabular geometry. Mineralization is hosted by amphibolites as massive, semi- massive and disseminated sulphides. The Selebi and South East Extension ore bodies strikes almost northeast-southwest, generally dips 32°- 58° towards the west/ north west with an average dip of 46° at Selebi and 37° at South East Extension as shown in Figure 8. The Phikwe Central ore body dips at 10°- 15° to the west, northwest with an average dip of 12°. The thickness of the ore-body varies from few meters to as much as 33 m, but the average thickness is around 5 m hence, 77 % of the ore body is less than 6 m thick. The structural interpretation of the

deposit and choice of appropriate mining method have been complicated by the three phases of folding that have occurred affecting the area. Mining challenges are created by variable ore body dips and geometry.

The generally competent hanging wall and footwall consists of hornblende-quartz-biotite-rich gneisses. Micaceous partings parallel to the schistosity are at highly variable and unpredictable distances from the ore-body and have the potential for failure along planes of weakness formed by shearing forces. The hanging-wall failing along weakness planes corresponds to strong foliation suggesting it has a strong, huge influence on the mechanical behavior of the gneiss. The possibility of failure is expanded where the hanging-wall has been penetrated up to these planes or beyond them and where these partings are thick from a few tens of millimeters to 5 cm. From underground mapping and core logging, it has been observed that the frequency of banding increases near the ore-body contact and the hanging-wall gneiss, thus increasing risk of failure. Figure 8 shows schematic long sections of BCL mine ore bodies.

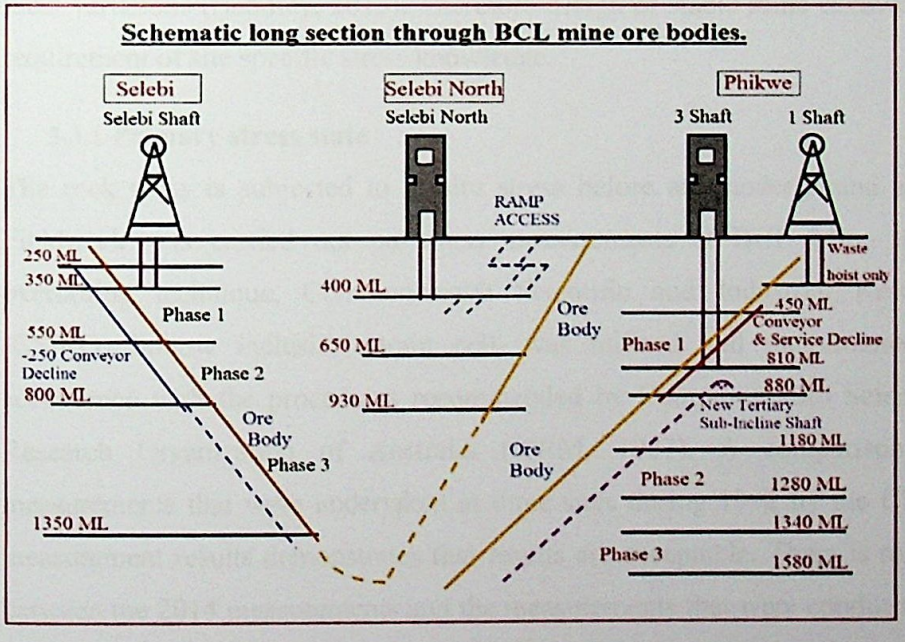


Figure 8: Schematic long section through BCL mines ore bodies (Maswebe, 2011).

3.3 The stress field around BCL mine and other mining districts

It is essential to have knowledge of the magnitude and orientation of in-situ stresses prior and after the rock mass has been disturbed by engineering activities to optimize rock engineering

design. The stresses in the rock mass could be classified into two main categories: primary (or virgin) stresses and secondary (or induced) stresses. Primary stress refers to the stresses in the rock mass that occur prior to any engineering work taking place. In other words, this state of stress is referred to as in-situ stress. The other stress form is the secondary stresses that are induced by the engineering works in the rock mass. Stress vocabulary used currently was suggested by Amadei and Stephansson (1997) founded on propositions from several authors (Fairhurst, 1986, Brown and Windsor, 1990, Zoback and Healy, 1992).

Variation in the stress regime was demonstrated by (Stacey and Wesseloo, 1998) who compiled a database of stress measurements in the South African mining industry. An evaluation of previous in-situ stress measurements, indicate that the magnitude and orientation of in-situ stresses can vary significantly across different mining districts and also within different geotechnical areas on a mine (Sellers et al., 2002). Proximity to mining, faults, dykes and joints and variation in host rock can influence the virgin stress regime and cause local variations (Handley, 2013). Therefore design of stable mine excavation is based on the requirement of site specific stress knowledge.

3.3.1 Primary stress state

The rock mass is subjected to in situ stress before any underground activity takes place. Fieldwork was carried out on stress measurements at BCL Mine in 2014. A proven overcoring technique, Commonwealth Scientific and Industrial Research Organization (CSIRO) hollow inclusion strain cell, was utilized and measurements were taken in accordance with the procedures recommended by Commonwealth Scientific and Industrial Research Organization of Australia (ISRM, 1987). A comparison of in-situ stress measurements that were undertaken at three sites during 1992 by the CSIRO and the 2014 measurement results demonstrates that results are acceptable. There is reasonable agreement between the 2014 measurements and the measurements that were conducted by the CSIRO in 1992. These results are appropriate for use as input into numerical methods of mine design.
BCL mine is characterized by the horizontal stress field, which has an influence on the mine planning. After compilation of the measured stress (Van der Heever et al., 2014), the results indicated large scatter of the stress levels at different depths and locations. According to Sellers et al. (2002) and Handley (2013) the factors that probably influenced variation in

stress measurements outcome are due to the inconsistency of the pre-mining stress tensor in the upper crust, the geomechanical factors such as varying rock properties, the presence of unidentified geological structures such as sills, dykes, faults and the ubiquitous joint sets near the measurement site along with added mining induced stresses and human error from the input data and analysis process.

The orientation and magnitude of the principal stresses in BCL mine are summarized in Table 5, which is the conclusion of the work conducted by (Van der Heever et al., 2014). These in-situ stress data has also been widely used in different geomechanical studies in BCL. The vertical stress can be estimated as the product of the depth and the unit weight of the overlying rock mass. Many computations of vertical stress worldwide at different Civil and Mining engineering grounds verify that this relationship is well founded. This stress is approximated from Equation 2 shown below:

Equation 2: The vertical stress estimation expression.

$$\sigma_v = \gamma z g \qquad (2)$$

Where σ_v is the vertical stress (MPa)

γ is the unit weight of the overlying rock (MN/m^3)

z is the depth below surface (m) and

g is the gravity acceleration ($9.81\ m/s^2$)

Measurements of horizontal stresses at varied mining and civil engineering areas internationally illustrates that the k ratio in Equation 3 tends to be high at shallow depth and that it decreases with depth (Brown and Hoek, 1978, Herget, 1988). The horizontal stress is estimated from the following relationship (Equation 3):

Equation 3: The horizontal stress approximation relationship.

$$\sigma_h = k\sigma_v \qquad (3)$$

Where σ_h is the horizontal stress (MPa)

k is the ratio of the average horizontal stress to the vertical stress

σ_v is the vertical stress (MPa)

The in situ stress measurements carried out at BCL mine are shown in Table 6. The direction and magnitude of principal stress are also illustrated in Table 6.

Table 6: Summary of stress components at BCL mine (Van der Heever et al., 2014).

Principal stress	Magnitude (MPa)	Plunge (°)	Direction
Major principal stress (Sigma 1)	40	13	South- Southwest
Intermediate principal stress (Sigma 2)	19	62	East
Minor principal stress (Sigma 3)	10	24	Northwest
K_{max}	2.1	-	
K_{min}	0.6	-	

3.3.2 Mining method

The techniques applied for the ore extraction at BCL Mine is the down dip open stope mining, sublevel open stoping, bord and pillar, and cut and fill mining method. In Phikwe central number 1 and 3 shaft, the mining method employed is bord and pillar in shallow, near horizontal dipping orebody, and cut and fill is applied in steeply dipping orebody, with sand and waste rock employed as backfill. In the Selebi and Selebi North shafts, the mining method in application is called sublevel open stoping (SLOS). Down dip open stoping is the mining method in operation at South East Extension and in some sections of Selebi mine.

A significant amount of ore dilution from unstable waste rock, corresponding to the weak rock mass conditions found at this mine, is associated with this SLOS mining method where the hanging wall is left unsupported. It is necessary to foresee the ground behavior for controlling and averting ground falls and stope dilution. The evaluation of engineering behavior of the rock mass is determined by adequately characterizing the rock mass. Characterizing rock mass is a challenging task especially in BCL mine where the rock mass is tectonically disturbed, highly faulted and sheared complex rock mass which represents unique geo-engineering conditions. Due to the nature of this research, the focus of the case study has been on the mining operations in the South East Extension, Selebi shaft and Phikwe central

shaft where most of the instability problems manifesting as FoG are experienced by the mine in various sections.

3.4 Characterization of FoG data

3.4.1 Compiling a FoG database

In order to describe the characteristics of the FoG event, a database containing the FoG size along with some of its influencing parameters was established. The fall of ground directory at BCL mine from 14th February 1995 through 2016 covering a 21 year period of ground falls was used as the main source of information for this study. The study findings are limited to the information reported as well as data available from the BCL database. Furthermore, FoG observations from the field for the events that occurred during the mine visit were employed to supplement this FoG data analysis work. Although mine operators are not required to list contributory factors, these data are often reported in the narratives, which offer brief summaries that typically identify the location and size of the falls and may provide other information. The documented FoG has happened in different mine shafts.

For BCL mine case study, thirteen parameters were selected as they were considered to be important in contributing to the complex nonlinear characteristics of the ground behavior in different mine openings. The choice of these parameters was dictated by the available data and recent published works (Adoko et al., 2016). The 13 parameters were categorized into three groups, namely: the rock mass characteristics, excavation geometry and engineering methods. The rock mass characteristics group consisted of rock type (X_1), rock structure (X_2), discontinuities (X_3), uniaxial compressive strength (X_4), cohesion (X_5) and friction angle (X_6). Excavation type (X_7), excavation depth (X_8), excavation width (X_9) and excavation height (X_{10}) represented the excavation geometry group parameters. The engineering methods group was represented by the excavation method e.g. use of blasting (X_{11}), unsupported span (X_{12}) and the implemented mining method (X_{13}). The FoG mass (X_{14}) represented the ground behavior index output parameter. All the parameters accepted to be affecting the ground behavior associated with FoG at BCL mine for this investigation were included and properly considered. The parameter importance will vary with rock mass characteristics, excavation geometry and the engineering methods at specific investigation site. In the selection of those parameters it has been found beneficial to combine those parameters from various groups

which have an effect on the ground behavior. Cai et al. (2004) stated that integration of various factors can be identified to be influencing ground behavior. Therefore the behavior of rock mass surrounding BCL mine openings is a function and result of the primary important parameters mentioned above. The most significant parameter on this research is the discontinuities. Geological discontinuities are a key factor in the failure mode and stability of rock around mine openings. The properties of discontinuities affect the engineering behavior of the surrounding rock masses causing wedges or blocks to fall from roof and sliding out of the walls.

In total, 129 datasets were compiled for the FoG database. Compilation of Fog data was based on field data collected and available data at BCL mine. The quality of BCL data sets was improved by removing the data which had missing parameters, reducing the number of FoG recorded from 590 to 98 data sets. The 95 data sets were incorporated in author's 34 FoG field data sets to make a total of 129 data sets. The fall of ground data collected was organized using Microsoft Excel spread sheet and plotted on graphs and histograms to view the averages and distributions of fall of ground dimensions that were recorded in the FoG directory and reported. A sample of the raw data from the FoG database is shown in Table 7.

Table 7: Raw data sample.

Data	X_1	X_2	X_3	X_4	X_5	X_6	X_7	X_8	X_9	X_{10}	X_{11}	X_{12}	X_{13}	FoG
1	Biotite Schist	Blocky	Bedding/ Lamination	40	1.54	24.5	Ramp	450	4	3	False	0	N/A	12
2	Gneiss	Blocky	Joint	185	32.8	51	Drive/ Haulage	810	5	3	True	0	N/A	350
3	Gneiss	Blocky	Joint	185	32.8	51	Stope face	750	8	3.1	False	0	Cut and Fill	5
4	Amphibolite	Bedded	Bedding/ Lamination	155	8.40	33	Stope face	810	1.7	2	False	3	Open Stoping	1740
5	Massive Sulphide	Fractured	Contact	130	8.50	32	Stope face	810	12	3	False	1.5	Cut and Fill	53
6	Gneiss	Blocky	Joint	185	32.8	51	Ramp	810	3	3	True	0	N/A	25
7	Massive Sulphide	Massive	Joint	130	8.50	32	Stope face	750	11	3.5	False	3	Cut and Fill	4.5
8	Hornblende Schist	Bedded	Bedding/ Lamination	40	1.54	24.5	Ramp	750	4	3.5	False	1	Other	8.1
9	Gneiss	Blocky	Fault/ Shear	185	32.8	51	Stope face	810	20	3	False	2.5	Cut and Fill	12
10	Massive Sulphide	Massive	Fault/ Shear	130	8.50	32	Stope back area	767	13	4.9	True	1	Room and Pillar	20
11	Massive Sulphide	Massive	Joint	130	8.50	32	Stope area	810	15	3.5	False	0	Development	1680
12	Mineralised Amphibolite	Blocky	Joint	155	8.40	33	Stope face	820	12	3.5	False	3	Cut and Fill	24
13	Gneiss	Blocky	Joint	185	32.8	51	Drive/ Haulage	810	5	3	True	0	N/A	12

3.4.2 Analysis of FoG

The FoG data analyzed from different mine shafts that have experienced the events included examining the elements influencing FoG. An analysis of the excavation width is represented in Figure 9 and can be realized that excavation width of 14 m-16 m is the most popular FoG event in Phikwe Central shaft and excavation width of 6 m-10 m and 14 m-18 m in Selebi stopes.

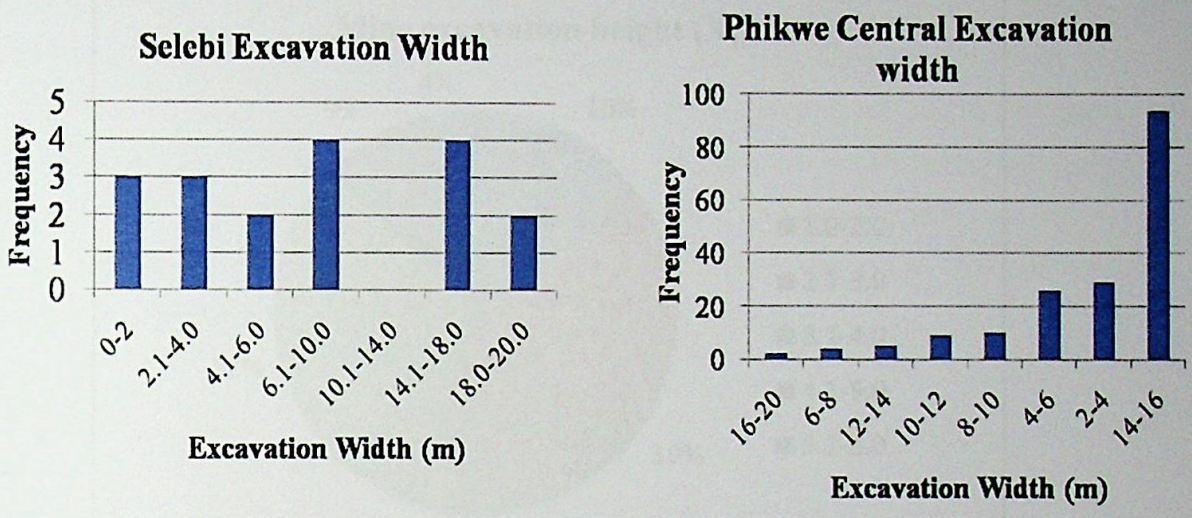


Figure 9: Various excavation width (X_9) at Selebi mine (left) and Phikwe Central mine (right).

From Figure 10 it is noticed that the multitude of mines have an excavation height from 2.1 m to 3 m which forms 39% of ground falls. At Selebi shaft, down dip open stoping mining technique is used with the usual excavation height of 3 m- 4 m, at South East Extension mine shaft several excavation height lie in the range of 1 m- 2 m and at Phikwe central shaft the frequent excavation height is 2.1 m- 3 m where cut and fill is mainly utilized. The excavation heights documented in the FoG data varied mainly due to different mining methods employed as shown in Figure 11. It is noted in Figure 11 that multitude of mines have an excavation height from 2.1 m to 3 m which forms 39% of ground falls.

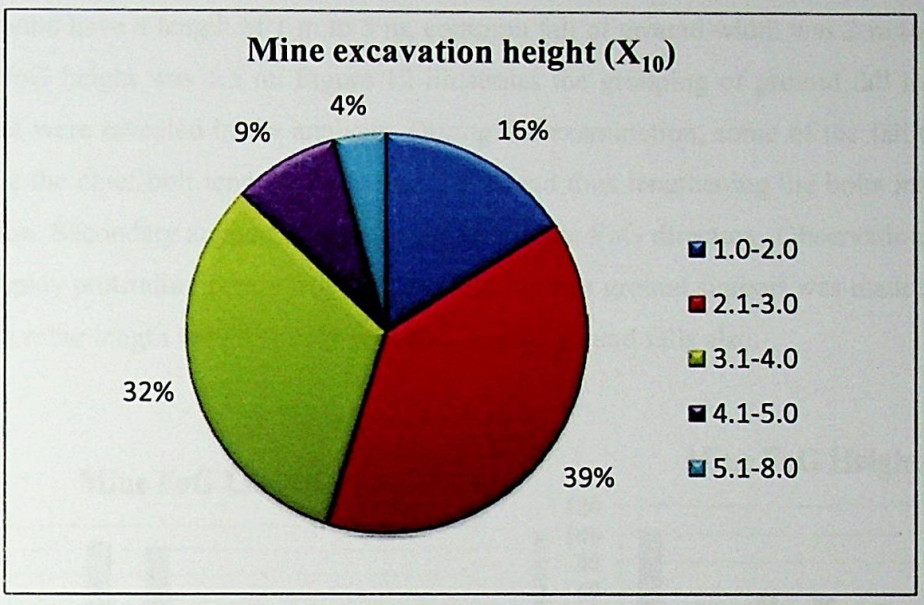


Figure 10: Different excavation heights (X_{10}) in the mine.

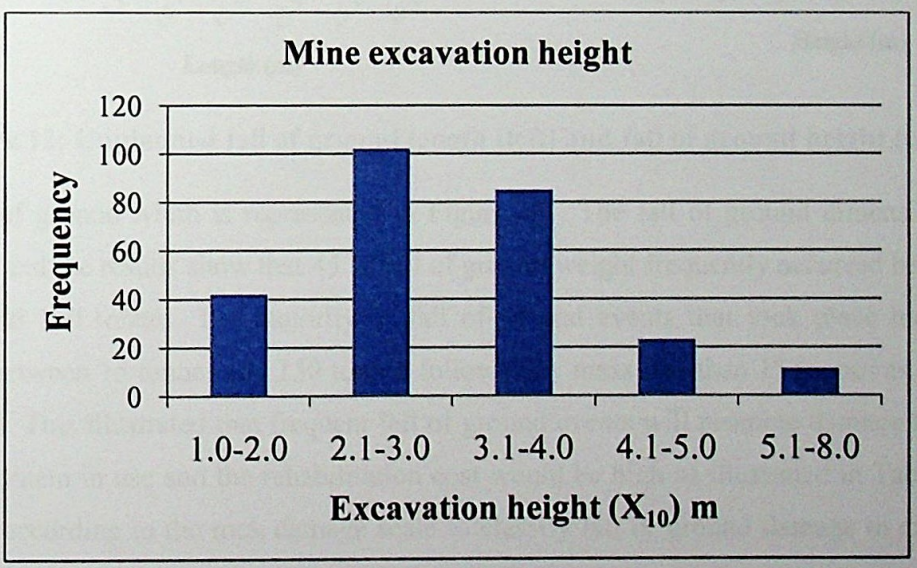


Figure 11: Mine wide excavation heights (X_{10}) distribution.

3.4.3 Unplanned fall of Ground Evaluation

Fascinating results were uncovered by surveying fall of ground data. According to the gathered data, it showed that numerous fall of ground thickness was less than 0.5 m; several

fall of ground have a length of 1 m to 5 m, common fall of ground width was 2 m to 4 m, the average FoG height was 1.5 m. Figure 12 illustrates the grouping of ground fall length and height that were revealed in the analysis. During the examination, some of the fall thickness was above the chief bolt length of 2 m and 2.4 m and thus lengthening the bolts may not be the solution. Secondary support was recorded also in the FoG directory. Observations of FoG events display protruding rebars from the roof hinting that ground support was inadequate and increasing rebar length would simply probably lead to ground falls also.

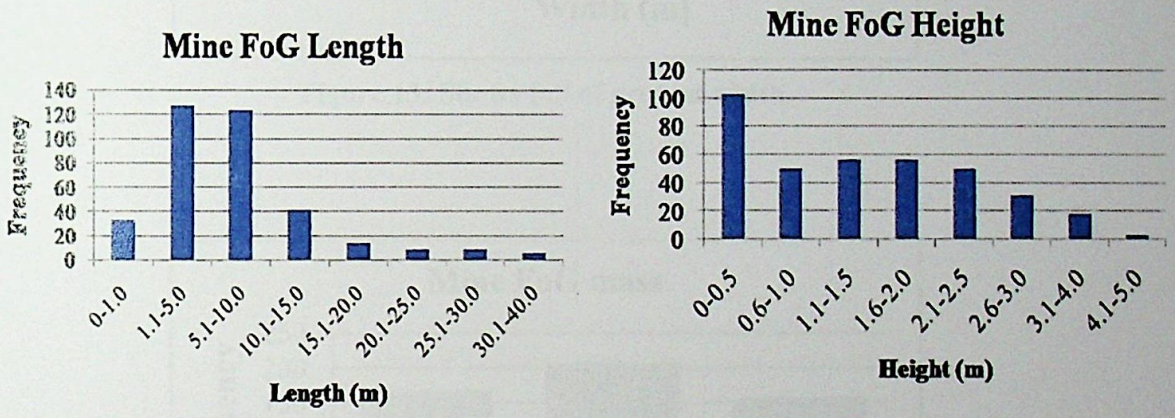


Figure 12: Unplanned fall of ground length (left) and fall of ground height (right).

The fall of ground width is represented in Figure 13. The fall of ground dimensions were analyzed and the results show that 45 % fall of ground weight frequently occurred between 15 tonnes and 150 tonnes. The majority of fall of ground events that took place had weight ranging between 15 tonnes and 150 tonnes followed by mass less than 15 tonnes as shown in Figure 14. This illustrated that frequent fall of ground events will promote damage to ground support system in use and the rehabilitation cost would be high as illustrated in Table 4. It is rated R4 according to the rock damage scale to classify fall of ground damage to excavation (Mikula, 2013, Duan, 2016).

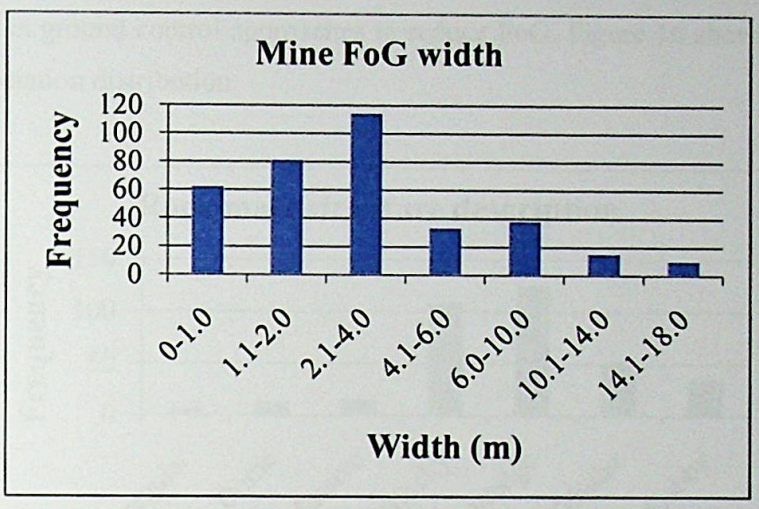


Figure 13: Shows fall of ground width.

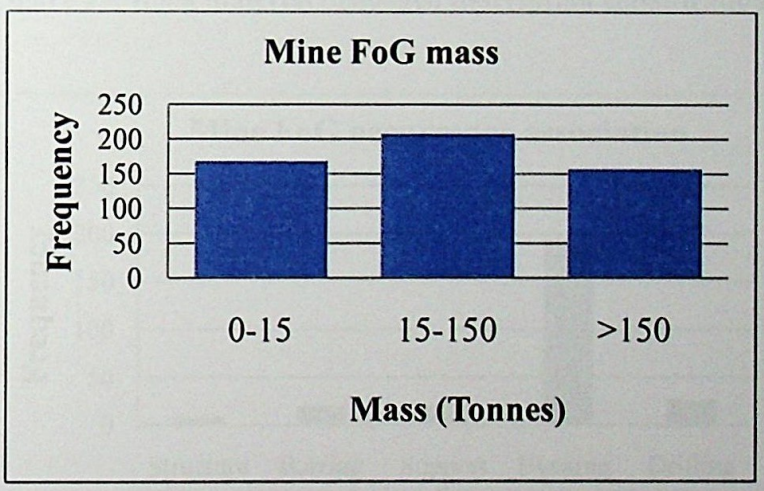


Figure 14: Illustrates unplanned fall of ground weight (X_{14}) distribution in the mine.

Conversation with rock mechanic officers at BCL mine and data analysis indicate that numerous rock material dislodged tend to be mostly wedges and followed by blocks. The rock mass structure was evaluted as massive and blocky. This signals that the failure of the rock mass along geological discontinuities and falls are driven by gravity. The rock material displacement description classification is shown in Figure 15. The FoG occurrence is related to blasting, suggesting that controlled blasting practise is required to minimise the hazards. Blasting is one of the important elements affecting falls of ground. Careful consideration

needs to be put in ground control approaches to reduce FoG. Figure 16 shows fall of ground occurrence association distribution.

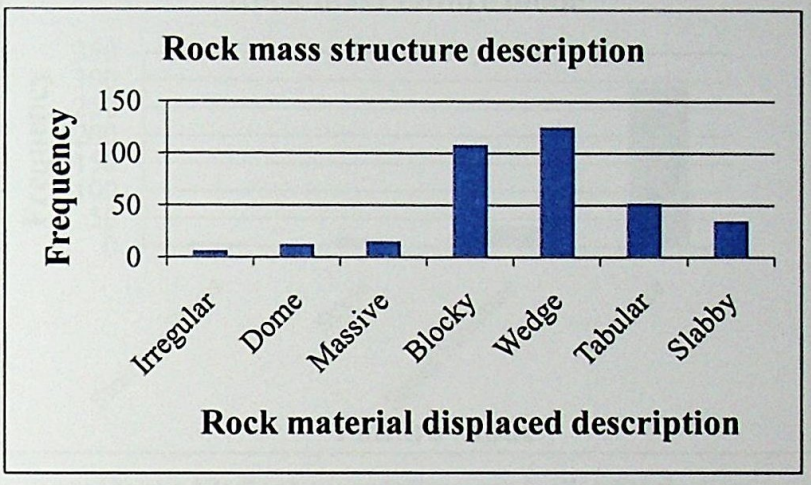


Figure 15: Rock material dislodged description classification.

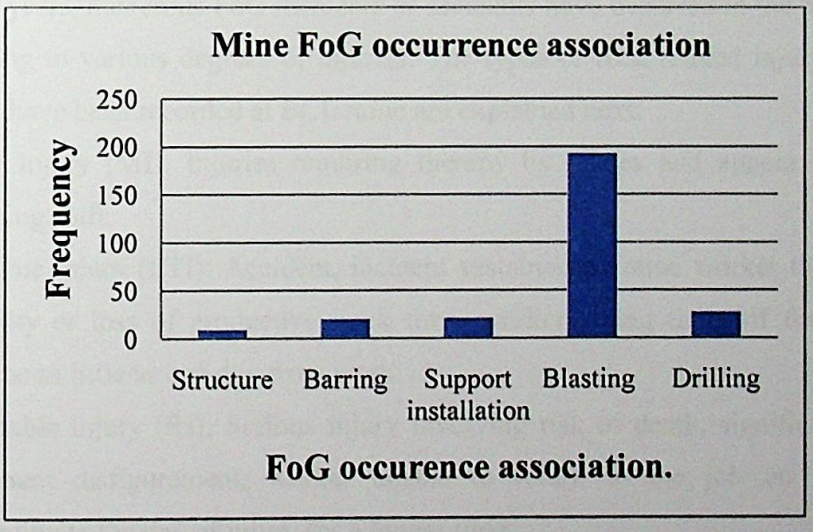


Figure 16: Fall of ground occurrence relation grouping.

From the examination of the rock mass failure mode data in Figure 17, a large number of falls of ground are a result of structurally controlled failure. The observed ground falls commonly develops from shear failure along geological structures. These instabilities can happen due to unfavourable intersection of geological discontinuities near the excavation boundary. The data will be analyzed further using numerical modelling methods to verify the failure modes

occuring in the mine. Figure 17 illustrates failure modes distribution in various BCL mine excavations.

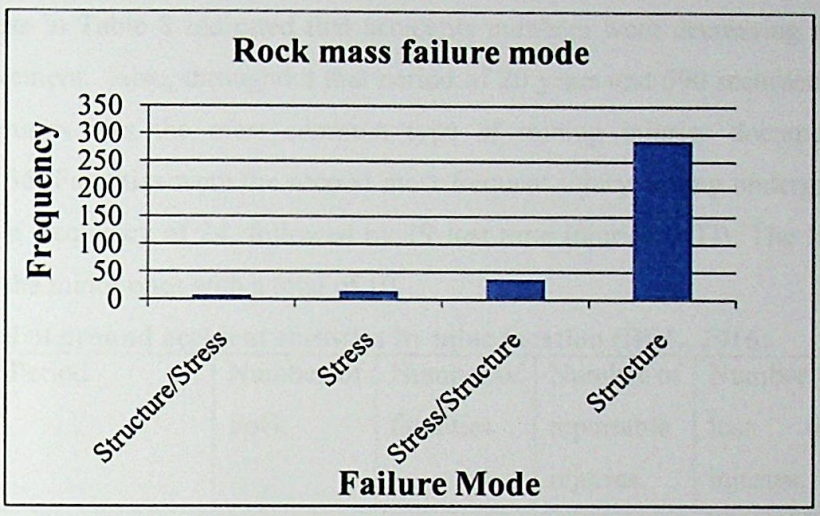


Figure 17: Rock mass failure mode distribution.

3.4.4 FoG accident statistics

Over the past years, numerous FoG incidents or accidents have occurred in the mine affecting workers leading to various degrees of injuries. The types of rock related injury and fatality accidents that have been recorded at BCL mine are explained next:

- Minor Injury (MI): Injuries requiring therapy by nurses and appear for work the following shift.
- Lost-time injury (LTI): Accident, incident sustained by mine worker that resulted in disability or loss of productive work time, worker taking time off for recovery. It could be as little as one day from work.
- Reportable injury (RI): Serious injury involving risk of death, significant degree of permanent disfigurement, worker unable to return to the job on working day succeeding to the day of injury for a longer time.
- Fatality (FI): A death of mine worker resulting from rock related accident.

Table 8 represents the distribution of injuries in spans of 5 years. The statistics shown in the table were gathered from the mines FoG database which were registered by the rock mechanics section. The sums of the instances that are grouped from March 1995 to January 2016 are represented by the total. From March 1995 through January 2016, falls of ground

events have been responsible for 24 fatalities, 36 reportable injuries, 19 lost time injuries and 10 minor injuries, according to BCL mine rock mechanics department FoG database. The grouped results in Table 8 indicated that accidents numbers were decreasing as a result of safety improvement. Also, throughout that period of 20 years and 590 recorded FoG events, reportable injuries was the most common type of mining injuries documented with a frequency of 36. Fatalities were the second most frequent injury among underground miners in BCL with a frequency of 24, followed by 19 lost time injuries (LTI). The least recorded injuries were the minor ones with a total of 10.

Table 8: Fall of ground accident statistics by mine location (BCL, 2016).

Mine Name	Time Period	Number of FoG.	Number of fatalities.	Number of reportable injuries.	Number of lost time injuries.	Number of minor injuries.
South East Extension	Oct 1995- Dec 1999	22	-	4	-	-
	Jan 2000-Dec 2004	52	2	4	2	4
	Jan 2005- Jan 2009	19	-	-	-	-
	Jan 2010-Dec 2013	2	1	-	-	-
Selebi	Mar 1995- May 1999	8	1	2	-	-
	May 2000- Jan 2004	8	-	4	-	1
	Jan 2007- Nov 2009	4	-	-	-	-
	Mar 2010- Jan 2016	9	-	4	-	-
Phikwe Central	Mar 1995- Dec 1999	176	11	10	1	-
	Jan 2000- Dec 2004	139	6	5	7	1
	Feb 2005- Jan 2009	90	2	-	2	-
	Feb 2010- Sep 2015	61	1	3	7	4
	Total (Mar 1995- Jan 2016)	590	24	36	19	10

The results in Figure 18 indicate that over the years, the number of fatalities related to FoG has been decreasing. This could be connected to improvements in ground control procedures and technology, work environment and training of mine workers on ground control. Figure 18 shows the number of fatalities recorded at BCL mine by 5 years period from 1999 to 2016.

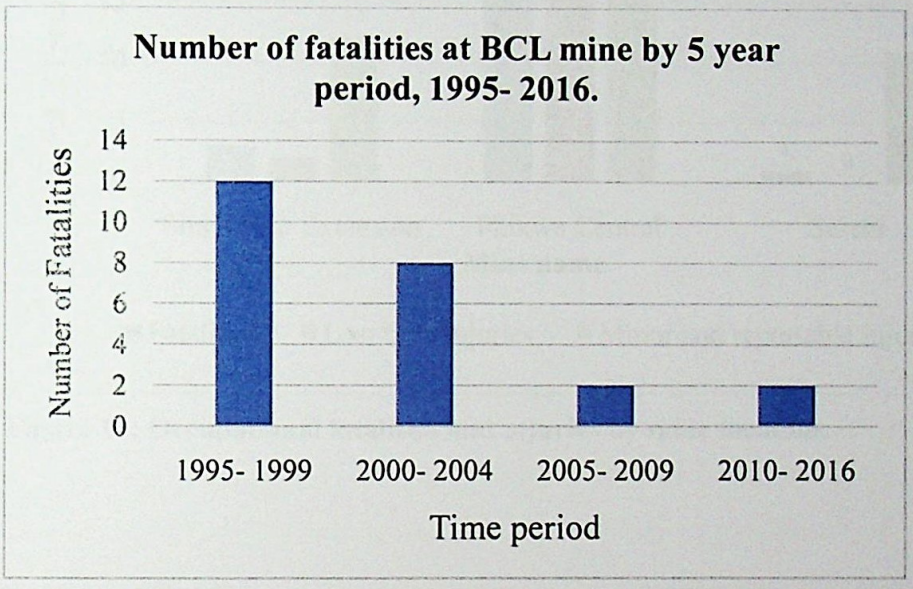


Figure 18: Number of fatalities at BCL mine by 5 year period.

Figure 19 results denote that the mine shaft with the highest number of fatalities and injuries was Phikwe Central which employs cut and fill mining method, followed by South East Extension with the second highest frequency of fatalities and injury of any degree that originated from fall of ground, then Selebi mine shaft. The results illustrated several hazards and types of injuries that underground miners are exposed to in BCL mine. Fall of ground is a common unsafe hazard that they will be working under. Of all the injuries, the cut and fill mining method delineate the highest number of injuries reported, number of fall of ground events, followed by down dip open stoping technique and followed by bord and pillar mining method. Lack of investment in hazards prevention and not changing working culture must be one of the reasons of those injuries. LTIs and Fatalities cause economic loss to mine operations and production stops because of rigorous FoG investigations taking place in the mine.

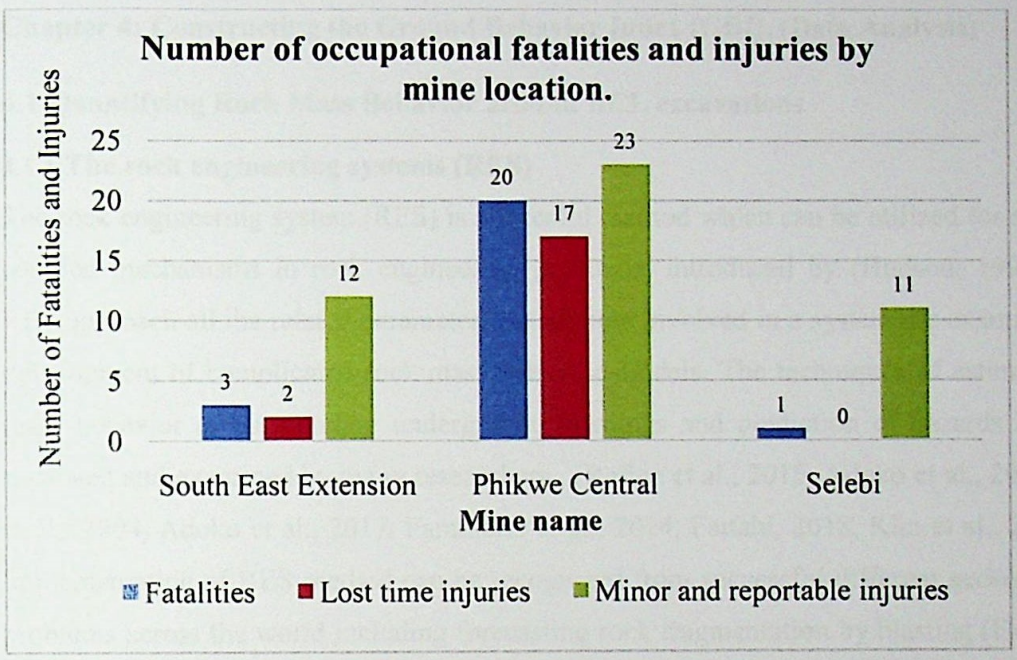


Figure 19: Occupational fatalities and injuries by mine location.

Chapter 4: Constructing the Ground Behavior Index (GBI), (Data Analysis)

4.1 Quantifying Rock Mass Behavior around BCL excavations

4.1.1 The rock engineering systems (RES)

The rock engineering system (RES) is a forceful method which can be utilized for analysis of coupled mechanisms in rock engineering problems, introduced by (Hudson, 1992). In the RES approach all the related parameters and factors involved in a system are examined in the development of complicated rock mass behavior models. The techniques of estimating rock mass behavior of surrounding underground openings and prediction of hazards have been reviewed and examined by many researchers , (Rafiee et al., 2015, Adoko et al., 2016, Zhang et al., 2004, Adoko et al., 2017, Faramarzi et al., 2014, Fattahi, 2018, Kim et al., 2008). The implementation of RES method can be recognized from successful different geo-engineering problems across the world including forecasting rock fragmentation by blasting (Faramarzi et al., 2013), evaluation of coal combustion potential in mines (Saffari et al., 2013), ground behavior and stability analysis of underground excavation (Benardos and Kaliampako, 2004, Lu and Hudson, 1993), techniques of rock fall hazard assessment for tunnel collapse (Shin et al., 2009) and slope stability problems in open pit mines and highways (Naghadehi et al., 2013, Tavoularis et al., 2015), and evaluation of rock mass cavability in block caving mines (Rafiee et al., 2016). Naghadehi et al. (2011) employed RES to survey the importance of factors impacting the rock slope stability. The ground collapse probability in tunneling based on rough set theory and rock engineering system was estimated by improving the Ground Index (Adoko et al., 2016). Kim et al. (2008) employed the RES to calculate the ground behavior index. The rock mass behavior surrounding underground space was evaluated utilizing RES and reviewed the approaches used to develop rock behavior index (Rafiee, 2014).

In the RES method, a given rock engineering situation is treated as a system (whole) where all the involved factors and their influence are considered for the entire situation. The key element of the RES method is the interaction matrix (IM) (Hudson, 1992). The IM is a methodological concept which allows representing correlations among multiple components of a given engineering problem. The principle is illustrated in Figure 20 and uses a cause-effect mechanism that relates every factor of the engineering situation to every other factor

with different weights according to their influence. The IM is constructed by positioning diagonally the subject components, X_i and X_j (engineering concepts, variables, factors etc…). Then, using a clockwise convention, their interactions are represented in the off-diagonal boxes.

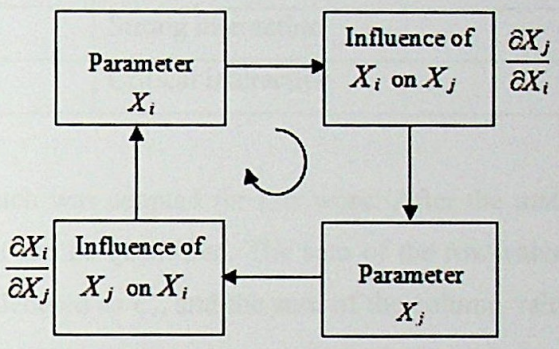


Figure 20: Principle of the interaction matrix (Hudson, 1992).

In Figure 20, the element situated at the right of X_i and above X_j represents the influence of X_i on X_j or the sensitivity of X_i toward X_j which can be represented by the first order partial derivative $\frac{\partial X_j}{\partial X_i}$ (Yang and Zhang, 1998, Naghadehi et al., 2013). For a multiple-dimensional interaction matrix containing n input parameters X_n, a $n \times n$ matrix (i.e. n rows by n columns) is obtained. The next task is usually referred to as the coding of the IM. Since the elements or components of a given Rock Engineering System are not necessarily numerical parameters, it is necessary to assign numerical values to the interactions (off-diagonal components $I_{ij}, (i \neq j)$). A coding method is required to estimate the necessary interactions intensities. The expert semi-quantitative (ESQ) method was developed by (Hudson, 1992) as illustrated in Table 9.

Table 9: ESQ method for interaction intensity coding (Hudson, 1992).

Code value	Description
0	No interaction
1	Weak interaction
2	Medium interaction
3	Strong interaction
4	Critical interaction

The ESQ coding approach was adopted for this work. After the matrix has been coded, the cause-effect interactions can be quantified. The sum of the row values for each parameter is called cause value and denoted as C_i, and the sum of the column values is the effect value E_i (Hudson, 1992).

4.1.2 Artificial Neural Network Background (ANN)

4.1.2.1 Basic concepts of ANN

Artificial Neural Networks (ANN) are sophisticated computer modeling approaches; a network of mathematical models prompted from biological neurons and is widely utilized in modeling geotechnical problems of nonlinear systems, general systems, complex functions and recognition of systems. Nowadays, ANN is regarded as one of the intelligent tools to forecast an output pattern when it identifies given input pattern. The ANN is built to model the neurons in the human brain (Gopalakrishnan et al., 2006). The ANN is a fast and forceful function of information processing that generally is determined by four factors namely: input-output properties of the system units, network topologies, connection weights and neuron thresholds. Basically, the input layer, hidden layer and an output layer form the ANN. Each layer comprises of one or more nodes and these layers are interrelated. Each layer consists of many neurons, regarding the magnitude of the issue to be solved. The user controls the number of neurons and layers in each later, and number of neuron can be used.

Over the years artificial neural network has proved to be a modern tool for analyzing geotechnical problems. Neural networks are mainly characterized by continuous nonlinearity, high parallel distributed processing and generalization capability (Jain et al., 1996). The transfer function, network architecture and learning law form the basic components of the

ANN (Simpson, 1990). Artificial neural networks have been successfully implemented to solve geo-engineering challenges fitting nonlinear functions and recognizing patterns. Success in the mining and civil division is being established by studies including assessment of rock mass collapse potential in tunnels and prediction of rock mass deformation due to tunneling in different qualities of rock mass, prediction of ground fragmentation, prediction of underground excavation stability, tunnel convergence (Mahdevari and Torabi, 2012), rock failure criteria and prediction of blast induced ground vibrations. The implementation of ANN have gained popularity in studies for prediction of uniaxial compressive strength (UCS) of rock samples from hardness test based on input parameters porosity, hardness, density, grain size and rock type formation of the rock sample. The prediction results of the ANN were closer to the measured values of UCS (Meulenkamp and Grima, 1999).

4.1.2.2 Back-propagation neural network

Back-propagation neural network (BPNN) was introduced by (Werbos, 1974) and is the most frequently used ANN type in science and engineering applications. The concept of BPNN is based on searching an error surface utilizing gradient algorithm for points with minimum error. Trial and error techniques is used to assess the number of hidden layers and neurons in hidden layers (Poulton, 2002, Baheer, 2000). In pattern classification, the multi layer perceptron neural network (Rosenblatt, 1958) can only address simple problems and nonlinear functions can be estimated by BP network within a multilayer ANN. The back propagation neural network is widely accepted as the prediction approach used for tunneling works for its ability to map nonlinear systems, its robustness and easy realization which provides the most efficient learning technique for multilayer neural networks. The feed forward back propagation comprises of three layers connected to each other through weights: input layer, hidden layer and output layer which make back-propagation network a multilayer network (Rumelhart and McClelland, 1986). Each layer comprises of neurons, which are elementary processing units. The signals are received by the neurons in the output layer from the other neurons in the input layer and hidden layer in the ANN model. The problem being solved determines the changes in the number of hidden layer and number of neurons in the hidden layer. Many authors have described the structure and operation of ANNs (Ripley, 1996, Fausett, 1994, Demuth and Beale, 1994, Shanin et al., 2001, Sayadi et al., 2013). A neural network generally consists of a layered structure, and each layer contains neurons: Input layer,

one or more hidden layers and an output layer. Figure 21 shows an artificial neural network structure (Fausett, 1994).

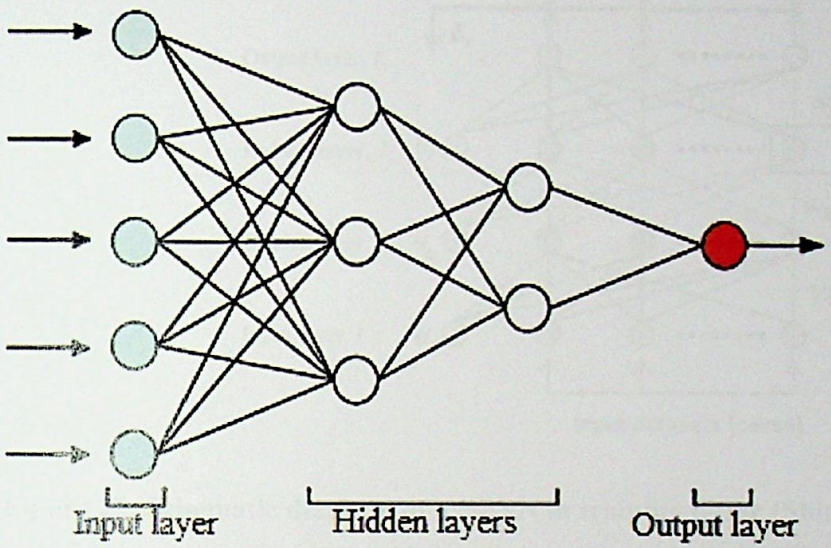


Figure 21: Artificial neural network structure (Fausett, 1994).

4.1.2.3 The first order partial derivatives of a trained Artificial Neural Network

To obtain a quantitative description of cause-effect in a Rock Engineering System (RES), a first order partial derivative of a trained ANN model can be computed (Adoko et al., 2017, Yang and Zhang, 1998, Naghadehi et al., 2013). This allows representing the variations of the output (effect) for small changes of the input variable (cause). In order to achieve better performances, it is recommended normalizing the input data before presenting to the network since they have different dimensions and units (Shin et al., 2009). In this study, a standard feed-forward neural network known as back propagation neural network (BPNN), (the feed-forward back propagation indicates that the network employs a forward activation flow of inputs and an error back-propagation algorithm for training of weight adjustments) is implemented. The back propagation was used to train the network as it is very fast. A schematic illustration of the multi layers BPNN in training phase is provided in Figure 22.

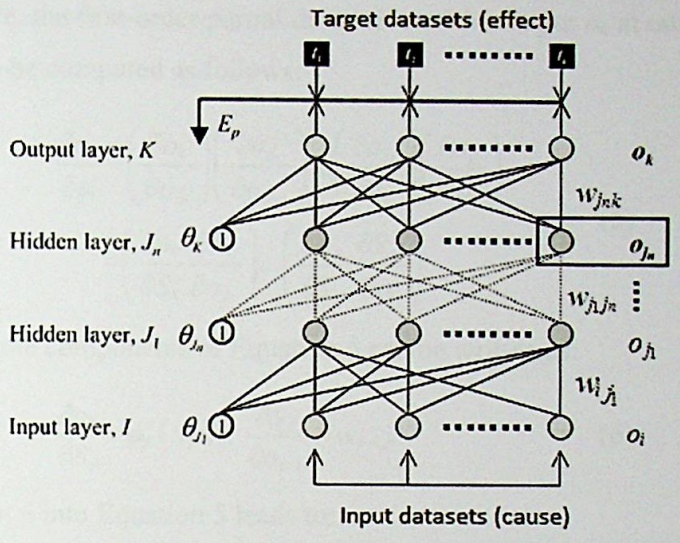


Figure 22: Schematic diagram of a BPNN in training phase (Shin et al., 2009).

The network consists of input layer I fed by input variables (cause), n hidden layers $J_1,\ldots,J_n$ and network output layer K processing the target variables (effect). As it can be seen in Figure 18, a neuron of an input layer transfers the input parameters without any processing to the hidden layers. The input signal S and output o for activation function ϕ at each neuron on the layers I, J_n and K with N_I, N_{J_n} and N_K the total number of neurons, respectively, and with connection weights w adjusted by the threshold θ at all the connections between neurons, are calculated as follows:

$$
\begin{aligned}
& o_{j_1}=\phi_{j_1}(S_{j_1});\ S_{j_1}=\sum_i o_i w_{ij_1}+\theta_i; \\
& \vdots \\
& o_{j_n}=\phi_{j_n}(S_{j_n});\ S_{j_n}=\sum_{j_{n-1}} o_{j_{n-1}} w_{j_{n-1}j_n}+\theta_{j_{n-1}} \\
& o_k=\phi_k(S_k);\ S_k=\sum_{j_n} o_{j_{n-1}} w_{j_n k}+\theta_{j_n}
\end{aligned}
\qquad (4)
$$

In Equation 4 the indices i, j_n and k stand for input units to the input layer, hidden units on the *nth* hidden layer J_n and output units on the output layer K, respectively (i=1,…,N_I , j_n=1,…,N_{J_n} ; k=1,…N_K). w_{pq} is the weight between the *pth* and the *qth* units on the layers. In Equation 4, the weights (w) and the thresholds (θ) are assumed as constants and only the components of the output vector o_k from the units on the hidden layer J_n are variables. By

using the chain rule, the first-order partial derivative of the output o_k at output layer K over o_i at input layer I can be computed as follows:

$$\frac{\partial o_k}{\partial o_i}=\left(\frac{\partial o_k}{\partial o_{j_n}}\right)\left(\frac{\partial o_{j_n}}{\partial o_{j_{n-1}}}\right)\cdots\left(\frac{\partial o_{j_2}}{\partial o_{j_1}}\right)\left(\frac{\partial o_{j_1}}{\partial o_i}\right)$$
$$=\left(\frac{\partial o_k}{\partial S_k}\frac{\partial S_k}{\partial o_{j_n}}\right)\cdots\left(\frac{\partial o_{j_1}}{\partial S_{j_1}}\frac{\partial S_{j_1}}{\partial o_i}\right) \quad (5)$$

Using Equation 4, the components of Equation 5 can be written as:

$$\frac{\partial o_p}{\partial S_p}=\phi_p'(S_p);\quad \frac{\partial S_p}{\partial o_{p-1}}=w_{p-1,p} \quad (6)$$

Replacing Equation 6 into Equation 5 leads to:

$$\frac{\partial o_k}{\partial o_i}=\sum_{j_1}\cdots\sum_{j_n}\phi_k' w_{j_n k}\phi_{j_n}' w_{j_{n-1}j_n}\cdots\phi_{j_2}' w_{j_1 j_2}\phi_{j_1}' w_{ij_1} \quad (7)$$

Equation 7 can be used in the general forward path procedure of a BPNN with multi hidden layers. However, if linear transfer function $\phi(S_k)=S_k$ and the sigmoid functions $\phi_j(S_j)=1/1+e^{-S_j}$; $\phi_j'=S_j(1-S_j)$ are implemented in the BPNN model as in this study, for a four-layer BPNN (with two hidden layer) the first-order partial derivative of the output over o_i at a given input layer I can be expressed as follows:

$$\frac{\partial o_k}{\partial o_i}=\sum_{j_1}\sum_{j_2}S_k(1-S_k)w_{j_2 k}S_{j_2}(1-S_{j_2})w_{j_1 j_2}S_{j_1}(1-S_{j_1})w_{ij_1} \quad (8)$$

Equation 8 is computed using the layer properties (input, weights and biases) which are obtained after training. The partial derivative defined by Equation 8 is an absolute input sensitivity and indicates the expected change in output variable o_k (effects) per unit change of input parameter X_p (causes), holding the other inputs constant. However, in engineering problems, the input parameters usually have different range, dimension and unit; hence it is not advisable to directly use the absolute input sensitivity in comparing with the relative effects of different input parameters on the output variable. Therefore, relative input sensitivity must be defined. But if the normalized data are used, Equation 8 could be employed to express relative input sensitivity with no further operation.

4.1.3 Defining the ground behavior index (GBI).

Using the same approach as in (Adoko et al., 2016), the cause C_i and effect E_j associated with the *ith* parameter P_i for the *ith* row and the *jth* column can be computed as (Hudson, 1992) using the following Equation 9:

$$C_i=\sum_{j=1}^{n}\frac{\partial P_j}{\partial P_i};\ E_j=\sum_{i=1}^{n}\frac{\partial P_j}{\partial P_i} \qquad (9)$$

Where $\partial P_j/\partial P_i$ represents the interactions of the IM; C_i is calculated over *jth* column while E_j is obtained over *ith* row. Accordingly, the interaction matrix defines in a comprehensive way the highly nonlinear relationship among the selected factors controlling the overall stability of the underground excavations. Then, the influence weights assigned to each controlling parameter of the ground behavior can be expressed as the percentage of the sum of the system's cause and effect for such parameters according to Equation 10:

$$W_i=\frac{C_i+E_i}{\sum C_i+\sum E_i}\times\frac{100}{N_{grade}}\times c \qquad (10)$$

Where N_{grade} is the number of grades assigned to the parameter P_i and c is a coefficient to scale W_i between 0 and 100. In this work, 5 grades were used for the parameters, except for rock structure (4 grades), discontinuities (3 grades) and the use of blasting (2 grades) (see Section 4.1.4.1).

The *GBI* describing the hazard level associated with the FoG is computed using Equation 11:

$$GBI=\sum W_i\times V_i \qquad (11)$$

In Equation 11 V_i denotes the rating values assigned to each parameter P_i for the ground behavior evaluation. The values of the *GBI* can range from 0 to 100. A higher value of *GBI* implies a higher hazard level. More details on the methodology could be found in (Adoko et al., 2017, Naghadehi et al., 2013, Adoko et al., 2016).

4.2 Developing the GBI

4.2.1 Dataset preparation

On the basis of the factors influencing the FoG, the parameters selected to compute the GBI include the rock mass characteristics, the excavations geometry, support, and the mining

methods namely: the rock type (X_1), rock structure (X_2), discontinuities (X_3), uniaxial compressive strength (X_4), cohesion (X_5), friction angle (X_6), excavation type (X_7), excavation depth (X_8), excavation width (X_9), excavation height (X_{10}), use of blasting (X_{11}), unsupported span (X_{12}), the implemented mining method (X_{13}) and the GBI output represented by the quantity of FoG. Details of the methodology can be found in (Adoko et al., 2017).

For the rating of these 13 parameters, intervals (classes) were used according to each attribute and each class is rated with values ranging from 0.0 to 1.0 (0.0; 0.3; 0.6; 0.8; and 1.0), except for rock structure (4 intervals), discontinuities (3 intervals) and the use of blasting (2 intervals). Those with qualitative attributes were translated into numerical values using a semi-quantitative encoding (Adoko et al., 2013, Adoko et al., 2016). As a result, the parameters with numerical attributes had their variable spaces divided into 5, 4, 3 or 2 intervals. The ratings were established in such a way that the higher the numerical value assigned to a given parameter, the higher the FoG hazard potential is likely to be. This parameter rating was based on well known rating systems and recommendations (Naghadehi et al., 2013). Table 10 shows the GBI parameter classification ratings.

Table 10: GBI parameter classification rating.

Parameter	Number of classes	Rating
X_1 (Rock type)	5 classes	Gneiss & Amphibolites: 0.0- 0.3
		Massive Sulphide & Mineralized: Pegmatite: 0.3-0.6
		Orebody: 0.6
		Schist: 0.8-1.0
X_2 (Rock structure)	4 classes	Massive: 0.1
		Bedded: 0.4
		Blocky: 0.8
		Fracture: 1.0
X_3 (Type of discontinuity)	3 classes	Lamination: 0.1
		Joint: 0.5
		Fault/Shear: 1.0
X_7 (Excavation type)	5 classes	Ramp/garage: 0.1
		Drive/haulage/pillar: 0.3
		Stope back: 0.6
		Stope ahead: 0.8
		Stope roof: 1.0
X_{11} (Use of blasting)	2 classes	Use of blasting: 1.0
		No use of blasting: 0.0
X_4- X_6; X_8- X_{10}; X_{12}- X_{13}	5 classes	
X_{13} (Mining method)	5 classes	N/A: 0.0
		Development: 0.3
		Room and pillar: 0.6
		Cut and fill: 0.8

Next, on the basis of field observation data FoG events that have occurred in BCL Mine between 1987 and 2015 were compiled. The amount of displaced material (mass) was used to quantify the level of severity of the FoG. It is assumed that the damage caused by a FoG event is directly proportional to its mass.

A three level hazard classification was used namely, hazard level 1 (HL1), hazard level 2 (HL2) and hazard level 3 (HL3) representing, good, fair and poor ground from FoG perspective, respectively. HL1 corresponds to FoG less than 15 tons, HL2 between 15 and 150 tons and HL3 more than 150 tons. By doing so, 108 datasets were selected. Table 11 provides a statistical description of the data.

.

Table 11: Statistical description of the data.

Parameters	Unit	Physical range	Mean	Std. deviation
Rock type (X_1)	Logic	-	-	-
Rock structure (X_2)	Logic	-	-	-
Discontinuities (X_3)	Logic	-	-	-
UCS (X_4)	MPa	41-185	117.2	39.15
Cohesion (X_5)	GPa	1.54-32.8	12.17	9.08
$\varphi(X_6)$	Degree (°)	24.5-51	38	7.5
Exca. type (X_7)	Logic	-	-	-
Exca. depth (X_8)	m	350-930	793.5	42.16
Exca. width (X_9)	m	1.7-20	11.5	4.715
Exca. height (X_{10})	m	2.0-20	3.67	1.53
Blasting (X_{11})	Logic	-	-	-
Unsupported span (X_{12})	m	0-42	3.35	4.55
Mining method (X_{13})	Logic	-	-	-
FoG	Tons	0.05-3640	180	490

4.2.2 Results

The steps that are involved in the calculations of the GBI are explained as follows:

1. Compose the encoding interaction matrix based on the trained BPNN that has been established (Section 4.1)
2. Calculate the causes C_i and effects E_i using Equation 9.
3. Calculate the interaction weights W_i of each parameters using Equation 10.
4. Compute the GBI based on Equation 11.

4.2.2.1 Composing the interaction matrix of the RES

The ANN model was created by importing FoG data into MATLAB, generating a network using *Neural Network tool* function, training, validation and testing. The training datasets described in Section 4.1.4.1 were used to train the neural network in order to get the sensitivity of the GBI parameters on one another. The encoding of the parameters was conducted as suggested by recent research (Adoko et al., 2016) and the Neural Network toolbox of MATLAB, a popular numerical computation software was implemented to compute the interaction matrix of the GBI system. Neural network tool allows you to import, create, use and export neural networks and data.

A network with 2 hidden layers was configured with the *feedforwardnet* function. The network architecture consisted of an input layer (13 nodes), an output layer (13 nodes) and two hidden layers (26 neurons each) as suggested by recent works (Naghadehi et al., 2013). This allows calculating the partial first derivative of each parameter once the training is completed. The traditional Levenberg-Marquardt back propagation algorithm was used, since the training process converges quickly as the solution is approached (Suratgar et al., 2005). The *trainlm* function was selected as it updates weight and bias values as stated by Levenberg-Marquardt. The *Learngdm* learning function was utilized as it accepts several inputs. The datasets were randomly selected and divided into training, validation and testing datasets in the model developed in this study. In order to generate the network, the performance function such as mean square error (MSE), number of layers, number of neutrons and transfer function are chosen. Figure 23 shows the performance of the training given by the mean square error (MSE); the best validation performance was 6.0334e-07 at epoch 145. After a series of training, validation and testing datasets using different network architectures, the optimum network architecture was selected. The model is treated as excellent and optimum because it had the best performance, least Root Mean Square Error (RMSE).

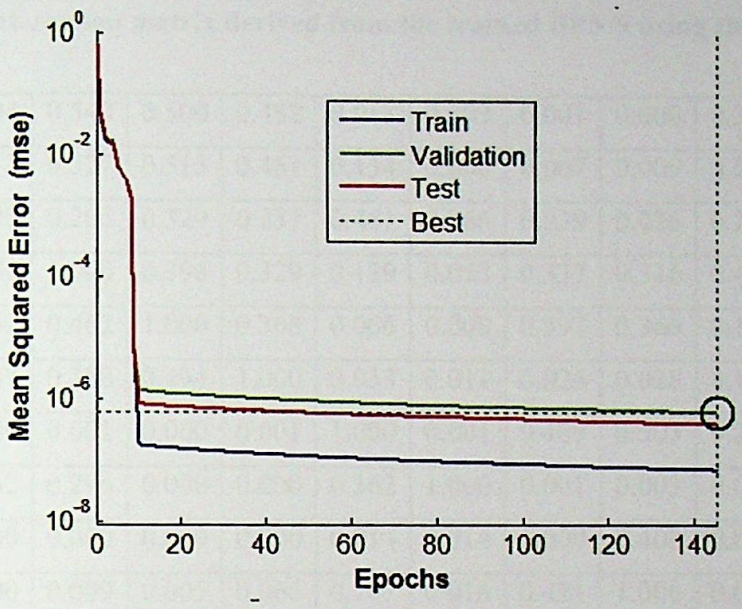


Figure 23: Training performance using the FoG datasets.

The computed components of the interaction matrix are summarized in Figure 23 and were calculated as per Equation 8. The components on the matrix diagonal in Table 12 represent classification categories. Each classification category determined by the trained ANN indicates the partial derivative of itself as 1.0 in Figure 23. Theoretically, a partial derivative of an identical component should always be 1.0. Since every value on the diagonal calculated by the trained ANN is close to 1.0 in Table 12, it can therefore be seen that ANN produced highly reliable partial derivative.

Table 12: The interaction matrix derived from the trained BPNN using the FoG datasets

1.000	0.261	0.494	0.540	0.500	0.488	0.013	0.003	0.001	0.000	0.395	0.512	0.274
0.454	1.000	0.513	0.527	0.513	0.461	0.134	0.000	0.007	0.009	0.274	0.368	0.197
0.500	0.559	1.000	0.205	0.329	0.237	0.461	0.066	0.039	0.026	0.230	0.600	0.528
0.361	0.162	0.184	1.000	0.396	0.329	0.139	0.053	0.337	0.316	0.400	0.366	0.450
0.165	0.011	0.362	0.462	1.000	0.368	0.066	0.008	0.397	0.366	0.118	0.296	0.342
0.145	0.009	0.347	0.388	0.494	1.000	0.053	0.011	0.026	0.028	0.105	0.230	0.273
0.001	0.001	0.000	0.001	0.000	0.001	1.000	0.001	0.469	0.503	0.279	0.404	0.453
0.362	0.362	0.362	0.296	0.000	0.000	0.362	1.000	0.001	0.003	0.000	0.001	0.230
0.003	0.005	0.000	0.000	0.000	0.000	0.014	0.014	1.000	0.408	0.003	0.494	0.001
0.000	0.000	0.000	0.009	0.005	0.066	0.107	0.016	0.421	1.000	0.001	0.379	0.002
0.000	0.000	0.002	0.000	0.000	0.000	0.256	0.000	0.001	0.000	1.000	0.475	0.133
0.000	0.000	0.001	0.001	0.000	0.000	0.268	0.000	0.001	0.000	0.000	1.000	0.007
0.013	0.011	0.039	0.066	0.002	0.001	0.397	0.141	0.353	0.329	0.405	0.529	1.000

4.2.2.2 Calculating the cause and effect

The function of each parameter on the ground behavior is illustrated in the cause-effect diagram in Figure 24. In this diagram the dominant factors in the system are situated in the bottom right section and the subsidiary factors are located in the top left section of the diagram. The cause effect plot is handy in comprehending the interaction degree of each factors and the system as a whole. The points dispersed along the main diagonal line show high degree of interaction, whereas low level interactivity is demonstrated by points distributed perpendicular to cause-effect (C=E) diagonal line (Mazzoccola and Hudson, 1996). From cause-effect diagram the parameters are mostly distributed in the right portion below the C=E diagonal line designating that X_1, X_2, X_3, X_4 and X_5 and are the most important, while X_{12} is the least important in that plot. Parameters X_{13}, X_7, X_6, X_9 and X_{10} spread along the main cause=effect diagonal line in Figure 24, indicates that parameters are interactive and make a good contribution to ground condition assessment .

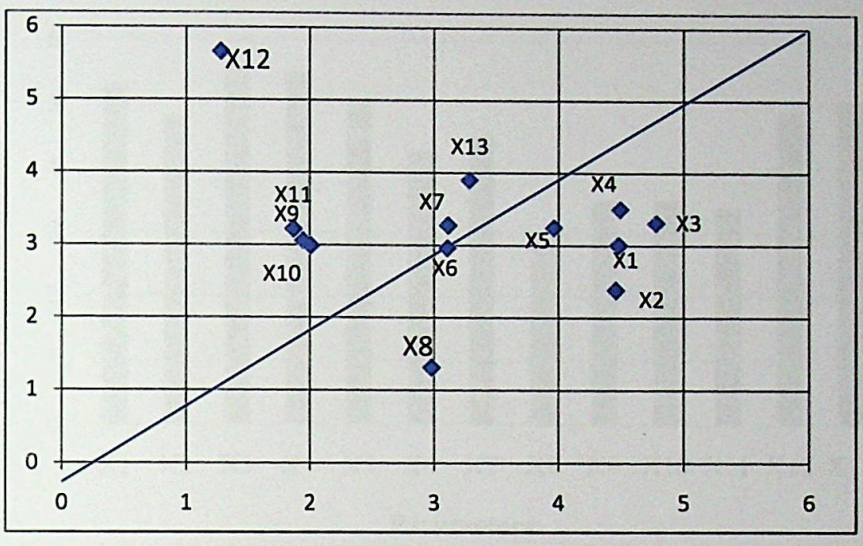


Figure 24: Cause-effect diagram for the GBI system.

Once the causes and the effects are calculated, the parameter intensities $(C+E)/\sqrt{2}$ can be calculated as well to identify the parameters interacting the most in the RES (Adoko et al., 2016). As it can be seen in Figure 25, X_1, X_2, X_3, X_4, X_5, X_{12}, and X_{13} are among the most important parameters of the GBI system. X_8 show low level of interactivity between factors, therefore is the least important parameter in the interactive intensity histogram illustrated in Figure 25.

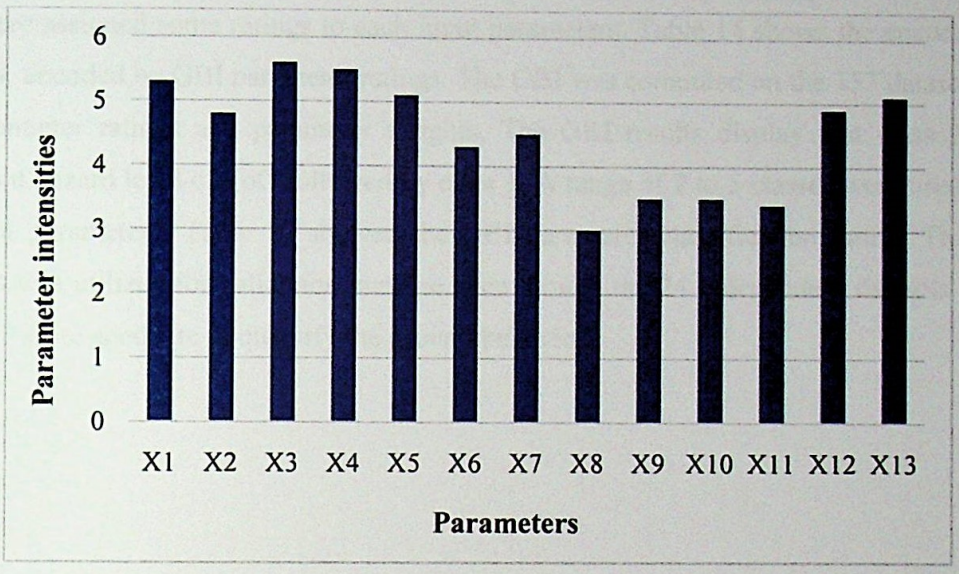


Figure 25: Interaction intensity for the parameters of the GBI.

4.2.2.3 The weights

The ANN is trained with the intention of determining weight values in order to accomplish the best network based on objective function. The network used random weights to compute some outputs using the transfer functions. The network error is acquired by comparing the computed outputs. The errors are minimized by modifying the linking weights using the learning rule. A pattern is presented to the network founded on the training process. The old weights, the node input values, errors and the learning rate are employed to calculate the new weights. Validation and testing are carried out to evaluate the correctness of the model. The calculated weights of parameters are summarized in Table 13 and were computed using Equation 10.

Table 13: Calculated parameter weights for ground behavior.

Parameter	X_1	X_2	X_3	X_4	X_5	X_6	X_7	X_8	X_9	X_{10}	X_{11}	X_{12}	X_{13}
Weight	7.6	8.7	13.7	8.1	7.3	6.2	6.5	4.4	5.1	5.1	12.9	7.1	7.3

4.2.2.4 The GBI values

An additional 157 independent datasets randomly selected which had not been previously used in BPNN training were examined. The 13 parameters that were used to compute the

GBI were assigned some ratings to each input parameters. Table 14 shows the encoded field datasets, encoded by GBI parameter ratings. The GBI was computed on the 157 datasets from the parameter ratings and parameter weights. The GBI results display that class 2 is the dominant hazard level of FoG followed by class 1. A range of 2 to 5 classes were used to rate different parameters. Table 10 showed the GBI parameter classification rating. This large datasets was utilized for validation purpose even though the 24 independent datasets used in Table 13 were adequate to quantify the ground behavior.

Table 14: Calculated GBI with a sample of encoded datasets.

X_1	X_2	X_3	X_4	X_5	X_6	X_7	X_8	X_9	X_{10}	X_{11}	X_{12}	X_{13}	GBI
0,6	0,1	0,1	0	0	0	0	0,3	0,6	0,3	0	0	0,3	14,89339
0,3	0,1	0,1	0	0	0	0	0,6	0,3	0,6	1	0,3	0,6	31,15357
0,3	0,1	0,1	0,3	0	0,3	0	0,3	0,6	0,6	1	0	0,3	31,35097
0,3	0,1	0,1	0,3	0,3	0,3	0	0,3	0,6	0,6	1	0	0	31,35821
0	0,1	0,1	0,3	0,6	0	0,3	0,3	0,3	0,6	1	0,3	0	31,96086
0	0,1	0,1	0,6	0,6	0	0	0,3	1	0,8	0	0,8	0,6	32,01403
0,3	0,1	0,1	0,3	0	0,3	0	0,3	0,6	0,8	1	0	0,3	32,36776
0,3	0,1	0,1	0,3	0	0,3	0	0,3	0,6	0,8	1	0	0,3	32,36776
0,3	0,1	0,5	0,6	0,3	0,6	0,6	0,3	0,3	1	0	0,8	0	38,26211
0,8	0,1	0,1	0	0,3	0	0,3	0,6	0,3	0,8	1	0,8	0	39,27317
0,8	0,1	0,1	0	0	0	0,8	0,6	0,3	0,8	1	0,8	0	40,32349
0	0,1	0,1	0,3	0,3	0,3	0,3	0,3	1	0,6	1	1	0,3	42,30609
0,3	0,1	0,1	0,6	0,6	0,3	0,8	0,3	0,8	0,8	1	0,6	0	47,46431
0,6	0,4	0,1	0,8	0,6	1	0	0,3	0,6	0,8	0	1	0,8	47,8309
0,3	0,1	0,1	0,3	0,6	0,3	1	0,6	0,6	0,8	1	0,8	0	48,02925
0	1	1	0	0	0,3	0	0,6	0,6	0,6	1	0,3	0	48,04067
0	1	1	0	0,3	0,3	0	0,6	0,6	0,6	1	0	0	48,12255
0	1	1	0	0,3	0,3	0	0,6	0,6	0,6	1	0	0	48,12255
0,8	0,1	0,1	0,3	0,3	0,3	0,8	0,6	0,3	0,8	1	0,8	0,3	49,00529
0	0,1	0,1	0,6	0,6	0	0,3	0,6	0,6	1	1	1	0,8	50,05591
0,3	0,1	0,5	0,8	0,8	0,8	0	0,8	0,8	0,8	0	1	0,6	50,39531
0,3	0,1	0,1	0,3	0,6	0,3	0,8	0,3	0,8	1	1	0,6	0,8	51,8862
0	0,4	0,5	0,3	0,6	0,6	0,3	0,6	0,8	0,8	1	0,8	0	52,16159
0	1	1	0	0,3	0,3	0	0,6	0,6	0,6	1	0,3	0,3	52,43146
0,3	1	0,1	1	0,8	1	0,3	0,8	0,8	0,8	1	0,8	0,6	69,06508

The final step is to compute the GBI values which define the hazard level associated with the FoG. To identify these hazard levels, the GBI values are plotted against each corresponding

field observation hazard level to visualize the data trend and the results are provided in Figure 26. Theoretically, the GBI can range between 0 and 100. As explained in Section 4.1.3, the higher the GBI value the higher the hazard level. In this study in particular, the GBI ranges between 14.42 and 72. Next adequate threshold values of the GBI capable of providing objectively a separation between hazard levels is defined through trial and error. The results indicate that three zones (with increasing hazard potential) can be identified with consistency in Figure 27: hazard level 1 (H.L.1), hazard level 2 (H.L.2) and hazard level 3 (H.L.3). H.L.2 is in between H.L.1 and H.L3 and is delimited by GBI values of about 30 and 50.

It was observed that the delimited zones overlapped each other. This is an avoidable situation since it is quasi impossible to calibrate the GBI system where the thresholds are constant. Besides, the GBI is empirical and based on some particular field data and therefore, cannot reproduce exactly the complex behavior of the rock masses surrounding the underground excavations. To tackle this issue, the lower boundaries of the overlapping zones are considered. However, by doing this, some computed GBI values would correspond to a FoG worse than actual observation, therefore more conservative than the other way around (i.e. considering upper limits of the overlapping zones) where the outcomes would appear better than reality.

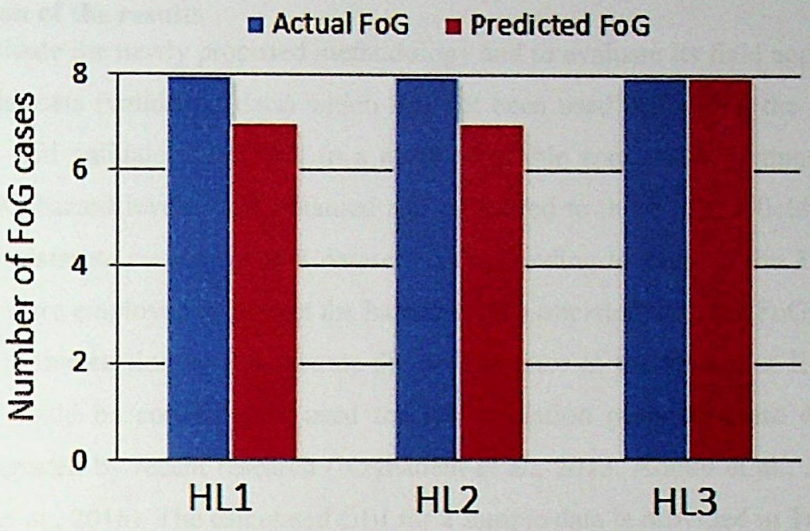


Figure 26: Comparison between predicted and actual FoG.

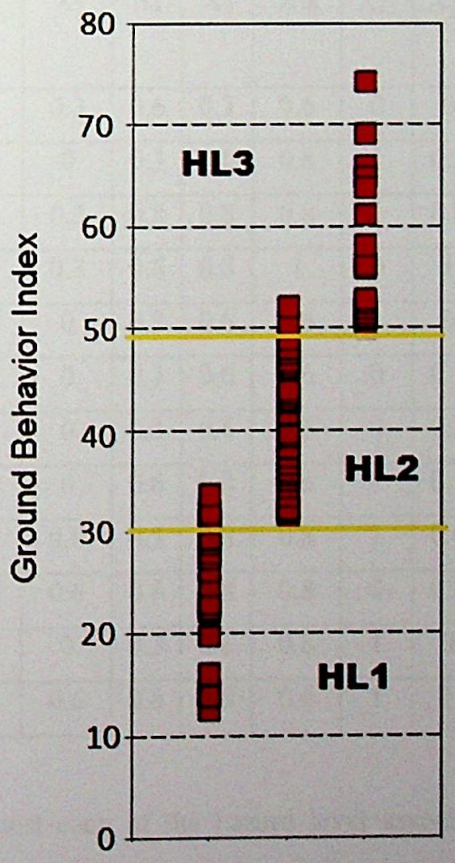


Figure 27: The GBI with the associated hazard level (H.L.).

4.2.3 Validation of the results

In order to validate the newly proposed methodology and to evaluate its field applicability, 24 independent datasets (validation data) which had not been used in training the BPNN, were considered. It will validate the BPNN in a more adaptable way. After computing the GBI values, the FoG hazard levels were obtained and compared to those of the field observation. The validation datasets consisting of 8 datasets corresponding to each of the 3 FoG classes (hazard level) were employed to predict the hazard level associated with the FoG). The results are presented in this section to demonstrate the performance of the networks. Even though a larger dataset could be conveniently used for the validation purpose, these datasets were enough as suggested by recent research (Naghadehi et al., 2013, Adoko et al., 2013, Rafiee, 2014, Adoko et al., 2016). The calculated GBI for a sample data is provided in Table 15 while Figure 26 presents a comparison between the predicted FoG and the field observations.

Table 15: Calculated GBI for a sample of validation datasets.

X_1	X_2	X_3	X_4	X_5	X_6	X_7	X_8	X_9	X_{10}	X_{11}	X_{12}	X_{13}	Actual HL.	GBI	Predicted HL.
0.6	0.1	0.1	0	0.3	0.3	0.3	0.6	0.3	0.6	0	0	0.3	1	22.20	1
1	0.1	0.1	0.3	0.3	0.3	0	0.3	0.6	0.8	1	0.3	0	2	39.83	2
0.6	1	0.1	1	0.8	1	0.3	0.8	0.8	0.8	1	0.8	0.6	3	71.35	3
0.6	0.4	0.1	1	0.6	0.8	0.3	0.8	0.8	1	0	1	1	3	55.85	3
0.6	0.1	0.1	0.3	0.3	0.3	0	0.3	0.6	0.6	1	0	0.6	2	38.03	2
0.3	0.4	0.1	0	0	0	0	0.3	0.6	0.6	0	0.3	0	1	16.67	1
0	0.1	0.5	0.3	0.3	0	0	0.3	0.6	0.6	0	0.3	0.6	1	26.28	1
0.3	0.4	0.1	0	0	0	0	0.6	0.3	0.6	1	0.3	0.6	1	33.76	2
0.3	0.1	0.1	0.6	0.6	0.8	0.8	0.3	0.8	0.8	1	0.6	0	2	52.84	3
0	1	1	0	0.3	0.3	0.6	0.6	0.8	0.8	0	0.8	0.6	3	51.16	3
0.3	0.1	0.5	0.3	0	0.3	0	0.3	0.6	0.8	1	0	0.3	2	37.86	2
0.6	0.4	0.1	0.8	0.8	1	0.6	0.6	0.8	0.6	1	1	0.6	3	65.97	3

The results show that, almost each of the hazard level associated with the FoG cases is correctly predicted. The GBI failed to calculate correctly one case each of hazard level 1 and hazard level 2. In terms of prediction accuracy of the hazard levels HL1, HL2 and HL3

87.5%, 87.5% and 100% of correct prediction, respectively, were achieved. Of course these results depend on not only the size of the validation data but also the adopted thresholds for delimitating the GBI into zones. An improvement was noted in comparison to a recent work where similar methodology was implemented (Adoko et al., 2016). To sum up, these results indicate good consistence between the predictions and the site observations. One of the merits of the current approach is the construction of the interaction matrix which is accomplished via a trained ANN. Larger datasets and more input parameters could yield a more refined GBI system and therefore resulting in more reliable results.

4.3 Conclusions

A methodology for quantifying the rock mass behavior around underground excavations in BCL Mine, Selebi-Phikwe, Botswana was proposed. The interactions between the factors affecting the rock mass behaviors were quantified using the Rock Engineering System (RES) and Artificial Neural Network (ANN) approaches which served as framework to establish the ground behavior index (GBI). The RES was applied as a convenient device for accounting for the complex and highly nonlinear correlation among the input parameters via the interaction matrices while ANN was implemented to objectively assign weights to the input parameters. The output parameter of the GBI system was the fall of ground (FoG) characteristics which were classified in three hazard levels (HL1, HL2 and HL 3). The input parameters related to the GBI included the rock type (X_1), rock structure (X_2), discontinuities (X_3), uniaxial compressive strength (X_4), cohesion (X5), friction angle (X_6), excavation type (X_7), excavation depth (X_8), excavation width (X_9), excavation height (X_{10}), use of blasting (X_{11}), unsupported span (X_{12}), implemented mining method (X_{13}). The Bamangwato Concessions Limited (BCL), an underground mine located in Selibe-Phikwe, Botswana was used as case study to compute the proposed GBI. On the basis of 84 selected datasets, the GBI was then computed. For validation purpose, 24 independent datasets (validation data) consisting of 8 datasets corresponding to each of the 3 FoG classes (hazard levels) were employed to predict the hazard level associated with the FoG and the results were compared to those of the field observation.

Firstly, the results from the interaction matrix indicated that: the most important parameters in the GBI system were the rock mass parameters and the mining methods. This agrees well with the theoretical and practical knowledge of rock engineering. Secondly, the comparison results

of proposed GBI showed good consistencies between the predictions and the site observations. It was concluded that the GBI could be used to translate a set of data into a single numerical attribute in form of index to represent the ground behaviors. Therefore, it could provide engineers with reliable quantitative information on the fall of ground as well as the corresponding hazard level. It is important to be noted that the GBI being empirical, the reliability of the predictions could be improved by implementing a larger validation data, and incorporating more influencing parameters. The GBI could be a complementary tool for ground control measures in underground mines.

Chapter 5: Numerical Modeling

5.1 Introduction

In this chapter, numerical modeling techniques were used to investigate structure controlled failure and stress controlled failures occurring around the underground mine openings in different selected sections of BCL mine. Rocscience software package (Rocscience, 2016b) and (Rocscience, 2016d) were employed to build model geometry of BCL mine for the different analysis. The stress characteristics around openings boundaries along with kinematic analysis of the structures were examined in order to corroborate the failure modes of the FoG events that had been observed in the mine. The model results are presented in the next sections.

Geological structures in the rock mass forming wedges and blocks were analyzed with Dips software (Rocscience, 2016a) determining how displacement of failed blocks is going to occur from the excavation boundaries and model a stable excavation by defining critical orientations that can cause instability. Stress analyses and combined structure/ stress analysis were undertaken using boundary element software package Examine2D (Rocscience, 2016b) and finite element software package rock and soil 2-dimensional (RS2) (Rocscience, 2016d) developed by Rocscience Inc. Examine2D and RS2 were selected to carry out stress and combined structure/stress analysis because the excavation geometry could be easily simulated, failure mode could be modeled using elasto- plastic brittle constitutive models, acceptable computation time of 1- 3 hours per analysis. Although GBI was established at BCL mine, it is limited as it does not capture the potential failure modes observed in the field. Numerical methods were used to model the structure and stress failure around a few selected BCL stopes. In order to fully characterize the FoG, this chapter comes as complement to Chapter 4 as the ground behavior index alone cannot be used to determine the failure mode.

5.2 Structure controlled failure mode analysis

Kinematic analysis is a method used to evaluate the potential failure modes that occur due to the presence of unfavorably oriented geological discontinuities in the excavated rock mass (Wyllie and Mah, 2004). Discontinuities are geological breaks in a rock such as joints, faults,

shear zones, foliation, bedding planes that can serve as failure planes. In Addition, according to (Hoek and Bray, 1981, Kliche, 1999), a wedge failure may occur when two discontinuities intersect forming wedge shaped block and angular relationships between discontinuities and excavation surface are implemented to examine the potential mode of failure along the plane of failure. Dips software Rocscience (2016a) was applied to determine possible failure modes occurring along unfavorable geological discontinuities in the stopes, sill drive and give an indication of stability conditions. All the recorded and availed different geological discontinuity orientations data from FoG database were imported as input parameters in Dips computer program to apply kinematic analyses. The dip angles and dip direction angles selected were used as input parameters in Dips software. The orientation of key geological structure sets in terms of dip and dip direction were in each stope and sill drive kinematically examined using methods suggested by (Goodman and Shi, 1985) and Dips software (Rocscience, 2016a). In this study, zones of cluster concentrations greater than 6% were considered significant and critical.

The results of the kinematic analyses showed that wedge failure was possible on the stopes and sill drive as determined by Dips. The results of kinematic analysis indicate that wedge sliding and falling failures are possible in the sill drive, limited to sill drive scale illustrating good agreement with field observations of structural failure mode on several mine openings (Figure 28).

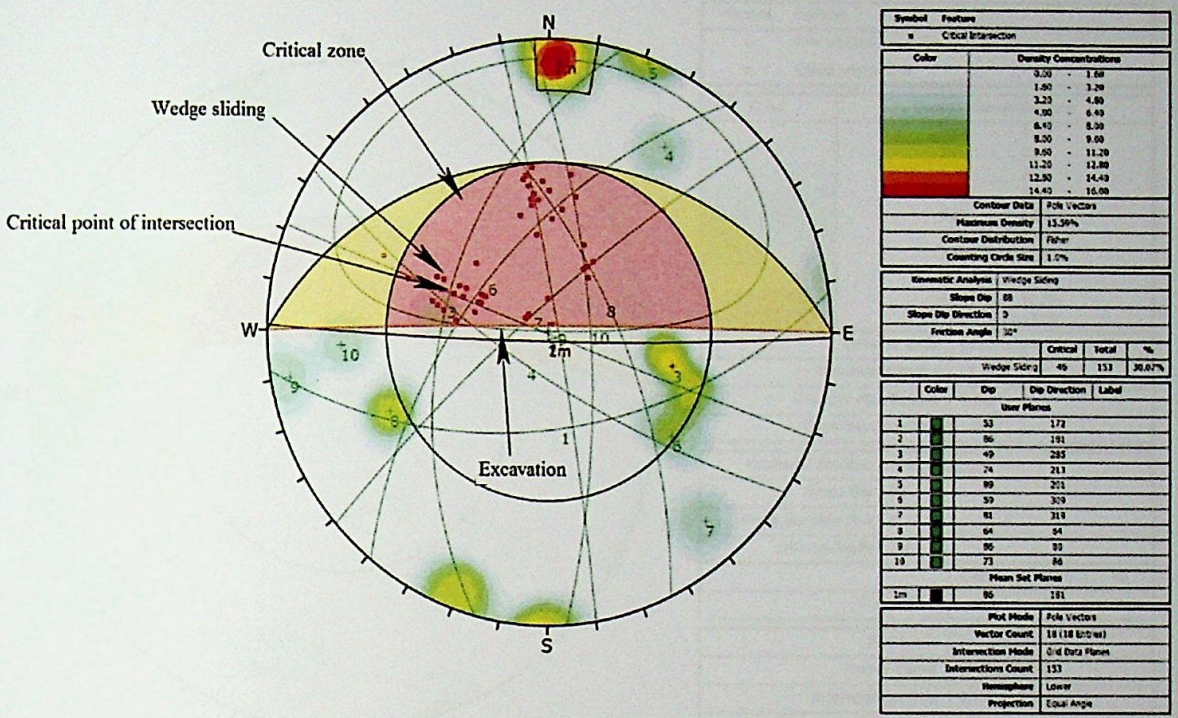
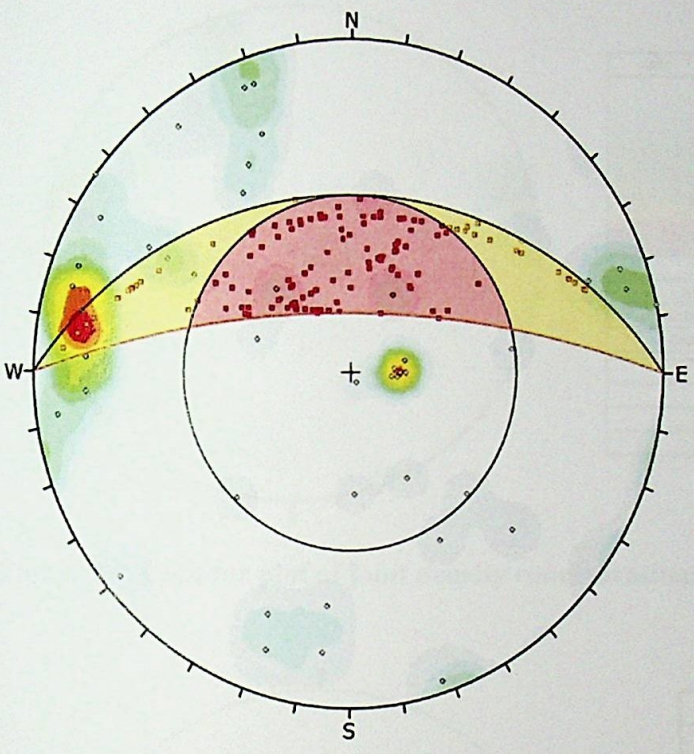


Figure 28: Stereonet projection with density contour and major geological structures forming sliding wedges in sill drive.

The wedges that meet the kinematic conditions for sliding to take place into the stope are delineated by zones of critical intersections which is pink colored zone in Figure 29.



Symbol	Feature
◇	Pole Vectors
◇	Critical Intersection

Color	Density Concentrations
	0.00 - 1.30
	1.30 - 2.60
	2.60 - 3.90
	3.90 - 5.20
	5.20 - 6.50
	6.50 - 7.80
	7.80 - 9.10
	9.10 - 10.40
	10.40 - 11.70
	11.70 - 13.00

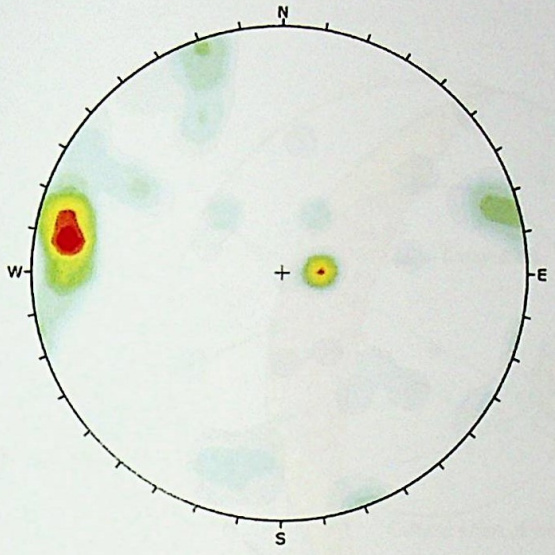
Contour Data	Pole Vectors
Maximum Density	12.62%
Contour Distribution	Fisher
Counting Circle Size	1.0%

Kinematic Analysis	Wedge Sliding		
Slope Dip	70		
Slope Dip Direction	0		
Friction Angle	34°		
	Critical	Total	%
Wedge Sliding	160	1368	11.70%

Plot Mode	Pole Vectors
Vector Count	53 (53 Entries)
Intersection Mode	Grid Data Planes
Intersections Count	1368
Hemisphere	Lower
Projection	Equal Angle

Figure 29: Pole plot of geological structures forming vital sliding and falling wedges in Phikwe stopes.

In contour plots of joints density concentrations, the cluster with a concentration greater that 6% is very significant. The highly concentrated areas of poles with density concentration greater than 6% were identified representing the leading and key discontinuity sets. Figure 30 shows contour plot of joint density concentration of Phikwe stopes. Figure 31 shows the pole plot of geological structures forming sliding and falling wedges which is the main failure mode taking place in Phikwe stope.

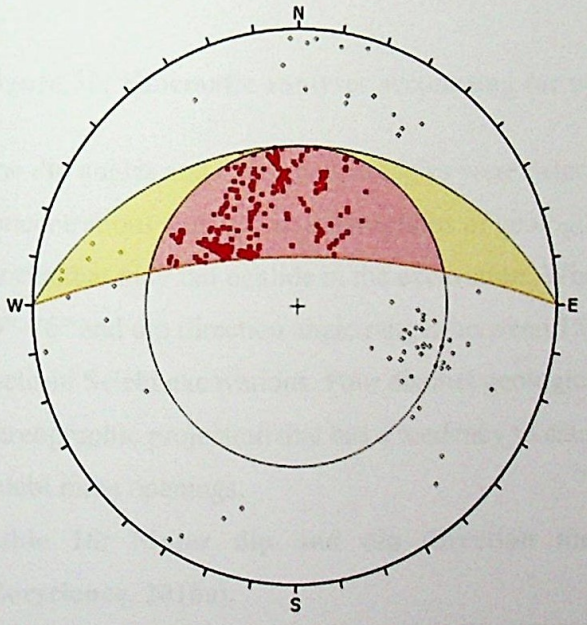


Color	Density Concentrations
	0.00 - 1.30
	1.30 - 2.60
	2.60 - 3.90
	3.90 - 5.20
	5.20 - 6.50
	6.50 - 7.80
	7.80 - 9.10
	9.10 - 10.40
	10.40 - 11.70
	11.70 - 13.00

Contour Data	Pole Vectors
Maximum Density	12.62%
Contour Distribution	Fisher
Counting Circle Size	1.0%

Plot Mode	Pole Vectors
Vector Count	53 (53 Entries)
Hemisphere	Lower
Projection	Equal Angle

Figure 30: Contour plot of joint density concentrations in Phikwe stopes.



Symbol	Feature
◇	Pole Vectors
▪	Critical Intersection

Kinematic Analysis	Wedge Sliding		
Slope Dip	70		
Slope Dip Direction	0		
Friction Angle	30°		
	Critical	Total	%
Wedge Sliding	351	2208	15.90%

Plot Mode	Pole Vectors
Vector Count	67 (67 Entries)
Intersection Mode	Grd Data Planes
Intersections Count	2208
Hemisphere	Lower
Projection	Equal Angle

Figure 31: Pole plot of geological structures forming vital sliding and falling wedges in Phikwe 835 m/ 3420 stopes.

The models outline failure that was activated by shear strain concentration allowing geological structures to activate movement of blocks and wedges.

According to the results of the kinematic analyses, wedge failures along intersection of the joint sets are expected to occur on the 950 m/3675 stope in Figure 32.

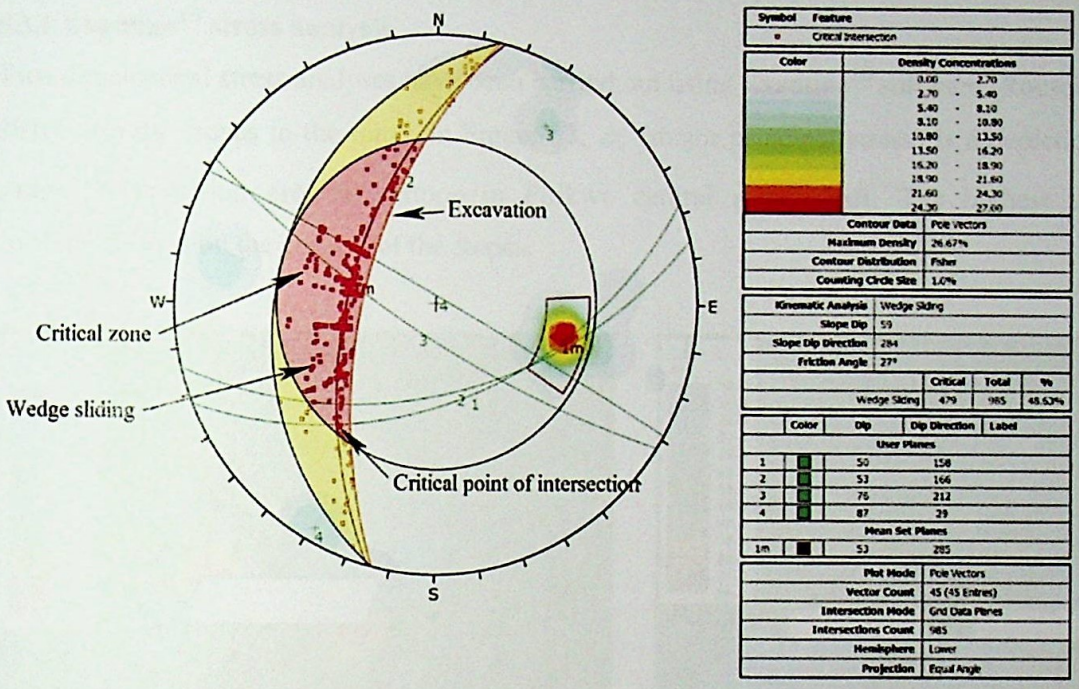


Figure 32: Kinematic analyses accounting for wedge sliding in Selebi 950 m/ 3875 stope.

The dip angles and dip direction angles were determined by points with high density pole concentrations and critical intersections of geological structures in the critical zone forming blocks that may fall or slide in the excavation. When the dip angle ranges from 50°- 86° and 49°-76° and dip direction angle ranges between 158°- 181° and 212°- 285°, FoG is likely to occur in Selebi excavations. Four distinct geological structures were found in the stereographic projection that has a tendency to cause fall of ground shown in Table 16 for Selebi mine openings.

Table 16: Major dip and dip direction measurements selected in Dips software (Rocscience, 2016a).

Geological structure set	Dip (°)	Dip direction (°)
1	86	181
2	49	285
3	64	064
4	76	212

5.3 Stress controlled failure mode analysis

5.3.1 Examine^{2D} stress analysis

Two dimensional stress analyses have been carried out using Examine^{2D} software (Rocscience, 2016b) on the stopes in the mine. In Figure 33, σ_1 (major principal stress) is a depiction of stress redistribution around a stope in Phikwe central mine shaft. The highest stress concentration is on the corners of the stopes.

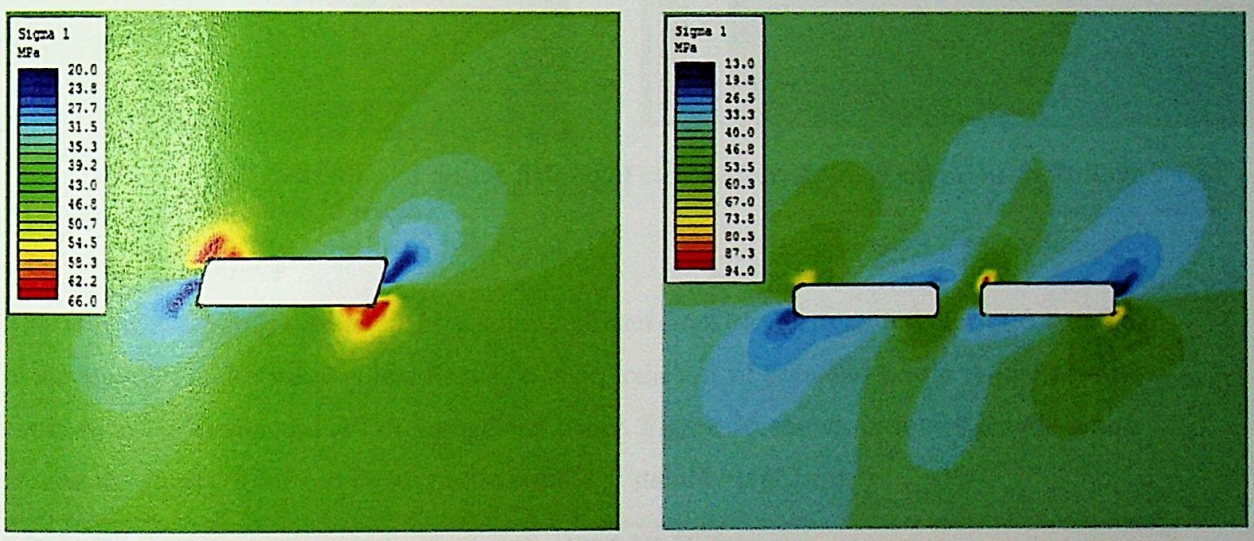


Figure 33: The distribution of major principal stress around Phikwe 3420 stope (left) and Selebi 3875 stope (right).

The stress distribution of minor principal stress after stope excavation is shown in Figure 34. The Phikwe 810 m/ 3420 stope and Selebi 950 m/ 3875 stopes are illustrated in this figure.

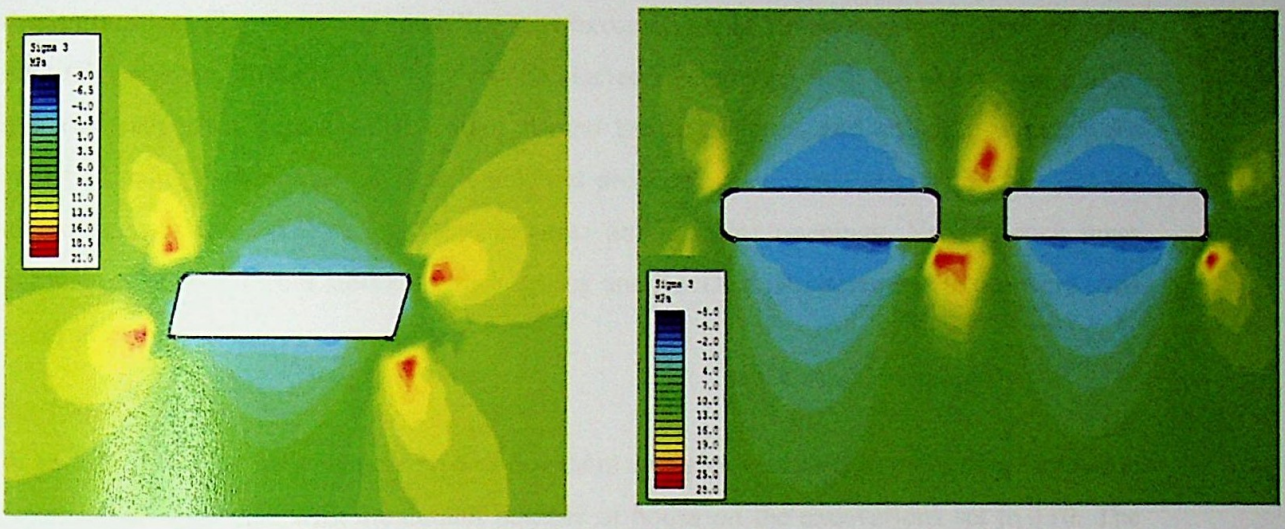


Figure 34: Stress distribution of minor principal stress after stope excavation in Phikwe 3420 (left) and Selebi 3875 (right).

5.3.1.1 Strength factor

Elastic model analysis display that the stope roof and floor has a strength factor of 0.1 to 0.6. If the strength factor value is less than 1, it is an indicator of potential brittle failure causing excavation instability and fall of ground can occur. Figure 35 shows various strength factors around the stopes. Roof and floor are susceptible to stability problems.

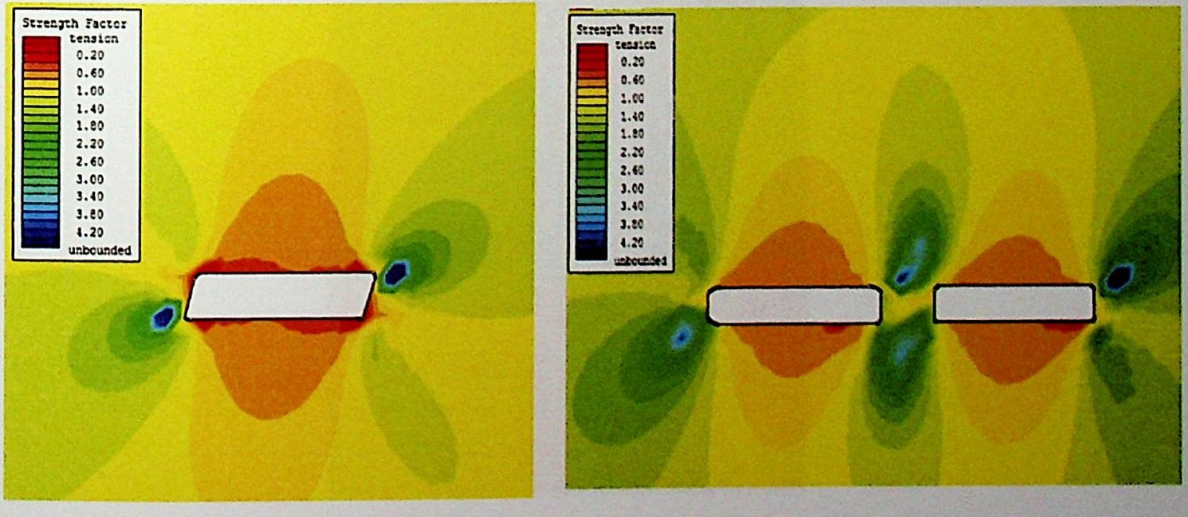


Figure 35: Strength factor around Phikwe stope (left) and Selebi stopes (right) after excavation.

5.3.2 Rock and Soil 2-dimensional (RS2) analysis

Numerical modeling was carried out to analyze the stress and combined structure/ stress failure mode stopes with rock masses with various properties, external forces and dense

discontinuities. The numerical modeling was executed using Rocscience computer program RS2 (Rocscience, 2016d). Modeling was conducted by applying both the elastic and plastic material properties. Stress redistribution around the excavations and strength factors were analyzed using elastic material. Plastic material property was utilized to examine the yielded elements, rock mass failure and displacements around mine openings. Various rock mass parameters obtained from laboratory rock testing and RocData (Rocscience, 2016c) were used as input parameters.

5.3.3 Model setup

A grided mesh type with element type of 6 nodded triangles was used in modeling. Gradation factor of 0.1 was used with the default number of nodes on the excavations set to 110. The number of nodes was used to evaluate the discretization of the excavation boundary. Underground auto restrains were applied to pin the external boundaries. Constant field stress was selected for modeling stresses to account for stress measurements made by (Van der Heever et al., 2014) in Table 6. The major, intermediate and minor principal stresses from Table 6 were used as input parameters. The direction of major principal stress is normal to strike of orebody. Figure 36 shows the general model setup of RS2.

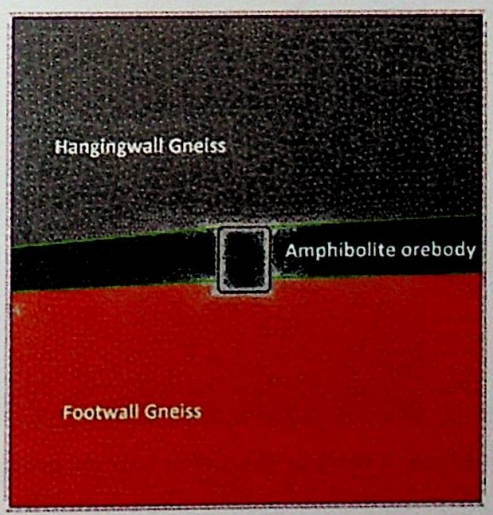


Figure 36: A general model setup for the Selebi sill drive.

5.3.4 Stress distribution

Stress distribution surrounding the stope is illustrated in Figure 37 and Figure 38. The distributed stresses are concentrated in the corners of the mine openings.

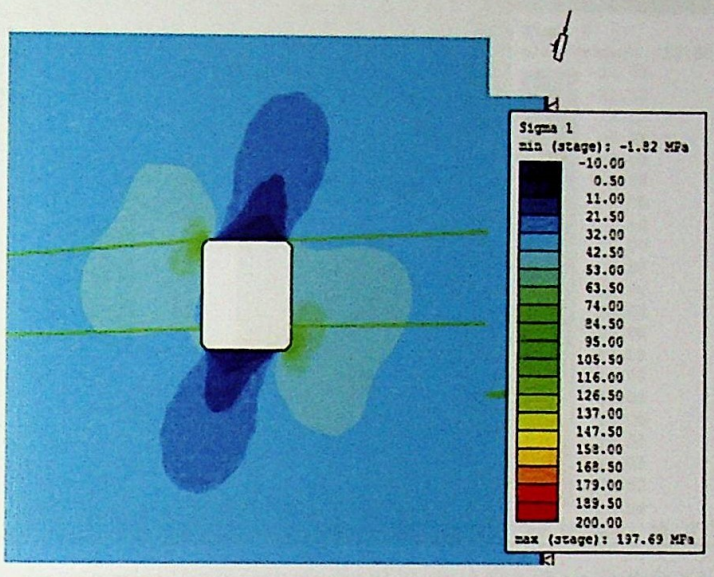


Figure 37: Stress distribution of major principal stress in Selebi 850 m sill drive (elastic model).

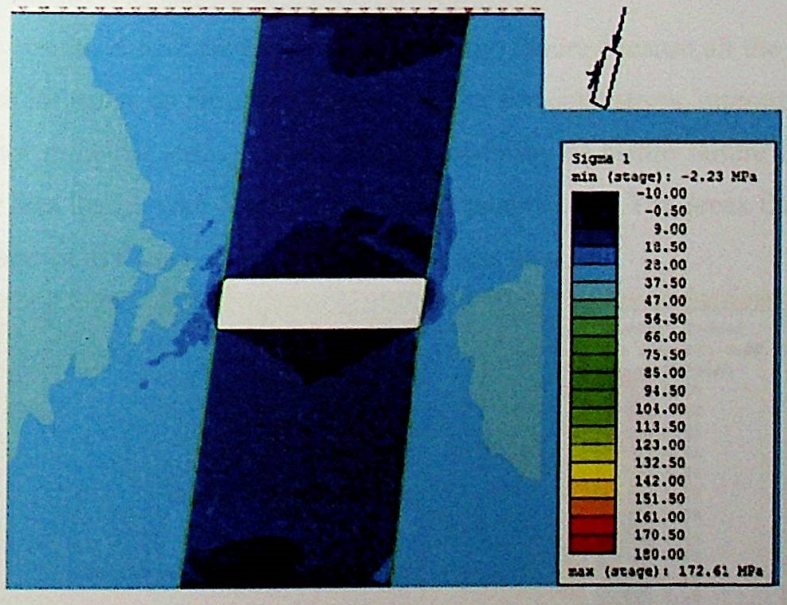


Figure 38: Stress distribution (major principal stress) around 835 m/ 3100 stope.

Figure 39 shows minor principal stress distribution around the sill drive. The negative stress will affect the surrounding rock mass causing stability problems. The stress failure that would cause fall of ground occurs when minor principal stress ranges between -4 MPa and -14 MPa and a strength factor of 0.95 to 0.10.

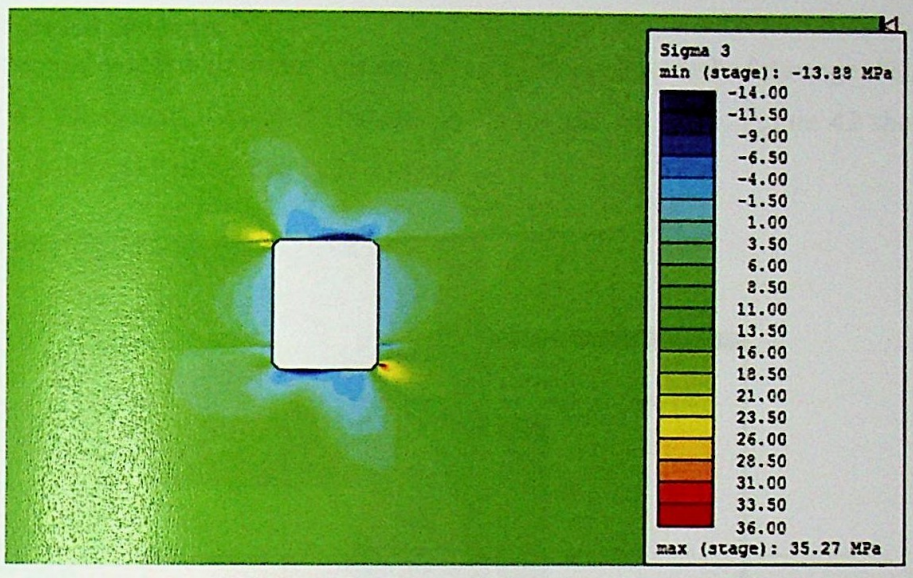


Figure 39: Stress distribution (minor principal stress) for the sill drive (elastic model).

5.3.5 Strength factor

Strength factor results in RS2 are handy in showing the failure because all the three principal stresses have an influence on the strength factor (major principal stress, intermediate principal stress and minor principal stress). Areas with a possibility of brittle failure are denoted by strength factor less than 1 with Hoek-Brown brittle parameters. The areas that are prone to instability are shown in Figure 40 by strength factor less than 1.

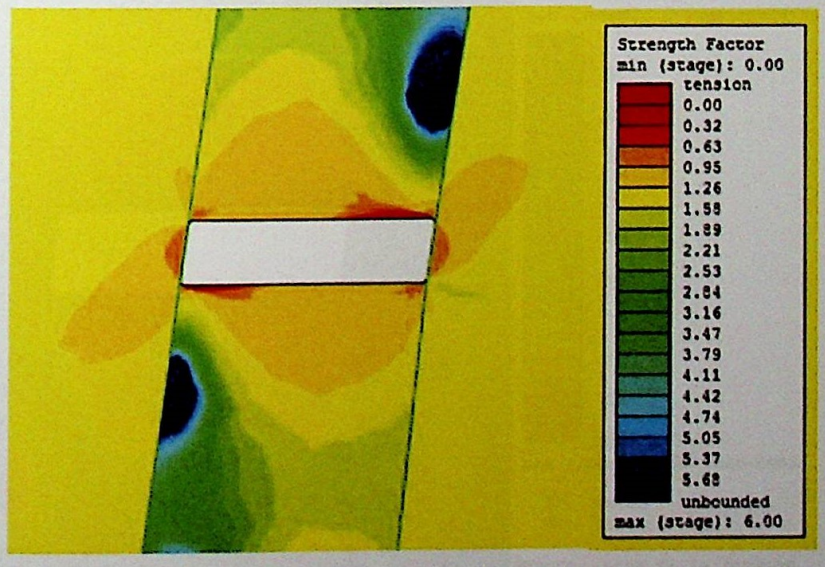


Figure 40: Potential brittle failure areas with strength factor less than 1 in an unsupported cut and fill 835 m/ 3100 stope (elastic model).

5.3.6 Yielded elements

The material yielded elements was employed to assess the level of damage. Figure 41 below illustrate the extent of yielded elements in stopes and sill drive. Figure 42 shows shear and tension failure at Phikwe 835 m/3100 stope.

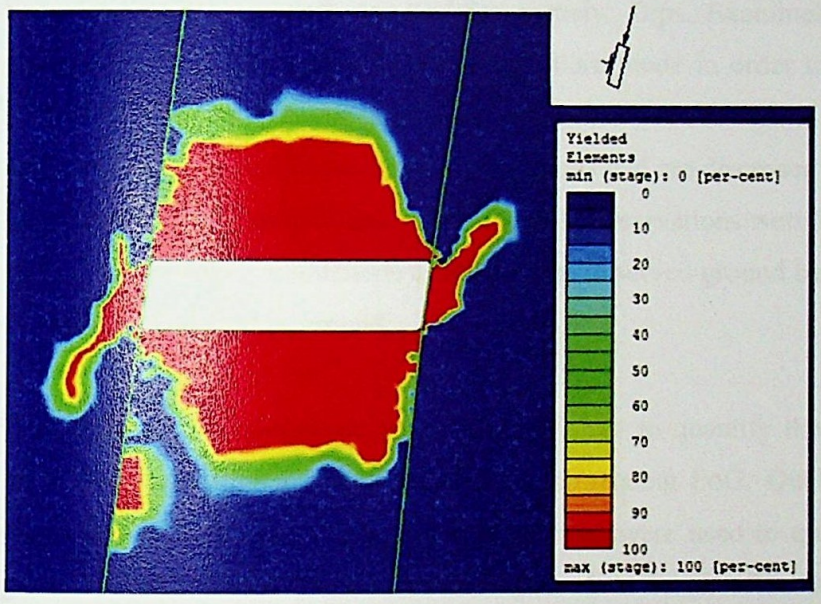


Figure 41: Yielded elements in a plastic model of Phikwe 835 m/ 3100 stope.

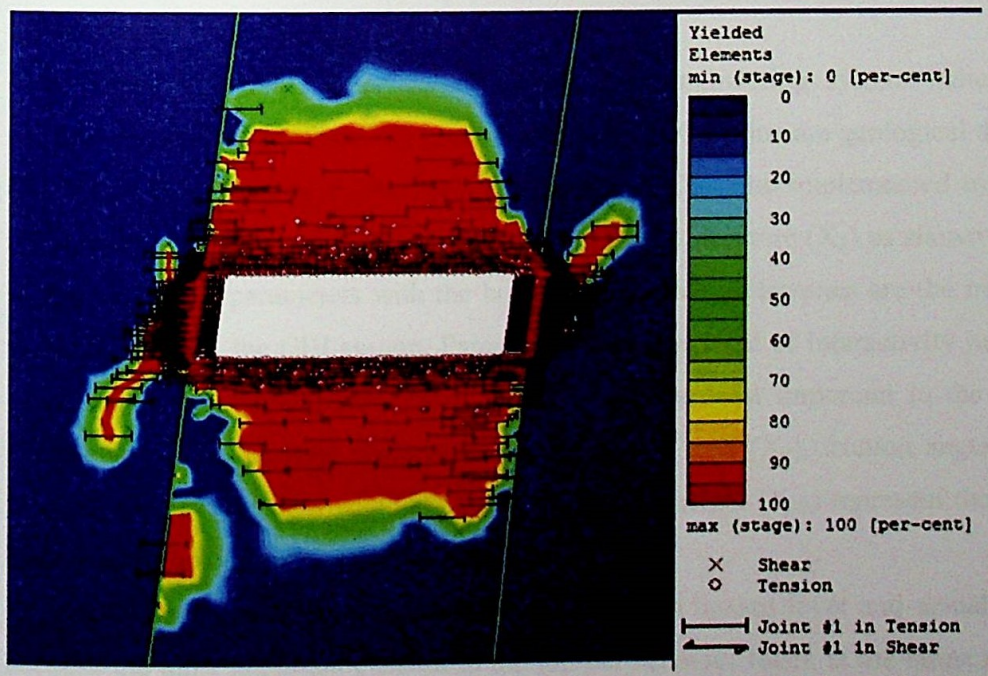


Figure 42: Shear and tension failure along discontinuities at Phikwe 835 m/ 3100 stope.

Chapter 6: Discussions

This chapter discusses results of the study and the implications for ground control at BCL mine. Statistical analysis, Rock Engineering system (RES) and Artificial Neural Network (ANN) were used to determine the factors that influence instability and assess BCL ground behavior. Rocscience software package namely: Dips, Examine2D and RS2 was used to analyze structurally controlled and stress failure mode in order to fully characterize fall of ground in BCL underground mine stopes and sill drive. The results of this research work were achieved by using the above mentioned methods and are discussed in depth in this section. In this study the FoG compilation results and field observations were integrated with RES, ANN as well as numerical simulations to analyze the observed ground behavior and failure mode at the mine causing fall of ground.

The study has established an empirical GBI chart to quantify the ground behavior of BCL mine and correlation between parameters influencing FoG. Qualitative methods, the rock engineering system and artificial neural network were used to quantify the behavior of the ground related to FoG. ANN and RES proved to be an effective tool for developing the ground behavior index. The key results can be identified in Figure 26 showing the calculated GBI values plotted on this chart. The GBI values were plotted on chart in order to calculate the associated hazard level.

The results of the interaction matrix of the rock engineering system indicate the most important parameters influencing ground behavior in BCL mine are geological discontinuities (X_3), uniaxial compressive strength (X_4), rock type (X_1), the implemented mining method (X_{13}), cohesion (X_5) , unsupported span (X_{12}) and rock structure (X_2) as shown in Figure 24. In Figure 24, the parameters with the highest interactivity intensities are the most important and influential in the GBI system. Parameters with low level of interactivity intensities, low cause and effect values plotted show that they are the least important in the GBI system. Parameter (X_{8}) is the least important. The excavation type (X_7), friction angle (X_6), use of blasting (X_{11}), excavation width (X_9), and excavation height (X_{10}) represent the intermediate important parameters of the GBI system.

The GBI range was selected to compare the predicted hazard level and actual hazard level because the most important element in the ground behavior index is the range not the value.

The GBI range focuses on the region zonation and how to evaluate the class of the ground using the GBI value grouped. The hazard levels associated with ground behavior at BCL mine were classified. The ground was divided into 3 classes with increasing hazard potential namely: Hazard level 1, hazard level 2 and hazard level 3 as shown in Figure 27. Hazard level 1 represents good ground, hazard level 2 represents fair ground and hazard level 3 represents poor ground. The use of GBI value may predict a value that is very close, accurate or bit different but still falls within the ground class. There is no need for particular accuracy as the ground conditions change affecting a large zone. The red dot in Figure 27 represents the GBI value. The data was calibrated into a system of values ranging 0-72. This was based on the collected data and compiled. These GBI values were grouped to constitute the hazard classes. Therefore the GBI range was adopted to assess the corresponding GBI value hazard class.

A connection between the most important parameters influencing ground behavior and the related fall of ground was established. If the rock mass characteristics, mining methods excavation geometry, blasting conditions and ground support conditions are known, the GBI value can be estimated and quantified. The identified most important parameters can be utilized in the ground control design stages after computing the GBI value to predict the hazard associated with that particular ground. The GBI values plotted on the GBI chart with associated hazard level range gives an idea on what hazard class would occur and whether is safe or not safe to continue mining.

As mining progresses to new ground, the GBI chart can be used for further hazard assessment related to that ground conditions. The new data could be used to update the GBI chart and recalibrate the GBI chart, recalibrate the range zone in order to improve and have more accurate GBI chart. BCL mine could collect more data and use this data to evaluate the corresponding ground behavior to see in which ground situations is FoG more likely to occur.

The GBI chart can be used to plot the GBI values to assess the hazard class related to new collected data. The input parameters need to be known and the proposed methodology can compute the GBI. The computed GBI can be used to plot the hazard level. With any dataset, the GBI can be computed and plotted on the GBI chart to see where the class falls using the engineering judgement to assess the GBI value. The ground behavior class was given by a certain GBI value and then it was grouped. Plot of the GBI values provided the range of GBI

with associated hazard level. The compiled data used for quantifying the ground behavior was analyzed, calibrated and validated with some testing datasets. During data validation the GBI values were used not the GBI range. The GBI chart was obtained as the final product of BCL ground behavior.

The mining method is considered as one the important parameters related to FoG located at the top of the cause=effect diagonal in Figure 24 and high interactivity in Figure 25 based to the following reasons. The mining method (X_{13}) is selected based on the characteristics of the rock mass and geomechanics properties of the ground not based on the fall of ground. In the cause effect diagram of Figure 24, the implemented mining method (X_{13}) contributed more on the cause and less on the effect. That is the reason why the mining method is on top of the cause=effect diagonal of the diagram. The mining method comes first and affects the results. The mining method affects the FoG. If mining method does not commensurate with rock mass properties and characteristics it will affect fall of ground. Fall of ground cannot influence the choice of mining method. The mining method does not have balanced cause=effect, has only one direction. The mining method only has cause or effect depending on whether is at the top or bottom of cause=effect diagonal of the diagram. However other parameters such as rock mass characteristics have an average cause=effect and FoG can influence change in these parameters.

Statistical analysis in Figure 15 and Figure 16 show that fall of ground in BCL mine is commonly associated with blasting event and geological material displaced in the form of blocks and wedges. The failure mode analysis in Figure 17 indicated that the fall of ground mainly occurs as structurally controlled failures.

The connection between rock mass properties and type, geological discontinuities, ground support and mining methods were assessed in the developed numerical model and proposed ground behavior index methodology. There is a link between fall of ground size, geological structures, hazard level, failure mode and ground behavior. The fall of ground mass and frequency is related to the stress failure, structurally controlled failure and hazard level. The increase in ground fall tonnage leads to escalated structurally controlled fall of ground and danger levels. Deterioration of ground conditions increases the possibility of high fall of ground size and structurally controlled failures.

Kinematic analysis where instabilities are occurring revealed structurally controlled failures in the form of wedges indicating that geological structures are one of the most important parameters influencing FoG. This evidence is also provided by RES and ANN tools showing that geological discontinuities are important parameters used to quantify ground behavior index. This implies that ground support is one of the factors that influence fall of ground in underground mine opening. The simulation results correspond to the failures observed in the field, indicating that the laboratory parameters are representative of in-situ field parameters. The RES and ANN results showed a very good correlation with observed fall of ground occurring around the stopes and sill drives. The ANN predicted between 87.5 % - 100 % the fall of ground against the observed field FoG.

Examine 2D and RS2 modeling approaches were implemented for assessing the stress failure and combined stress and structurally controlled failure around the excavations. Performed analysis illustrated that the failure mode and the extent of failure zone depends on the in situ stress state orientation and geological discontinuities orientations. The stability of underground mine excavations and the rock mass behavior is influenced by the magnitude and direction of in situ stress field and dip angle/ dip direction angle of geological structures. The change in stress direction in the numerical model showed a wide variation in major principal stress, minor principal stress, yielding and strength factor. The modeling results in Figure 33 and Figure 37 indicated that the stress failure would occur when major principal stress is within the range of 63 MPa to 95 MPa. The stress failure that would cause fall of ground occurs when minor principal stress ranges between -4 MPa and -14 MPa in Figure 39 and – 2 MPa to – 8 MPa in Figure 34. In Figure 35 the strength factor of Phikwe and Selebi stopes in Figure 35 are 0.60 to 0.10 indicating that the stopes are susceptible to stability problems as the strength factor is less than 1. Phikwe stope has a strength factor of 0.95 to 0.10 in Figure 40 revealing the potential of brittle failure in rock mass with strength factor less than 1. The damage index introduced by (Martin et al., 1999) was applied to compute the damage index around the mine openings in order to assess the ground behavior and failure mode in order to validate the numerical models. The numerical models result show that BCL mine stope alignments have a favorable to intermediate favorable orientation with respect to the major principal horizontal stress, minor principal effective stress and while avoiding critical geological discontinuity orientations that may cause instabilities. The failure zone that

appears around the stopes is the outcome of strength of rock mass, far field stresses, geological structures and opening geometry (Kaiser et al., 2000) and (Martin et al., 1999). Thus, stress and combined structure/stress analysis show that the permanent BCL mine openings are aligned nearly parallel to major horizontal stress direction and the stopes are aligned near perpendicular to the major horizontal stress decreasing the stress impact on the rock mass around excavations. Therefore, the stopes are stabilized by high clamping pressures provided by high horizontal stresses minimizing block and wedge failures. The stress situation and mining induced stress has the potential to cause tensile failures, spalling and strain bursts when stress progressively builds up in the pillars and sidewalls.

6.1 Failure

All failures indicated from the developed models of the mine stopes indicate shear dominated failure and tension failure in stope roof, floor and minor in sidewall rock masses as shown in Figure 42. The tension stresses weaken the rock mass by opening the fractures and geological structures. Failure is initiated along geological discontinuities due to horizontal stresses in the immediate roof and floor accompanied by separation of weak parting planes, fractures propagating and coalescing with other structures, disconnection of roof rock units applying dead weight on the roof bolts and side bolts causing the fall of ground leaving the ground support damaged and protruding. 2- Dimensional simulation models showing failure around BCL mine stopes were produced at Phikwe central 835 m depth in Figure 40, Figure 41, Figure 42 and Selebi 950 m depth in Figure 35 using Examine 2D and RS2.

The mining induced stresses, intersection of geological structures and deterioration in ground conditions change the rock mass behavior results in potential of block fall, block sliding and shear failure modes that cause fall of ground if not adequately supported. Although, it is impossible to estimate exactly how this affects the stope stability, it can be assumed that a larger area of yielding is less favorable than a small zone extending into the rock mass. The study illustrates that fall of ground in stopes is mainly caused by discontinuities. Other means could be the change of stope shape to assist in relieving stress concentration in the stope corners and reducing excavation span. Also from field observations it can be noted that the fall of ground occurring in the mine openings is promoted by the deterioration in ground conditions influenced by changes in rock mass characteristics.

The research shows that to reduce the impact of brittle failure and fall of ground in stopes it is suitable to change mining methods, the size of stopes, stope sequencing as mining advances encounters alteration in stress state, changes in rock mass parameters such as quality, type and strength. Thus is beneficial because changing the mining method and minimizing stope spans will decrease possibility of exposing geological structures that can form wedges.

6.2 Rock mass quality

The rock mass in Phikwe central stopes and Selebi stopes was generally classed as fair to good rock, in some areas poor rock mass based on the ground behavior index chart in Figure 27. The computed GBI can be utilized in ground support design and evaluating stability problems resulting from block falls and blocks sliding, in low stress mining environments (Palmström and Stille, 2010).

The fall of ground severity differs from location to location due to many factors involved that affect the stability of underground mine openings. The tonnage of rock material dislodged was used to evaluate the fall of ground severity in various mine locations. Further, the total weight of rock material displaced was determined to be higher in poor quality and low strength rock mass, poor ground conditions and in stopes that experience higher degree of failure.

The observed FoG failure modes were predominantly structurally controlled followed by stress failure. This was noticed in the field where events took place, in Figure 17, Figure 28, Figure 32 and Figure 41. Dips models demonstrated that block falls and sliding of wedges along geological structures is the principal failure mode. The existence of geological discontinuities such as faults, shear zones, foliation and joints have been observed in stope and other mine openings boundaries which are believed to have an impact on fall of ground occurrences but their role is not fully understood. In some parts of the mine in Selebi and Phikwe central stopes the majority of failure was stress/structure induced. This was provided by evidence of failure in numerical modeling as shown in Figure 41 and Figure 42.

Incorporation of field observations, ground behavior index, kinematic analysis and numerical modeling results imply that there is a relationship between fall of ground size, hazard level and failure mode. The evaluation of ground behavior index accounted for different hazard levels, the ground response is connected with gravity driven structurally controlled failure modes and stress failure mode. This leads to forecasting and prove that the gravity driven

structurally controlled failure modes are the dominant type for the BCL rock mass structure as geological structures is one of the most important parameters influencing ground behavior index that lead to fall of ground. However, the results may help to understand the role of geological discontinuities, mining methods, stress and rock mass parameters on the rock mass behavior that can cause fall of ground in hard rock underground mines.

Fall of ground characterization results can be used further in assessing the hazard level of FoG, factors that influence fall of ground and as inputs to improve the ground control design decisions especially mining methods and ground support systems.

6.3 Summary

This research work has revealed that ground behavior index chart can be used to predict the hazard level associated with that particular ground. ANN and RES identified the most essential factors that influence observed fall of ground and predicted the ground fall occurrence. The most important parameters that affect the FoG in BCL stopes are geological discontinuities, rock type, rock mass structure, cohesion, mining methods and unsupported excavation span. It showed that RES and ANN are reliable tools that can be used to predict fall of ground in underground excavations. Statistical analysis using graphs showed that structurally controlled failure mode is main failure mode taking place in BCL mine opening. Kinematic analysis using Dips software indicated block fall and block sliding failure mode, signifying that structurally controlled gravity driven falls of ground is the fundamental failure mode. Numerical analysis using RS2 and Examine2D indicated shear and tension failure in stopes. This shows that stress state such as in situ stress orientation, mining induced stress and geological structures are one of the principal factors promoting excavation instability. Structurally controlled failure contributes the majority of the modeled failures occurring through the rock mass.

Chapter 7: Conclusion

The main conclusions drawn from this study are given in the following paragraphs.

This study necessitated knowledge of BCL mine stopes rock structure, ground behavior, structurally controlled and stress failure modes. The Rock Engineering system (RES) and Artificial Neural Networks (ANN) were employed to establish ground behavior index (GBI) empirical chart used to quantify the behavior of the ground around BCL mine opening. The RES was applied to quantify the highly nonlinear most important parameters influencing the rock mass behavior leading to Fall of ground (FoG). The ANN method was implemented to evaluate and assign the weights of input parameters involved which served as a framework to form the GBI. The output parameter of the GBI system was the fall of ground characteristics which were classified in three hazard levels (Hazard level 1, hazard level 2 and hazard level 3). In BCL mine stopes, hazard level 2 is the most frequently occurring followed by hazard level 1 then hazard level 3. This suggests that BCL mine stope grounds are good to fair from GBI perspective. The results from parameter interaction matrix indicated that the most important parameters in BCL mines GBI system were geological discontinuities (X_3), uniaxial compressive strength (X_4), rock type (X_1), mining method (X_{13}), cohesion (X_5), unsupported span (X_{12}) and rock structure (X_2). The least important parameter is the excavation depth (X_8) in the GBI system. The GBI chart can be used to evaluate the hazard level related to ground behavior.

A simple statistical analysis model was performed using graphs to quantify principal factors and most important elements of fall of ground. The statistical analysis results indicated wedges and block falls, structural failure, stress failure and combined structure/stress failure mode. Also, the statistical analysis results revealed that most FoG takes place in active stopes due to blasting. The ground falls were mainly caused by geological discontinuities, mining induced stresses and engineering methods.

The second aspect of this thesis focused on numerical modeling to analyze structurally controlled failure and stress failure mode. The results of the kinematic analysis on the stopes demonstrate that wedge type failure on the critical intersections and orientations of structures was possible on the stopes and sill drives. Fall of ground has a tendency of occurring when the dip angle / dip direction angle of geological structures varies between of 49°- 74°/212°-329° and 67°- 76°/64°- 104° forming critical intersections in Phikwe stopes. In Selibe stopes,

fall of ground has a propensity for taking place when the dip angles of geological structures forming wedges ranges from 50°- 86° and 49°-76° and dip direction ranges between 158°-181° and 212°- 285°. The stress failure would take place when major principal stress is within the range of 63 MPa to 95 MPa. The stress failure that would cause fall of ground occurs when minor principal stress ranges between -4 MPa and -14 MPa, -2 MPa to -8 MPa and at a strength factor of 0.95 to 0.10 which is in agreement with the field observations. Assessment of kinematic analyses and field observations suggest that geological discontinuities are one of the most essential parameters that lead to FoG events. The excavation geometry, excavation methods, rock mass characteristics and orientation of geological structures have significant influence on the failure mode and failure control occurring in the mine openings.

The rock and soil 2-dimensional (RS2) modeling results revealed shear and tension failure. Predominant structurally controlled gravity driven failure and in some areas accompanied by structurally controlled/ stress failure that occur are repeated in different stopes accompanied by various stress failure modes.

The conclusions are also founded on the field observation and ground investigations results. The structurally controlled and stress failure mode results are consistent with the field observations. The BCL mine stopes and sill drives rock mass structure was identified as mainly jointed/ blocky/ bedded and intact/massive. It can be said that the ground behavior was evaluated as stable with potential of discontinuity controlled, gravity induced block fall, sliding blocks and shallow stress induced shear failure in combination with structurally controlled block falls. Hence, the primary failure mode leading to fall of ground was assessed as discontinuity controlled induced falling and sliding of blocks, occasional stress and shear failure along pre-existing geological structures. The possible failure examined in BCL is block fall and shear failure. For structurally controlled failure such as block falls, sliding blocks and shear failure modes, it can be stated that empirical support design charts of good rock may be sufficient to stabilize possible rock wedges in the stope roof and walls.

The results of this research work presented in Chapter 4 and Chapter 5 of this thesis has illustrated that numerical modeling, RES and ANN can be a useful tool for providing an important insight of BCL mine structurally controlled failure and stress modes, quantify ground behavior and predict hazard level associated with the fall of ground. The results showed good correspondence between predictions and field observations.

These results provide vital insights of fall of ground characteristics and aids engineers in designing mine ground control techniques which encompasses all the important factors influencing fall of ground hence advances workers safety and minimize production delays. The recommendations for ground control improvements and future research are made to tackle some of the questions that could not be managed, problems and solutions that this research answered.

7.1 Recommendations and future numerical modeling

Based on the results obtained in this study, in connection with managing FoG and improving the ground control at BCL mines the following are recommended:

1. Because the mining methods and unsupported span of the excavations were among the most important parameters controlling the FoG behavior, special attention should be put on the stope design and the mining methods.
2. The use of empirical method for stope design such as the Matthew's stability graph (Mathews et al., 1981, Mawdesley et al., 2001) combined with numerical methods should be implemented in order to properly take into consideration the mining aspects (stope sequencing, mining layout, support requirement, backfilling, dynamic load, etc…) and the rock mass discontinuity conditions.
3. Inspections of ground support should be carried out to look for signs of blast damage, corrosion and assess performance.
4. Future ground control methods should integrate the parameters that influence the ground behavior and fall of ground to prevent and control instability in underground mines.
5. Use of the GBI chart for further ground conditions assessment and to predict FoG events.
6. Collection of structural data including dip angles and dip direction angles of geological discontinuities is necessary in all areas of the mine to allow ease of kinematic analysis and integrate structural data with other data in ground control designs such as mining direction and ground support systems.
7. Kinematic analysis should be performed systematically for non-temporal excavations if unfavorable structural conditions prevail so that critical discontinuity orientations could be avoided.

8. Ground displacements and stress monitoring instruments around stopes should be placed in the mine to make it suitable for numerical models to be calibrated, improved back analysis data of fall of ground and advanced forecasting of fall of ground in various sections of the mine.
9. The numerical analysis input parameters are required to be updated when available to increase the level of precision in determining the failure modes such as stress measurements and rock mass parameters such as rock mechanical properties and rock mass characteristics.
10. The stress state that will be generated around the mine openings and its influence on the stability of stopes will need to be assessed in detail utilizing 3-dimensional stress analysis software as 3 dimensional models provide better accuracy.
11. Excavation damage zone should be minimized by use of smooth blasting.
12. Following this work it was recommended that longer than 2 m rock bolts must be utilized as ground support. Rock bolts, shotcrete and wire mesh be used in poor ground conditions.

7.2 Future Research

Investigate the influence of geological discontinuities and mining induced stresses in the occurrence of fall of ground in detail. Evaluate the function of ground support in minimizing, preventing fall of ground due to mining induced stress failures in underground mines.

Limited and missing field data were integrated to compile FoG database in order to accomplish this research work. It is proposed that in order to improve the analysis of collected data, more geological structural data such as dip angles and dip direction angles should be gathered, recording all the parameters to reduce the amount of missing data for the future.

It is also suggested that that other significant factors that influence instability and associated with fall of ground such as blasting, excavation geometry, mining method and rock type and geological structures be included in model development. This will make the proposed model more relevant to the field observed conditions.

Inspect further the significant factors that influence fall of ground and the methods of predicting and controlling fall of ground.

Reference

1. Abedellah, W., Raju, G. D., Mtri, H. S. & Thibodeau, D. 2014. Stability Of Underground Mine Development Intersections During The Life Of A Mine Plan. *International Journal Of Rock Mechanics And Mining Sciences* 72, 173-181.
2. Adoko, A. C., Gokceoglu, C., Wu, L. & Zuo, Q. J. 2013. Knowledge- Based And Data Driven Fuzzy Modelling For Rockburst Prediction. *International Journal Of Rock Mechanics And Mining Sciences,* 61, 86-95.
3. Adoko, A. C., Phumaphi, P. T. & Zvarivadza, T. Quantifying Rock Mass Behavior Around Underground Excavations. *In:* Arma, Ed. 51st Us Rock Mechanics/ Geomenchanics Symposium 2017 San, Francisco, California, United States. American Rock Mechanics Association, 25-28 June 2017.
4. Adoko, A. C., Wang, H., Jiao, Y. Y. & Seitshiro, I. T. Developing The Ground Index (Gi) For Rock Collapse Assessment In Tunneling. The 50th U.S. Rock Mechanics/Geomechanics Symposium, Houston, 26-29 June 2016, 26-29 June 2016 Houston, Texas. Arma: American Rock Mechanics Association.
5. Amadei, B. & Stephansson, O. 1997. *Rock Stress And Its Measurement,* London, Chapman And Hall.
6. Andreev, G. E. 1995. *Brittle Failure Of Rock Materials: Test Results And Constitutive Models,* Rotterdam, Balkema, A.A.
7. Badal, R. 1994. Controlled Blasting In Jointed Rocks. *International Journal Of Rock Mechanics & Mining Sciences,* 31, 79-84.
8. Baheer, I. 2000. Selection Of Methodology For Modeling Hysteresis Behavior Of Soils Using Neural Networks. *Journal Of Computer Aided Civil Infrastructure Engineering,* 5, 445-463.
9. Bajpayee, T. S., Pappas, D., M & & Ellenberger, J., L. 2014. Roof Instability: What Reportable Noninjury Roof Falls In Underground Coal Mines Can Tell Us. *Professional Safety,* 59, 57-62.
10. Barton, J. M., Klemd, R. & Zeh, A. 2006. The Limpopo Belt: A Result Of Archean To Proterozoic, Turkic-Type Orogenesis. *In:* Reimold, W. U., Gibson, R.L (Ed.). Geological Society Of America Special Paper.
11. Bcl 2016. Fall Of Ground Directory. *In:* Section, B. R. M. (Ed.). Bcl Mine, Selebi-Phikwe.
12. Benardos, A. G. & Kaliampako, D. C. 2004. A Methodology For Assessing Geotechnical Hazards For Tbm Tunneling- Illustrated By The Athens Metro, Greece. *International Journal Of Rock Mechanics And Mining Sciences,* 41.
13. Bertoncini, C. A. & Hinders, M. K. 2010. Fuzzy Classification Of Roof Fall Predictors In Microseismic Monitoring. *Measurement,* 43, 1690-1701.
14. Biswas, K. & Zipf, R. K. 2003. Root Causes Of Ground Fall Related Incidents In Us Mining Industry. *In: 22nd International Conference On Ground Control In Mining.*
15. Brown, E. T. & Hoek, E. 1978. Trends In Relationships Between Measured Rock In Situ Stress And Depth. *International Journal Of Rock Mechanics, Mining Science And Geomechanics*, 211-215.
16. Brown, E. T. & Windsor, C. R. 1990. Near Surface Stresses In Australia And Their Influence On Underground Construction. *Seventh Australian Tunnelling Conference.*
17. Brown, P. J. 1988. *Petrogenesis Of Ni-Cu Ore Bodies, Their Host Rocks And Country Rocks At Selebi-Phikwe, Eastern Botswana.* Phd, University Of Southampton.

18. Cai, M. 2016. Prediction And Prevention Of Rockburst In Metal Mines- A Case Study Of Sanshandao Gold Mine *Journal Of Rock Mechanics And Geotechnical Engineering,* 8, 204-211.
19. Cai, M., Kaiser, P. K., Uno, H., Tasaka, Y. & Minami, M. 2004. Estimation Of Rock Mass Deformation Modulus And Strength Of Jointed Hard Rock Masses Using Gsi System. *International Journal Of Rock Mechanics & Mining Sciences,* 41, 3-19.
20. Calleja, J. & Porter, I. Coalburst Control Methods. 16th Coal Operator's Conference, 10-12 February 2016 2016 Wollongong, Australia. The Australian Institute Of Mining And Metallurgy, 321-329.
21. Chikande, T. & Zvarivadza, T. 2016. Review Of Support System Used In Poor Ground Conditions In Platinum Room And Pillar Mining: A Zimbabwean Case Study. *Journal Of Southern African Institute Of Mining And Metallurgy,* 116.
22. Chinner, G. A. & Sweatman, T. R. 1968. A Former Association Of Enstatite And Kynite. *A Journal Of Mineral Sciences.* Adelaide: Mineralogical Society.
23. Christiansson, R., Hakala, M., Kemppainen, K., Siren, T. & C.D, M. 2012. Findings From Large Scale In-Situ Experiments To Establish The Initiation Of Spalling. *Isrm International Symposium- Eurock 2012.* Stockholm, Sweden.
24. Demuth, H. & Beale, M. 1994. Neural Network Toolbox User's Guide. Natick, Usa: The Math Work, Inc.
25. Deng, H. 2000. *Predicting The Extent Of Rock Failure/ Loosening Above Underground Excavations In Massive And Jointed Rocks.* Master Of Science, University Of Manitoba.
26. Direk, C. 2015. *Risk Assessment By Fault Tree Analysis Of Roof And Rib Fall Accidents In An Underground Coal Mine.* Master Of Science, Middle East Technical University.
27. Dou, L., Lu, C.-P., Mu, Z.-L. & Gao, M.-S. 2009. Preventing And Forecasting Of Rock Burst Hazards In Coal Mines. *Mining Science And Technology (China),* 19, 585-591.
28. Duan, W. 2016. *An Assessment Of The Significance Of Factors Affecting The Occurence Of Rockburst Damage.* Master Of Philosophy, The University Of Western Australia.
29. Esterhuizen, G. S. & Bajpayee, T. S. Horizontal Stress Related Failure In Bedded Mine Roofs: Insights From Field Observations And Numerical Models. Proceedings Of The 46th U.S Rock Mechanics/Geomechanics Symposium 2012 Chicago. 68-77.
30. Esterhuizen, G. S., Dolinar, D. R., Ellenberger, J. L., Prosser, L. J. & Iannacchione, A. T. Roof Stability Issues In Underground Limestone Mines In The United States Proceeding Of The 26th International Conference On Ground Control In Mining, 2007 Morgantown. 336-343.
31. Fairhurst, C. In-Situ Stress Determination- An Appraisal Of Its Significance In Rock Mechanics. International Symposium On Rock Stress And Measurements 1986 Stockholm. Centek Publ, Lulea, 3- 17.
32. Faramarzi, F., Mansouri, H. & Ebrahimi Farsangi, M. A. 2013. A Rock Engineering Systems Based Model To Predict Rock Fragmentation By Blasting. *International Journal Of Rock Mechanics And Mining Sciences,* 60, 82-94.
33. Faramarzi, F., Mansouri, H. & Farsangi, M. 2014. Development Of Rock Engineering Systems- Based Models For Flyrock Risk Analysis And Prediction Of Flyrock

Distance In Surface Blasting *Journal Of Rock Mechanics And Rock Engineering,* 47, 1291- 1306.
34. Fattahi, H. 2018. Applying Rock Engineering Systems To Evaluate Shaft Resistance Of A Pile Embedded In Rock. *Geotechnical And Geological Engineering* 1-11.
35. Fausett, L. V. 1994. *Fundamentals Neural Networks: Architecture, Algorithms, And Applications,* Englewood Cliffs, New Jersey, Prentice-Hall, Inc.
36. Finn, C. A., Deszcz-Pan, M., Anderson, E. D. & John, D. A. 2007. Three-Dimensional Geophysical Mapping Of Rock Alteration And Water Content At Mount Adams, Washington: Implications For Lahar Hazards. *Journal Of Geophysical Research B: Solid Earth,* 112.
37. Flaten, M. 2015. *Stress Induced Stability Assessment Of The Underground Caverns For Moglice Hydropower Project, Albania.* Msc, Norwegian University Of Science And Technology.
38. Gallon, M. L. Structural Re-Interpretation Of The Selebi-Phikwe Nickel-Copper Sulphide Deposits, Eastern Botswana. *In:* Anhaeusser, C. R. & Maske, S., Eds. Mineral Deposits Of Southern Africa, 1986. Geological Society Of South Africa, 1663-1669.
39. Goodman, R. E. & Shi, G. H. 1985. *Block Theory And Its Application To Rock Engineering,* New Jersey, Usa, Prentice-Hall Press, Englewood Cliifs.
40. Gopalakrishnan, K., Manik, A. & Khaitan, S. K. 2006. Runway Stiffness Evaluation Using An Artificial Neural System Approach *International Journal Of Computer Engineering*, 517-523.
41. Goricki, A., Schubert, W. & Riedmueller, G. 2004. New Developments For The Design And Construction Of Tunnels In Complex Rock Masses. *International Journal Of Rock Mechanics And Mining Sciences,* 41, 720-725.
42. Grau , R. H. & Prosser, L. J. 1997. Scaling Roof Accidents In Underground Stone Mines. *Rock Products.*
43. Guo, Y. H. & Jiang, F. X. 2009. Application Of Comprehensive Fuzzy Evaluation In Burst-Proneness Risk Of Coal Seam. *2nd International Conference On Future Information Technology And Management Engineering.* Los Alamitos: Ieee Computer Society.
44. Handley, M. F. 2013. Pre-Mining Stress Model For Subsurface Excavations In Southern Africa. *The Journal Of The Southern African Institute Of Mining And Metallurgy*, 449-471.
45. Hao, Y. H. & Azzam, R. 2005. The Plastic Zones And Displacements Around Underground Openings In Rock Masses Containing A Fault. *Tunnelling And Underground Space Technology,* 20, 49- 61.
46. Herget, G. 1988. *Stresses In Rock,* Rotterdam, Balkema.
47. Hoek , E. & Bray, J. W. 1981. *Rock Slope Engineering,* London, England, The Institute Of Mining And Metallurgy
48. Hoek , E. & Brown, E. T. 1980. *Underground Excavations In Rock,* London: The Institute Of Mining And Metallurgy.
49. Hoek , E., Brown, E.T 1980. Empirical Strength Criterion For Rock Masses. *Journal Of Geotechnical Engineering Division Asce,* 106, 1013-1035.
50. Hoek , E., Carranza-Torres, C. & Corkum, B. Hoek-Brown Failure Criterion- 2002 Edition. 5th North American Rock Mechanics Symposium And The 17th Tunneling

Association Of Canada Conference (Narms-Tac 220), 2002 Toronto, Canada. Mining Innovation And Technology, 267-273.
51. Hudson, J. A. 1992. *Rock Engineering Systems: Theory And Practice,* Chichester, Ellis Horwood.
52. Iannacchione, A. T., Dolinar, D. R., Marshall, T. E., Oyler, D. C. & Compton, C. S. Controlling Roof Beam Failures From High Horizontal Stresses In Underground Stone Mines Proceedings Of The 17th International Conference On Ground Control In Mining 1998 Morgantown, West Virginia. 102-112.
53. Iramina, W. S., Eston, S. M., Hennies, W. T. & Candia, R. C. 2014. Fatal Accidents And Rockfalls In Peruvian Underground Mines. *In:* Drebenstedt, C., Singhal, R (Ed.) *Proceedings Of The 22nd Mine Planning And Equipment Selection Conference* Dresden, Germany.
54. Irfan, T. Y. 1999. Characterization Of Weathered Volcanic Rocks In Hong Kong. *Journal Of Engineering Geology Ahd Hydrogeology,* 32, 317-348.
55. Isrm 1987. Suggested Methods For Rock Stress Determination. *International Journal Of Rock Mechanics, Mining Science And Geomechanics*, 53-73.
56. Iverson, R. S., William, W. A. & Johnson, J. C. 2013. A New Perimeter Control Blast Deisgn Concept For Underground Metal/Nonmetal Drifting Applications. Pittsburgh, Pa: National Institute For Occupational Safety And Health.
57. Iverson, S., Mchugh, E., Dwyer, J., Warneke, J. & Caceres, C. 2007. Ground Control And Safety Implications Of Blast Damage In Underground Mines. *In:* Luo-Y, P.-S. M.-C. F.-G. T.-S. K.-A. H.-K., Ed. Proceedings Of The 26th International Conference On Ground Control In Mining, 2007 Morgantown, West Virginia. 328-335.
58. Jain, A. K., Mao, J. & Mohiuddin, K. M. 1996. Artificial Neural Networks: A Tutorial. *Computer,* 29, 31-44.
59. Jian, Z., Xibing, L. & Xiuzhi, S. 2012. Long Term Prediction Model Of Rockburst In Underground Openings Using Heuristic Algorithms And Support Vector Machines. *Safety Science,* 50, 629-644.
60. Kainthola, A. 2015. Tunnelling Challenges And Solutions- Indian Scenario. *Tunnelling Association Of India,* 4, 89.
61. Kaiser, P. K. Underground Rock Engineering To Match The Rock's Behaviour-Challenges Of Managing Highly Stressed Ground In Civil And Mining Projects. 50th Us Rock Mechanics Symposium 2016 Houston, Texas, Usa. American Rock Mechanics Association (Arma).
62. Kaiser, P. K. & Cai, M. 2012. Design Of Rock Support System Under Rockburst Condition. *Journal Of Rock Mechanics And Geotechnical Engineering,* 4, 215-227.
63. Kaiser, P. K., Diederichs, M. S., Martin, C. D., Sharp, J. & Steiner, W. Underground Works In Hard Rock Tunneling And Mining Proceedings Of Geoeng 2000 Conference, 2000 Lancaster. Technomic Publishers Co Inc, 841-926.
64. Kaiser, P. K. & Kim, B.-H. 2008. Rock Mechanics Advances For Underground Construction In Civil Engineering And Mining. *Korea Rock Mechanics Symposium.* Seoul.
65. Kaiser, P. K. A. & Cai, M. Critical Review Of Design Principles For Rock Support In Burst-Prone Ground–Time To Rethink. . *In:* Potvin, Y. & Brady, B., Eds. Proceedings Of The Vii International Symposium On Ground Support In Mining And

Underground Construction, 2013 Australian Centre For Geomechanics, Perth, Wa. Australian Centre For Geomechanics, 3–38.
66. Kashyap, S. K., Parhi, D. R. K., Sinha, A., Singh, M. K. & Singh, B. K. 2008. Optimization Of Mine Siupport Parameters Using Neural Network Approach. *International Association For Computer Methods And Advances In Geomechanics (Iacmag)*. Goa, India.
67. Katongo, C. Ground Conditions And Support Systems At 1 Shaft, Konkola Mine, Chililabombwe, Zambia. In: Proceedings Of The Third Southern African Conference On Base Metals, 2005 Kitwe, Zambia. The South African Institute Of Mining And Metallurgy, 253-280.
68. Key, R., M. 1976. The Geology Of The Area Around Francistown And Phikwe, Northeast And Central Districts, Botswana. *Geological Survey Of Botswana District Memoir*. Lobatse, Botswana.
69. Kidybinski, A. 1986. Design Criteria For A Roadway Supports To Resist Dynamic Loads. *International Journal Of Mining And Geological Engineering*, 4, 91-109.
70. Kim, M. K., &, Y. Y.-I. & J.-J, S. 2008. Methodology To Quantify Rock Behavior Around Shallow Tunnels By Rock Engineering Systems. *Geosystem Engineering* 11, 37-42.
71. Kliche, C. A. 1999. *Rock Slope Stability*, Colorado, Usa, Society For Mining, Metallurgy, And Exploration, Inc. (Sme).
72. Koldas, K. S. 2003. Rockburst And Fall Of Ground Investigations In Deep Level Gold Mines: South Africa Example. *17th International Mining Congress And Exhibition Of Turkey*. Ankara, Turkey: Chamber Of Mining Engineers Of Turkey.
73. Konicek, B. R., Deb, D., Prasad, M. & Sankar, U. S. 2011. Numerical Modelling- An Effective Tool For Strata Control In Coal Mines. *National Seminar On Underground Coal Mining*.
74. Lang, L., Fu-Bao, Z. 2010. A Comprehensive Hazard Evaluation System For Spontaneous Combustion Of Coal In Underground Mining. *International Journal Of Coal Geology*, 27-36.
75. Lear, P., A 1979. The Ore Mineralogy Of The Phikwe And Selebi Nickel-Copper Deposits, Botswana. *Geological Society Of South Africa, Special Publication*, 5, 117-132.
76. Lehmann, C. & Konietzky, H., H 2015. Geomechanical Issues In Longwall Mining-An Introduction.
77. Li, B. & Liu, Y. 2015. Determination Of Classification Of Rockburst Risk Based On Random Forest Approach And Its Application. *Science Technology*, 33, 57-67.
78. Li, N., Xianda, F. & Jimenez, R. 2016. Predicting Rockburst Hazard With Incomplete Data Using Bayesian Networks. *Tunnelling And Underground Space Technology*, 61, 61-70.
79. Li, Y., Zhou, H., Zhu, W., Li, S. & Liu, J. 2015. Numerical Study On Crack Propagation In Brittle Jointed Rock Mass Influenced By Fracture Water Pressure. *Journal Of Materials*, 8, 3364-3376.
80. Liu, Q. S., Zhang, W., Lu, X. L. & Fu, J. J. 2010. Safety Monitoring And Stability Analysis Of Large-Scaler Roadway In Fault Fracture Zone. *Chinese Journal Of Rock Mechanics And Engineering*, 29, 1954-1962.

81. Lu, P. & Hudson, J. A. A Fuzzy Evaluation Approach To The Stability Of Underground Excavations Isrm Symposium: Eurock'93, 1993. 615-622.
82. Mahdevari, S. & Torabi, R. S. 2012. Prediction Of Tunnel Convergence Using Artificial Neural Networks. *Tunnelling And Underground Space Technology,* 28, 218-228.
83. Mansurov, V. A. 2001. Prediction Of Rockbursts By Analysis Of Induced Seismicity Data. *International Journal Of Rock Mechanics And Mining Sciences,* 38, 893-901.
84. Marinos, V. P. Geological Behaviour Of Rock Masses In Underground Excavations. Proceedings Of The 12th International Congress
85. 2010 Patras. Bulletin Of The Geological Society Of Greece, 1238-1247.
86. Mark, C. The Science Of Design In Mining Rock Mechanics. In Proceedings From The 34th International Conference On Ground Control In Mining, 2015 West Virginia. Morgantown 225-237.
87. Mark, C. 2016. Science Of Empirical Design In Mining Ground Control. *International Journal Of Mining Science And Technology,* 26, 461-470.
88. Mark, C. & Barczak, T. M. The Impact Of Ground Control Research On The Safety Of Underground Coal Miners: 1910-2010. *In:* Brune, J. F., Ed. 41st U.S Rock Mechanics Symposium. Extracting The Science: A Century Of Mining Research, 2010. Society For Mining, Metallurgy And Exploration, 177-188.
89. Mark, C. & Gauna, M. 2017. Preventing Roof Fall Fatalities During Pillar Recovery: A Ground Control Success Story. *International Journal Of Mining Science And Technology,* 27, 107- 113.
90. Mark, C., Pappas, D. M. & Barczak, T. M. 2011. Current Trends In Reducing Groundfall Accidents In U.S Coal Mines *Society Of Mining Engineers.*
91. Mark, C. & Zelanko, J. C. 2005. Reducing Roof Fall Accidents On Retreat Mining Sections. *Coal Age,* 110, 26-31.
92. Marques, E. A. G., Barroso, E. V., Menezes-Filho, A. P. & Vargas Jr., E. A. 2010. Weathering Zones On Metamorphic Rocks From Rio De Janeiro- Physical, Mineralogical And Geomechanical Characterization. *Engineering Geology,* 111, 1-18.
93. Martin, C. D., Christiansoon, R. & SÖederhäell, J. 2001. Rock Stability Considerations For Siting And Constructing A Kes-3 Repository. Based On Experiences From Aespoe Hrl, Aecl's Url, Tunelling And Mining. Sweden.
94. Martin, C. D., Kaiser, P. K. & Christiansoon, R. 2003. Stress, Instability And Design Of Underground Excavations. *International Journal Of Rock Mechanics & Mining Sciences.*
95. Martin, C. D., Kaiser, P. K. & Mccreath, D. R. 1999. Hoek-Brown Parameters For Predicting The Depth Of Brittle Failure Around Tunnels *Canadian Geotechinal Journal,* 36, 136-151.
96. Martyka, J. & Hetmanczyk, P. 2013. The State Of Natural And Technical Hazards In Polish Hard Coal Mines In 2013. *Report Under Prof Kabiesz Lidership.* Katowice.
97. Mason, R. 1973. The Geology Of The Southern Tati Area. Lobatse: Unpublished Report, Geological Survey Of Botswana.
98. Maswebe, D. 2011. Sill Pillar Reclamation At Selebi Shaft, Bcl Mine, Botswana. Selebi-Phikwe, Botswana: Bcl Mine.
99. Mathews, K., Hoek, E., Wyllie, D. & Stewart, S. 1981. Prediction Of Stable Excavation Spans At Depths Below 1000m In Hard Rock Mines. *Canmet Report.*

100. Mawdesley, C., Trueman, R. & Whiten, W. J. 2001. Extending The Mathews Stability Graph For Open–Stope Design. *Mining Technology,* 110, 27-39.
101. Mazzoccola, D., F & & Hudson, J. A. 1996. A Comprehensive Method Of Rock Mass Characterization For Indicating Natural Slope Instability. *Quartely Journal Of Engineering Geology,* 29, 37-56.
102. Mccourt, S., Kampunzu, A. B., Bagai, Z. & Armstrong, R. A. 2004. The Crustal Architecture Of Archaean Terranes In Northeastern Botswana. *South African Journal Of Geology*, 147-158.
103. Meulenkamp, M. & Grima, M. A. 1999. Application Of Neural Networks For The Prediction Of Unconfined Compressive Strength (Ucs) From Equotip Hardness. *International Journal Of Rock Mechanics And Mining Sciences,* 38, 29-39.
104. Miao, S., Cai, M. & Guo, Q. 2016. Rockburst Prediction On In-Situ Stress And Energy Accumulation Theory. *International Journal Of Rock Mechanics And Mining Sciences,* 83, 86-94.
105. Mikula, P. A. 2013. The Effect Of Choice Of Magnitude Scale On Empirical Charting Of Dynamic Ground Support Performance *Ims Conference.* Hobart, Tasmania.
106. Molinda, G. M. 2003. Geologic Hazards And Roof Stability In Coal Mines. *In: Characterization And Control Of Coal Mine Roof In Weak Ground.* Pittsburgh: U.S Department Of Health And Human Services, Public Health Services, Centers For Disease Control And Prevention, National Institute Of Occupational Safety And Health, Dhhs (Niosh)
107. Molinda, G. M. & Mark, C. 2010. Ground Failures In Coal Mines With Weak Roof. *Electronic Journal Of Geotechnical Engineering,* 15, 547-588.
108. Moshab 1997. Geotechnical Considerations In Underground Mines: Guideline, Mines Occupational Safety And Health Advisory Board. *In:* Resources, D. O. I. A. (Ed.). Government Of Western Australia.
109. Naghadehi, Z. M., Jimenez, R., Khalokakaie, R. & Jalali, E. S. M. 2011. A Probabilistic Systems Methodology To Analyze The Importance Of Factors Affecting The Stability Of Rock Slopes. *Engineering Geology,* 118, 82-92.
110. Naghadehi, Z. M., Jimenez, R., Khalokakaie, R. & Jalali, E. S. M. 2013. A New Open-Pit Mine Slope Instability Index Defined Using The Improved Rock Engineering Systems Approach. *International Journal Of Rock Mechanics & Mining Sciences,* 61, 1-14.
111. Ndlovu, X. & Stacey, T. R. 2007. Observations And Analyses Of Roof Guttering In A Coal Mine. *Journal Of The South African Institute Of Mining And Metallurgy,* 107, 477-491.
112. Newman, H. R. 2013. The Mineral Industry Of Botswana *U.S. Geological Survey Minerals Yearbook—2012.* U.S Geological Survey.
113. Nilsen, B. & Palmström , A. 2000. Handbook Nr. 2: Engineering Geology And Rock Engineering *Nowergian Group Of Rock Mechanics*, 249.
114. Palmström , A. & Stille, H. 2007. Ground Behaviour And Rock Engineering Tools For Underground Excavations. *Tunnelling And Underground Space Technology,* 22, 363-376.
115. Palmström, A. & Stille, H. 2010. *Rock Engineering,* London, Thomas Telford Limited.

116. Pappas, D. & Mark, C. 2010. Roof And Rib Fall Accidents And Statistics – An Update, In Characterization And Control Of Coal Mine Roof In Weak Ground. Niosh Information Circular.
117. Pappas, D. M. & Mark, C. 2012. Roof And Rib Fall Incident Trends: A 10 Year Profile. *Transactions Of Society For Mining, Metallurgy And Exploration*, 462-478.
118. Peng, Q., Qian, A. & Xiao, Y. 2010. Research On Prediction System For Rockburst Based On Artificial Intelligence Application Methods. *Journal Of Sichuan University: (Engineering Science)*, 42, 18-24.
119. Peng, S. S. 2015. Topical Areas Of Research Needs In Ground Control- A State Of The Art Review On Coal Mine Ground Control *International Journal Of Mining Science And Technology*, 25, 1-6.
120. Peng, Y., Peng, K., Zhou, J. & Liu, Z. 2014. Prediction Of Classification Of Rockburst Risk Based On Genetic Algorithms With Svm. *In: 2nd International Conference On Machinery, Material Science And Energy Engineering (Icmmsee)*. Changsha, China: Trans Tech Publications Ltd, Zurich, Switzerland.
121. Pola, A., Crosta, G. B., Fusi, N. & Castellanza, R. 2014. General Characterization Of The Mechanical Behavior Of Different Volcanic Rocks With Respect To Alteration. *Engineering Geology*, 169, 1-13.
122. Potvin, Y., Nedin, P., Sandy, M., Rosengren, K. & Rosengren, M. 2001. Towards Elimination Of Rockfall Fatalities In Australian Mines. Perth: Autralian Centre For Geomechanics.
123. Poulton, M. M. 2002. Neural Networks As An Intelligence Amplification Tool: A Review Of Applications. *Journal Of Geophysics*, 67, 979-993.
124. Prusek, S., Rajwa, S., Wrana, A. & Krzemien, A. 2017. Risk Assessment Of Roof Fall In Longwall Coal Mines. *International Journal Of Mining, Reclamation And Environment*, 31, 558-574.
125. Queensland, G. 2004. Reduction Of Exposure To Rockfalls In Underground Metalliferous Mines. *In:* Petroleum, D. O. M. A. (Ed.). Queensland: Queensland Government.
126. Rafiee, R. 2014. Development Rock Behavior Index Around Underground Space Using A Rock Engineering System. *Journal Of Geology And Mining Research*, 6, 46-56.
127. Rafiee, R., Ataei, M., Khalokakaie, R., Jalali, S. M. E. & Sereshki, F. 2015. Determination And Assessment Of Parameters Influencing Rock Mass Cavability In Block Caving Mines Using The Probabilistic Rock Engineering System. *Rock Mechanics And Rock Engineering*, 48, 1207-1220.
128. Rafiee, R., Ataei, M., Khalokakaie, R., Jalali, S. M. E. & Sereshki, F. 2016. A Fuzzy Rock Engineering System To Assess Rock Mass Cavability In Block Caving Mines. *Neural Computing And Applications*, 27, 2083-2094.
129. Rahimi, B. & Sharifzadeh, M. 2017. Evaluation Of Ground Management In Underground Excavation Design. *In:* Wesseloo, D. J. (Ed.) *Deep Mining 2017: International Conference On Deep And High Stress Mining*. Perth: Australian Centre For Geomechanics.
130. Ripley, B. D. 1996. *Pattern Recognition And Neural Networks*, Cambridge University Press.

131. Rocscience, I. 2016a. Dips Version 7.0: Streographic Projection Program For The Interactive Analysis Of Orientation Based Geological Data. Toronto, Canada: Rocscience.
132. Rocscience, I. 2016b. Examine2d Version 8.0: 2 Dimensional Boundary Element Program For Stress Analysis Of Underground Excavations. Toronto, Canada.
133. Rocscience, I. 2016c. Rocdata Version 5.0: Toolkit For The Analysis Of Rock And Soil Strength Data, Strength Envelopes And Other Physical Paramaters. Toronto, Canada: Rocscience.
134. Rocscience, I. 2016d. Rs2 Version 9.0: 2 Dimensional Rock And Soil Finite Element Program For Analyzing Slopes And Underground Excavations. Toronto, Canada: Rocscience.
135. Rosenblatt, F. 1958. The Perceptron: A Probabilistic Model For Information Storage And Organization In The Brain. *Psychological Review,* 65, 386-408.
136. Rumelhart, D. E. & Mcclelland, J. L. 1986. *Parallel Distributed Processing,* Cambridge, Usa, Mit Press.
137. Saffari, A., Sereshki, F., Atei, M. & Ghanbari, K. 2013. Applying Rock Engineering Systems (Res) Approach To Evaluate And Classify The Coal Spontaneous Combustion Potential In Eastern Alborz Coal Mines. *International Journal Of Mining And Geo-Engineering,* 47, 115-127.
138. Saharan, M. R. & Mitri, H. 2011. Destress Blasting As Mines Safety Tool: Some Fundamental Challenges For Successful Applications. *Procedia Engineering,* 26, 37-47.
139. Sayadi, A., Monjezi, M., Talebi, N. & Khandelwal, M. 2013. A Comparative Study On The Application Of Various Artificial Neural Networks To Simultaneous Prediction Of Rock Fragmentation *Journal Of Rock Mechanics And Geotechnical Engineering,* 5.
140. Schubert, W., Steindorfer, A. Advanced Monitoring Data Evaluation And Display For Tunnels. *In:* Negro Jr, A., Ferreira, A., A, Ed. Proceedings Of The International Symposium On Tunnels And Metropolises, 1998 Sao Paulo. Balkema, Rotterdam, 1205-1208.
141. Sellers, E. J., Coetzer, S. J. & Kamstra, R. 2002. Understanding And Determining The Variability In Primitive Stress. Johannesburg: Safety In Mines Research Advisory Committee.
142. Shahriar, K., Oraee, K. & Bakhtavar, E. Roof Falls: An Inherent Risk In Undergroundcoal Mining. The 28th International Conference On Ground Control In Mining, 2009 Morgantown, Wv, Usa.
143. Shanin, M. A., Jaksa, M. B. & Maier, H. R. 2001. Artificial Neural Network Applications In Geotechnical Engineering. *Australian Geomechanics Journal,* 36, 49-62.
144. Shin, H.-S., Kwon, Y.-C., Jung, Y.-S., Bae, G.-J. & Kim, Y.-G. 2009. Methodology For Quantitative Hazard Assessment For Tunnel Collapses Based On Case Histories In Korea. *International Journal Of Rock Mechanics And Mining Sciences,* 46, 1072-1087.
145. Simpson, P. K. 1990. *Artificial Neural Systems. Foundation, Paradigms, Applications And Implementations.,* New York, Ny, Pergamon Press.

146. Singh, P. K., Roy, M. P., Ranjit, K., Paswan, R. K., Dubey, R. K. & Drebenstedt, C. 2015. Blast Vibration Effect In An Underground Mine Caused By Open-Pit Mining. *International Journal Of Rock Mechanics And Mining Sciences,* 80, 79-88.
147. Sinkala, P. & Krishna, R. Improving The Geomechanics Conditions For Effective Ground Control; A Case Study Of Chibuluma South Mine, Zambia. International Conference On Management Science And Management Innovation (Msmi 2014), 2014 Changsha, China.
148. Stacey, T. R. & Gumede, H. 2007. Evaluation Of Risk Of Rock Fall Accidents In Gold Mine Stopes Based On Measured Joint Data. *The Journal Of The Southern African Institute Of Mining And Metallurgy,* 107, 345-350.
149. Stacey, T. R. & Wesseloo, J. 1998. Evaluation And Upgrading Of Stress Measurement Data In The Mining Industry. Johannesburg: Simrac Report Gap 511, Mine Health And Safety.
150. Suratgar, H., Tavakoli, M. B. & Hoseinabadi, A. Modified Levenberg- Marquardt Method For Neural Networks Training. Proceedings Of World Academy Of Science, Engineering And Technology, 2005. 46-48.
151. Tavoularis, N., Koumantakis, I., Rozos, D. & Koukis, G. 2015. An Implementation Of Rock Enginering System (Res) For Ranking The Instability Potential Of Slopes In Greek Territory. An Application In Tsakona Area (Peloponnese- Prefecture Of Arcadia). *Bulletin Of Geological Society Of Greece,* 49, 38-58.
152. Van Der Heever, P., &, P. P. S. & Handley, M. F. 2014. In-Situ Stress Measurements On 1480 Level, Bcl Mine, Selebi-Phikwe. Johannesburg: Confidential Report.
153. Van Der Merwe, J. N., Van Vuuren, J. J., Butcher, R. & Canbulat, I. 2001. Causes Of Falls Of Roof In South African Collieries. Safety In Mines Research Advisory Committee.
154. Varnes, D. J. 1978. Slope Movement Types And Processes. *In:* Schuster, R. L., Krizek, R.J (Ed.) *In Special Report 176: Landslides: Analysis And Control.* Washington, D.C: National Academy Of Science.
155. Verma, K. H., Samadhiya, K. N., Singh, M. & Prasad, V. V. R. 2014. Blast Induced Damage To Surrounding Rock Mass In An Underground Excavation. *Journal Of Geological Resource And Engineering,* 2, 13-19.
156. Wang, J. A. & Park, H. D. 2001. Comprehensive Prediction Of Rockburst Based On Analysis Of Strain Energy In Rocks. *Tunnelling And Underground Space Technology,* 16, 49-57.
157. Watters, R. J., Zimbelman, D., Bowman, S. & Crowley, J. 2000. Rock Mass Strength Assessment And Significance To Edifice Stability, Mount Rainier And Mount Hood, Cascade Range Volcanoes. *Pure Applied Geophysics,* 157.
158. Werbos, P. J. 1974. *Beyond Regression: New Tools For Prediction And Analysis In The Behavioral Sciences* Phd, Havard University.
159. Whyatt, J., Girand, J. & Johnson, J. Feasibility Of Using Controlled Blasting Techniques To Improve Ground Control Safety In Underground Mines. Proceedings Of The 39th U.S Rock Mechanics Conference, 2003 Cambridge, Massachusetts. Cambridge, 1774-1724.
160. Wyllie, D. C. & Mah, C. W. 2004. *Rock Slope Engineering, Civil And Mining (4th Edition),* New York, Spon Press.

161. Xie, Z., Zhang, N., Qian, D., Han, C., An, Y. & Wang, Y. 2018. Rapid Ecxavation And Stability Control Of Deep Roadways For An Underground Coal Mine With High Production In Inner Mongolia. *Journal Of Sustainability,* 10, 1160.
162. Yang, Y. & Zhang, Q. 1998. The Application Of Neural Networks To Rock Engineering Systems (Res). *International Journal Of Rock Mechanics And Mining Sciences,* 35, 727-745.
163. Yu, H. C., Liu, H. N., Lu, X. S. & Liu, H. D. 2009. Prediction Method Of Rockburst Proneness Based On Rough Set Theory And Genetic Algorithm. *Journal Of Coal Science Engineering (China),* 15, 367-373.
164. Zhang, L. Q., Yang, Z. F., Liao, Q. L. & Chen, J. 2004. An Application Of The Rock Engineering Systems (Res) Methodology In Rockfall Hazard Assessment On The Cheng- Du–Lhasa Highway, China. *International Journal Of Rock Mechanics And Mining Science,* 41, 833-838.
165. Zhang, P., Peterson, S., Neilans, D., Wade, S., Mcgrady, R. & Pugh, J. Geotechnical Risk Management To Prevent Coal Outburst In Room And Pillar Mining. Proceedings Of The 34th International Conference On Ground Control In Mining, 2015 Morgantown, Wv. 68-79.
166. Zhou, J., Shi, X. Z., Dong, L., Hu, H. Y. & Wang, H. Y. 2010. Fisher Discriminant Analysis Model And Its Application For Prediction Of Classification Of Rockburst In Deep Buried Long Tunnel. *Journal Of Coal Science And Engineering (China),* 16, 144-149.
167. Zhu, W., Xu, J. & Xu, G. 2017. Mechanism And Control Of Roof Fall And Support Failure Incidents Occuring Near Longwall Recovery Roadways. *Journal Of Southern African Institute Of Mining And Metallurgy,* 117.
168. Zimbelman, D. R., Rye, R. O. & Breit, G. N. 2003. Origin Of Sulfate Minerals In Active Andesitic Stratovolcanoes. *Chemical Geology,* 215, 37-60.
169. Zimbelman, D. R., Watters, R. J., Firth, I. R., Breit, G. N. & Carrasco-Nunez, G. 2004. Stratovolcano Stability Assessment Methods And Results From Citlaltepetl, Mexico. *Bulletin Of Volcanology,* 66, 66-79.
170. Zoback, M. D. & Healy, J. H. 1992. In-Situ Stress Measurements To 3.5 Km Depth In The Cajon Pass Scientific Research Borehole. *Journal Of Geophysical Research* 97, 5039-5058.